63-3-6

ASD-TDR-63-113

406 691

DETECTION OF HYDROGEN-AIR FIRES AND EXPLOSIONS IN AEROSPACE VEHICLES VIA OH BAND AND WATER BAND EMISSION

~~TECHNICAL DOCUMENTARY REPORT NO. ASD-TDR-63-113~~

April 1963

Directorate of Aeromechanics
Aeronautical Systems Division
Air Force Systems Command
Wright-Patterson Air Force Base, Ohio

Project No. 6075, Task No. 607501

(Prepared under Contract No. AF33(657)-8969 by the Reaction Motors Division of Thiokol Chemical Corporation, Denville, New Jersey; K. Hill and B. Hornstein, Authors)

NOTICES

When Government drawings, specifications, or other data are used for any purpose other than in connection with a definitely related Government procurement operation, the United States Government thereby incurs no responsibility nor any obligation whatsoever; and the fact that the Government may have formulated, furnished, or in any way supplied the said drawings, specifications, or other data, is not to be regarded by implication or otherwise as in any manner licensing the holder or any other person or corporation, or conveying any rights or permission to manufacture, use, or sell any patented invention that may in any way be related thereto.

Qualified requesters may obtain copies of this report from the Armed Services Technical Information Agency, (ASTIA), Arlington Hall Station, Arlington 12, Virginia.

This report has been released to the Office of Technical Services, U.S. Department of Commerce, Washington 25, D.C., in stock quantities for sale to the general public.

Copies of this report should not be returned to the Aeronautical Systems Division unless return is required by security considerations, contractual obligations, or notice on a specific document.

30-763M, 400, 6-11-63

Aeronautical Systems Division, Directorate of Aeromechanics, Flight Accessories Lab, Wright-Patterson AFB, Ohio.
Rpt No. ASD-TDR-63-113. DETECTION OF HYDROGEN-AIR FIRES AND EXPLOSIONS IN AEROSPACE VEHICLES VIA OH BAND AND WATER BAND EMISSION. Final report, Apr 63, 96p., incl illus, tables and refs.

Unclassified Report.

To provide a basis for reliable hydrogen-air fire and explosion detection in aerospace vehicles, measurements of the absolute value of radiant intensity were made over the OH bands of the ultraviolet and the water bands in the infrared. A surprising

(over)

result was the increase in OH radiant intensity with decreasing pressure. Diffusion flame variables were hydrogen flow rate, port diameter, and pressure from 760 to less than 20 mm Hg. For explosions, mixture ratio as well as pressure were varied; the rate of increase of emission and pressure after ignition were measured to determine detection lead time. Results where possible are presented as fundamental quantities which can be applied with reasonable rigor to a variety of design situations. Detection based upon monitoring OH radiation is recommended over other properties such as IR radiation, ionization, temperature rise, or pressure rise. Application of the data to specific designs is discussed.

1. Fire Detection Hydrogen-Air
2. Aerospace Vehicles
3. Radiation, Infrared
4. Radiation, Ultraviolet

I. AFSC Project 6075 Task 607501
II. Contract AF 33 (657)-8969
III. Thiokol Chemical Corp., Reaction Motors Division, Denville, N. J.
IV. K. Hill
B. Hornstein

V. Aval fr OTS
VI. In ASTIA collection

Aeronautical Systems Division, Directorate of Aeromechanics, Flight Accessories Lab, Wright-Patterson AFB, Ohio.
Rpt No. ASD-TDR-63-113. DETECTION OF HYDROGEN-AIR FIRES AND EXPLOSIONS IN AEROSPACE VEHICLES VIA OH BAND AND WATER BAND EMISSION. Final report, Apr 63, 96p., incl illus, tables and refs.

Unclassified Report.

To provide a basis for reliable hydrogen-air fire and explosion detection in aerospace vehicles, measurements of the absolute value of radiant intensity were made over the OH bands of the ultraviolet and the water bands in the infrared. A surprising

(over)

result was the increase in OH radiant intensity with decreasing pressure. Diffusion flame variables were hydrogen flow rate, port diameter, and pressure from 760 to less than 20 mm Hg. For explosions, mixture ratio as well as pressure were varied; the rate of increase of emission and pressure after ignition were measured to determine detection lead time. Results where possible are presented as fundamental quantities which can be applied with reasonable rigor to a variety of design situations. Detection based upon monitoring OH radiation is recommended over other properties such as IR radiation, ionization, temperature rise, or pressure rise. Application of the data to specific designs is discussed.

1. Fire Detection Hydrogen-Air
2. Aerospace Vehicles
3. Radiation, Infrared
4. Radiation, Ultraviolet

I. AFSC Project 6075 Task 607501
II. Contract AF 33 (657)-8969
III. Thiokol Chemical Corp., Reaction Motors Division, Denville, N. J.
IV. K. Hill
B. Hornstein

V. Aval fr OTS
VI. In ASTIA collection

FOREWORD

This report covers research performed in the Physics and Advanced Systems Department of Reaction Motors Division under USAF Contract No. AF33(657)-8969. This contract was initiated under Project No. 6075, "Characteristics of Propellant Flames for Detection", Task No. 607501, "Detection and Controlling of Hydrogen Fires and Explosions". The work was administered under the direction of the Flight Accessories Laboratory, Aeronautical Systems Division, with Mr. Terry Trumble acting as project engineer.

This report covers a period of work from 1 June 1962 through 30 November 1962.

The authors, Kenneth Hill and Bernard Hornstein, appreciate the extensive assistance of Wallace Sutton in conducting the experiments and reducing the data. They are indebted to Hans Wolfhard, Department Manager, for discussions and suggestions regarding the direction and results of the research.

The technical project monitor at ASD was Terry Trumble. His assistance in delineating the scope of the research is acknowledged.

This report bears the Thiokol Chemical Corporation designation RMD 5508-F.

ABSTRACT

To provide a basis for reliable hydrogen-air fire and explosion detection in aerospace vehicles, measurements of the absolute value of radiant intensity were made over the OH bands of the ultraviolet and the water bands in the infrared. A surprising result was the increase in OH radiant intensity with decreasing pressure. Diffusion flame variables were hydrogen flow rate, port diameter, and pressure from 760 to less than 20 mm Hg. For explosions, mixture ratio as well as pressure were varied; the rate of increase of emission and pressure after ignition were measured to determine detection lead time. Results where possible are presented as fundamental quantities which can be applied with reasonable rigor to a variety of design situations. Detection based upon monitoring OH radiation is recommended over other properties such as IR radiation, ionization, temperature rise, or pressure rise. Application of the data to specific designs is discussed.

This technical documentary report has been reviewed and is approved.

WILLIAM C. SAVAGE
Chief, Environmental Branch
Flight Accessories Laboratory

TABLE OF CONTENTS

TABLE OF CONTENTS (Cont.)

LIST OF TABLES

LIST OF ILLUSTRATIONS

LIST OF ILLUSTRATIONS (Cont.)

LIST OF ILLUSTRATIONS (Cont.)

1. INTRODUCTION

1.1 Purpose and Scope of Program

In manned aerospace vehicles carrying stored liquid hydrogen, fuel can leak into a vented or closed compartment, and burn or explode with air. For safety, three sequential requirements must be met:

(1) To detect the presence of hydrogen and inert the compartment before ignition takes place.

(2) If ignition does occur, to detect reliably, under all flight conditions, the resulting fire or explosion in time to activate suppression or safety measures before damage occurs.

(3) Apply effective suppression measures.

The investigation herein reported concerns the detection of fires and explosions. Its object is to furnish recommendations as to the best techniques for reliable and timely detection of all hazardous hydrogen-air fires and explosions, which can occur in closed and vented compartments, from sea level to space altitudes.

For reasons to follow, monitoring of ultraviolet or infrared radiant energy from the reaction zone offered the best promise for unequivocal, simple detection under all hazardous conditions. Therefore the more direct purpose of the investigation is to evaluate the scope and limitations, if any, of such methods, through evaluating the power radiated from flames and explosions which could occur under vehicle operating conditions.

It was necessary that our approach to this problem be fundamental rather than in the context of any immediately foreseeable vehicle or compartment design, so as not to restrict the applicability of conclusions reached. This implied for example:

(1) The ignition process itself should not be studied, because as indicated in Section 2, ignition is dependent upon type of ignition source*, time and intensity of ignition duration, catalytic activity of surfaces, flow conditions, geometry and other compartment design details in addition to the composition and pressure of the gas mixture involved. Ignition has not yet proved amenable to quantitative generalization.

---

* e.g. spark, arc discharge, small hot surface, large hot surface, hot gas jet

---

Manuscript released by authors December 1962 for publication as an ASD Technical Documentary Report.

(2) Certain structural environmental effects on flame and explosion properties cannot be considered in detail, such as compartment shape, irregularities, roughness, flame holding projections, or heat sinks. These are vehicle design factors and cannot be evaluated until compartment design is specified.

(3) Our conclusions should not be constrained by the state of development of detection instruments available now, but rather should consider the fundamental flame and explosion properties and the inherent nature of devices which can detect these properties.

(4) Suppression techniques per se are outside our scope, as these and their activators are independent of the detection process itself.

1.2 Problem and Approach

Accordingly the physical problem was defined as follows:

The source of hazard is a leak (or jet) of hydrogen from storage or transfer equipment, into a compartment containing an ignition source, at any altitude from sea level up to space. If the compartment is closed, the air within it is always at or near atmospheric pressure, and fires or explosions that occur will be initially at one atmosphere. If the compartment is vented to ambient, the pressure at the time of ignition will be between 1 atmosphere and zero depending upon altitude, and the question of the actual existence and intensity of flames and explosions arises as well as the variation with pressure of detectable properties.

Whether a fire or explosion occurs depends upon whether the leak is ignited as soon as it develops, or whether the hydrogen mixes freely with the compartment air and is ignited at some subsequent time. In the former case, a diffusion flame is formed at the leak which will persist as long as a supply of air is available at the leak site. In the latter case, an explosion wave can propagate through the gas mixture, and may leave a diffusion flame burning at the leak if the air supply is renewed (vented compartment), provided that the force of the explosion does not blow out the flame. A flame can also be reignited on surfaces heated by the preceding explosion.

Accordingly, in the experimental aspect of the program, attention was paid to diffusion flames and explosions at one atmosphere and below. Detonations were not investigated as existing data (See Section 2) indicated that under the conditions being considered, the transformation of an explosion (deflagration) into a detonation was improbable unless the intensity of the original ignition source was strong enough in itself to be structurally damaging (e.g. an incident shock wave).

At the outset of the program it was established from existing background information that the property we should examine as most suitable for detection was the emitted radiation from the reaction zone. For the H_2-air system this comprises principally the OH radiation in the ultraviolet and the water bands in the near infra-red.

Radiation can be detected at a distance from the reaction zone and burnt gases, and emitted radiation can be detected from any point in a solid angle viewed by a detector such as a photomultiplier tube.

In contrast other flame properties such as temperature, ionization,* or reaction product appearance, can be detected only when the reaction zone or burnt gases are in contact with the detector element, which requires anticipating all points of ignition, delaying detection until propagation brings the reaction to the detector, or using a multiplicity of detectors.

Detection by monitoring pressure rise was a priori unattractive, although a pressure wave is propagated from a flame or subsonic wave. The slow propagation velocity can, however, result in a dangerously long time lag for detection, especially in the case of explosions. Moreover pressure in a vented compartment is altitude dependent. Thus a pressure change would not signal the presence of a fire and the rate of pressure change would have to be utilized for detection.

These considerations of general detection techniques are amply discussed in reference 9.

1.3 Detailed Program

Based upon the foregoing, this investigation undertood to determine the following data:

(1) Absolute measurements of radiant power from hydrogen-air flames of varying sizes and fuel consumption rate as a function of pressure, with special attention to small flames and flames at their lower limits of stability, which are presumably limiting cases for detectability.

(2) Absolute measurements of radiant power and pressure rise from hydrogen-air explosions versus time from ignition, as functions of stoichiometry and initial pressure.

---

* Ionization can be in principle detected by absorption methods, but this is a "line-of-sight" rather than a "volume" detector, and so tends to the same drawbacks as the "point" detectors here mentioned. The same consideration applies to absorption detection of combustion products in the opitcal spectral region.

(3) Derived from the explosion measurements, a measure of the time interval between detection of the reaction and the attainment of a dangerous pressure level.

A review of the literature was made, Section 2 of this report, which qualitatively supported the selection of radiation properties for study, but which did not yield the absolute values of radiation versus reaction conditions needed for evaluation and design.

The required data was obtained by experiments which are discussed in subsequent sections.

2. BACKGROUND AND LITERATURE

2.1 General

A tremendous body of information is summarized in general reference works upon properties of flames[1, 2, 3], explosions[1, 5] and detonations[1, 5]. These general works contain extensive references to original and more detailed sources for the interested reader. A brief exposition of the effect upon ignition and flammability of gas composition, environmental conditions and ignition source is in reference (4). The availability of these works precludes the need for an exhaustive review here. Rather, the following paragraphs will be limited to a brief statement of those properties which especially pertain to the magnitude and detectability of flame and explosion phenomena.

2.2 Categories of Flame and Explosion Reactions

(1) Premixed Flames

A combustion wave will propagate through a flammable homogeneous fuel-oxidizer vapor mixture with a characteristic burning velocity, the value of which depends upon the fuel and oxidizer species (Fig. 1), their mixture ratio (Fig. 1), initial temperature (Fig. 2), and to some extent the pressure of the unburned gas. If the unburned gas is flowing from an orifice at some rate greater than the flame velocity and below a blow off velocity, a flame stationary in space will result, having a temperature and composition profile represented by Figure 3. Propagation is by heat and active particle transfer from the burned gases into the unburned gases, thus preheating the gas mixture, so that reactions occur at an increasing rate with temperature, until the fuel and oxidizer is spent and the gases leave the reaction zone.

(2) Diffusion Flames

A diffusion flame is formed when a jet of fuel issues into an oxidizing atmosphere. A reaction zone is established at the boundary between the fuel and oxidizer, products flow by diffusion away from the flame zone into both the fuel and the oxidizer, while fuel and oxidizer flow by diffusion into the reaction zone. Figure 4 is an idealized diagram of a diffusion flame, showing the change in composition across the flame front.

Certain characteristics distinguish the diffusion flame from the premixed flame. In the diffusion flame, the flame front is located at the point of highest temperature and where the fuel and oxidizer are in stoichiometric proportion. Location of this point is determined by diffusion of reactants rather than by gross stoichiometry, and the flame temperature in the reaction zone is thus essentially independent of gross stoichiometry. In the premixed flame, however, temperature in the flame zone is a function of stoichiometry, since either excess oxidizer or fuel acts as an inert diluent.

(3) Deflagrations and Detonations

When a stationary homogeneous fuel oxidizer mixture, within the flammability limits is ignited, a flame front, identical with the premixed flame cited above, will begin to propagate through the mixture (relative to the unburnt gas) with a velocity characteristic of the mixture, identical with the burning velocity previously mentioned. If the mixture is contained in a closed volume*, the expansion of the burned gas will pressurize the volume, including the unburned gas, and weak, sonic pressure waves will propagate into the unburned gas. Owing to this pressurization, and distortion and turbulence in the flame front due to wall friction, both the propagation velocity of the flame front and the intensity of the pressure waves increase. These waves can develop in time into a shock wave which under suitable conditions can become sufficiently intense to initiate reaction directly in its wake where the energy of reaction sustains the shock. A detonation thus can develop from a deflagration under proper conditions and with a suitable induction distance. A detonation can of course develop with little induction if the original ignition of the flammable mixture is sufficiently intense, such as by another incident shock wave, caused by very strong sparks or explosions. Two main differences between a detonation and high order detonation are in the velocity of propagation and the total pressure rise. For a stoichiometric hydrogen-air detonation, under normal circumstances, a velocity of 2200 meters/sec[18] and a pressure

* or if ignited at the closed end of a tube open at one end.

ratio of 16[1] are obtained. The values for deflagrations are variable, and can approach those of a detonation. Peak pressures, in fact, can be much higher in deflagrations than in detonations. *

(4) Transition from Deflagrations to Detonations

In the environments under consideration in this program, the development of an H_2-air deflagration wave into a detonations is considered unlikely. Experiments at RMD[6] in a 54.6 cm diameter by 9.85 meter long explosion tube showed that H_2-air did not detonate at one atmosphere, unless the air was artificially enriched from an oxygen concentration of 21% to one of 29%. Comparison experiments in a 3.8 cm diameter by 9.15 meter tube produced H_2-air detonations at one atmosphere only when the air was enriched to 23% oxygen, or with normal air, when the initial pressure was 6 atmospheres. This data is interpreted to mean that at one atmosphere and with normal air, the induction distance is greater than 9 meters, even though 18 joules and 6 joules of spark energy were used for ignition in the large and small tube respectively.

Induction distance increases at reduced pressure (Table I, p. increases with increasing temperature (Table II, p. 48), increases with increasing tube diameter (Table III, p. 49) and decreases with tube surface roughness.[5]

We did not find data in the literature on the development of detonations in hydrogen-air mixtures which could apply to the environments of interest here. Our statement above, that detonations were not liable to be encountered, is based upon the general trends and the data cited. It must at the same time be remembered that owing to the geometry and size dependence of induction distance, a detonation hazard might exist for some (unspecified) compartment designs.

(5) Fuel Sprays, or Mists

A jet of liquid fuel penetrating into gaseous oxidizer can give rise to a spray of droplets. Droplet combustion has been treated by several authors.[3, 8] In general it is not possible to predict propagation in droplet arrays since the size distribution is highly dependent on atomization conditions, which thus govern droplet evaporation rate and flame propagation. However a

---

* As reported in Ref. (6), deflagrations of hydrocarbon with enriched air in a 54.6 cm diam. x 9.85 meter long closed tube produced pressure ratios of about 65, and hydrogen with enriched air produced pressure ratios up to 81. Note that the "air" contained more than 21% O_2; with "air" at 21% O_2, these over-pressures did not occur but might, however, be found for certain other geometries.

summarizing statement[3] suggests that for fine droplets (less then 10 microns for hydrocarbons) a mist of fuel in air shows flammability limits and propagation rates representative of premixed fuel-air systems. For larger droplets, the combustion becomes more and more a series of diffusion flames around individual droplets which propagate from droplet to droplet.

2.3 Hydrogen-Air Premixed Flames

Premixed flame systems are characterized by ignition energies, flammability limits, burning velocities, quenching distances and minimum flame sizes for propagation.

(1) Ignition Energies

Since this program is concerned with properties of flames and explosions after ignition takes place, it is appropriate to review only superficially the ignition process, which is in fact very dependent upon experimental conditions as will be indicated. Information sources are indicated, however, for the interested reader.

Lewis and von Elbe[1] have an extensive summary of data on ignition by sparks, and to a lesser extent by hot surfaces and hot wires.

Spark Ignition

Data for hydrogen air and hydrocarbons are presented in terms of minimum ignition energies and quenching distances versus mixture ratio and pressure. For H_2-air, the minimum energy is 0.02 millijoules at 1 atmosphere and is lowest for a near stoichiometric mixture. The quenching distance is 0.06 cm. The minimum energies and quenching diameters increase greatly as the rich and lean limit mixtures are approached.

For comparison, the minimum ignition energy at 1 atmosphere for propane-air is 0.25 millijoules and the quenching distance is 0.2 cm. Thus the hydrogen-air system is easily ignited and flames are more stable than nearly any other conceivable fuel-air system.

Ignition energy and quenching distance increase as pressure decreases. As a rough guideline ignition energy is proportional to $1/p2$ (p being pressure) whereas quenching distance and minimum flame dimensions are proportional to $1/p$.

Ignition by Hot Surfaces

Ignition by hot surfaces (except for self ignition temperature (SIT) measurements, see below) shows the same inverse energy-pressure relation as spark ignition, but specific data for H_2-air is lacking.

Hot surface ignition (whether wire or extended surface) is highly sensitive to ignition conditions. Owing to competition between purely thermal diffusion loss from the surface to the reactant system and the rate at which the initial volume of reactant is heated to the reaction point, there is a surface temperature-time relationship to consider. A hotter surface requires a briefer heating time to ignition, and by virtue of the lower total heat loss from the surface for brief heating periods, the total time-integrated energy for hot surface ignition decreases with increasing surface temperature and briefer induction periods.

For example it is reported that in a 20% (slightly lean) H_2-air mixture, a 0.0433 mm diameter nichrome wire heated electrically, required a total energy of about 20 millijoules to ignite the mixture in 10 milliseconds and about 38 millijoules when a 50 millisecond heating period was required. (1)

The time-energy values were similar for 11% methane-air mixture even though hydrogen mixtures have a much lower "ignition energy". The total energies for both fuel mixtures decreased with increasing wire diameter. The similarity for methane and hydrogen, and the variation with wire diameter are consistent with the dependence of hot surface ignition upon diffusive heat loss. In the former case, the lower thermal conductivity of methane resulted in a higher thermal gradient from the wire to the gas so that a higher fraction of the energy from the wire was concentrated in a hot volume surrounding it. In the latter, increased heat capacity of the heavier wire and lower surface to volume ratio maintained the wire at a higher temperature for a given energy input, and thus more effectively heated the surrounding gas volume.

Wolfhard(10) discusses other aspects of low pressure ignition, amplifying on the drastic increase of ignition energy at low pressures.

The nature of a hot surface affects ignition temperature, an extreme example being pointed out in Figure 100 of reference (3), where a platinum surface had to be at a temperature at least 130°C higher than a nickel surface to ignite a natural gas-air mixture. The platinum gave rise to a catalized surface reaction where a large fraction of the heat of reaction was transferred back to the platinum rather than to the reactant gases, decreasing the net flow of energy into the gas mixture to be ignited.

Further complexity in the ignition of a reactant system is indicated in Wolfhard[10] and the review by Wigg[11] on the increase of ignition energy with flow velocity and on the increase of hot surface ignition temperature with flow velocity in a flowing ignitable mixture (Figs. 5 and 6).

Barnett and Hibbard[3] is recommended also for an exposition of the complex effects of flow, temperature, surface and other variables upon ignition. Most of the data is for hydrocarbon systems; some H_2-air data is found. The qualitative trends, common to ignitable systems in general are however of real interest.

A special case of ignition by hot surfaces is the SIT (self ignition temperature) measurement where a volume of mixture is heated uniformly by slowly heating the containing vessel[1, 3] until ignition takes place. Figure 7 shows the SIT-pressure dependence of ignition for stoichiometric H_2-O_2. Of interest is the region between 4 mm Hg and 350 mm Hg, where the SIT decreases with decreasing pressure, owing to the change in the balance of competing reaction steps, including wall deactivation of chain carriers, in the H_2-O_2 reaction. Thus, despite the generalities mentioned above concerning the increasing difficulty of igniting low pressure mixtures, the details of the reaction as well as environment and geometry must be considered for each case.

Hot Jet Ignition

Another mode of ignition occurs when a jet of hot air issues into a fuel.[12] For the case of a hot air jet into H_2 at 1 atmosphere, the critical hot gas ignition temperature is 670°C.

Table IV (p. 49) compares ignition temperatures of various fuels with air as determined by different techniques.

(2) Flammability Limits

The flammability limits of explosive mixtures are not theoretically calculable but are measured by standardized techniques[13]. For H_2-air, at 1 atmosphere and room temperature, the measured limits are:

	Limits, % H_2 by volume	
	Lower	Higher
Upward propagation	4.1	74
Horizontal propagation	6.0	--
Downward propagation	9.0	74

The 4.1% lower limit refers to partial combustion with cellular flame structure and therefore cannot be taken as a true limit.

The limits widen with increasing temperature. For downward propagation, the lower limit decreases linearly to 6.3% at 400°C, and the higher increases linearly to 81.5% at 400°C. The corresponding narrowing of limits with reduced temperature is expected, but not documented.

The effect of reduced pressure is not well established. Reference (13) indicates an increase of the lower limit from 9.35 to 10.6% at one half atmosphere, and "a small lowering of the lower limit between 500 and 200 mm followed by a rapid rise in the lower limit between 200 and 100 mm". In other experiments reviewed in reference (13), no mixture propagated flame below [illegible] mm Hg. It is obvious from other data that 50 mm Hg cannot represent a lower propagation limit for H_2-air, but rather results, in the data quoted, from the increase of quenching diameter with lower pressure (See Section 2.3(3)) until it coincides with the dimensions of the test apparatus. For all practical purposes it can be assumed that no low pressure limit for flame propagation exists, for sufficiently large vessels, and that under ideal conditions the limits of inflammability are little affected by decreasing the pressure below 1 atmosphere.

(3) Quenching Distances

The quenching distance of a premixed flame (e.g., the minimum diameter tube through which it will propagate) is of significance in propagation of a flame through a tube between compartments, and its dependence on the pressure affects the flammability limits of a combustible mixture in real situations (see Flammability Limits, Section (2.3(2)).

Extensive discussions are found in references (1), (3) and (10).

The salient points are that the quenching distance varies with the reactants (c.f. H_2-air and propane air, Section 2.3(1), Spark Ignition), mixture ratio, (being lowest for near stoichiometric mixtures) and varies very nearly as 1/pressure.

For H_2-air, the quenching distance is .06 cm (parallel plates) at 1 atmosphere, stoichiometric, and increases to 0.3 cm at the limit (see Fig. 8, which shows quenching distance as a function of stoichiometry and pressure). For cylinders, the quenching diameter is about 0.7 times the parallel plate quenching distance[10, 14]. Although not directly documented, it is expected that quenching distances will decrease with increasing temperature.

A significant implication of the pressure dependence of quenching distance is that the minimum burner diameter to sustain a premixed flame varies as 1/p. In fact one means of determining the pressure dependence of quenching is from a flame stability plot such as Figure 9, which shows stable regimes for acetylene-air flames. Each region is bounded by the blow-off limit above, and the flash back limit below; these limits converge to define a minimum flame at a given pressure.

An important consequence of the pressure effect on quenching diameter is that as pressure decreases, the minimum mass flow rate to maintain a stable flame increases since cross section area of the burner increases as the square of the diameter, while linear velocity stays approximately constant. This relationship is shown in Figure 10, which is replotted from the data in Figure 9.

The form of the relationship shown for acetylene-air is common to all gaseous flame systems. While a stability plot for H_2-air is not available, the quantitative behavior can be taken to be the same as that in Figure 10 since the quenching distance for acetylene-air is nearly the same as H_2-air at one atmosphere.

(4) Burning Velocities

The burning velocities of the $H_2/N_2/O_2$ system are plotted in Figure 1 and are shown to be sensitive to composition (oxygen enrichment) and stoichiometry.

A temperature sensitivity can also be expected as indicated in Figure 2. This can be of importance where a cooled flammable mixture is formed by the evaporation of liquid hydrogen into air,[15] or conversely where a flammable mixture is heated by the compartment environment and then ignited. The effect of temperature upon H_2-air burning velocity has not, however, been measured but could be of value in assessing hazards involving liquid hydrogen.

There has been some uncertainty regarding the effect of pressure on burning velocity[2, 3]. In general it appears that for hot flames (e. g. oxygen-supported) burning velocity is independent of pressure, and for cooler air-supported flames, burning velocity is nearly independent of pressure, showing usually a slight increase as pressure is reduced. The above statements assume that burner diameters or propagation channels are large enough to preclude quenching effects. (See also Flammability Limits, Section 2. 3(2).)

2.4 Hydrogen-Air Diffusion Flames

The diffusion flame is of particular interest because a jet of hydrogen issuing into an air-containing compartment will upon ignition form a diffusion flame. Unfortunately diffusion flames have been studied fundamentally to a much lesser extent than premixed flames.

If the compartment is closed, the flame will gradually consume the oxygen and diminish in intensity as it is vitiated, eventually extinguishing. This vitiation produces changes in flame shape, size, temperature, radiation, etc. and is a subject that has been rather extensively investigated[16]. However, vitiated combustion does not appear to be of interest in the fire-detection context, since detection should be accomplished promptly after ignition, before vitiation has become significant. A possible exception is a leak which results in a lean explosive mixture which is ignited, and after the explosion is complete, a flame remains at the leak burning in the residual oxygen. The properties of vitiated H_2-air flames have not been reported.

The size of a diffusion flame depends upon the diameter of the fuel jet and its velocity. Figure 11 shows the variation of flame length, in the laminar and turbulent regions, as a function of fuel velocity at constant pressure from a given port diameter. In the laminar region flame height is proportional to flow rate. Under turbulent conditions, flame height is constant until the blow-off limit is reached.

In the laminar region for fuel flowing into a concentric stream of excess air, the flame height is expressed approximately* by[2]:

$$y = \frac{V}{2\,D}$$

where: y = flame height
V = volumetric flow rate
D = diffusion coefficient of air into fuel

Interesting implications are:

(1) For the same mass flow rate and the same burner, flame size is independent of pressure because V and D both vary inversely with pressure.

---

* extremely simplified, see references for more complete analysis of flame behavior.

(2) At constant pressure and mass flow, flame height is independent of fuel-port diameter, since doubling the diameter results in 1/4 the linear velocity, which is compensated by the time for diffusion, proportional to the square of the diffusion path length.

Diffusion flames have pressure-flow stability conditions as do premixed flames. Although these limits have not been determined for H_2-air, data on other systems illustrate the nature of pressure, flow, and burner diameter dependence, discussed more fully in reference[10]. Figure 12 shows the flame lift-off limits for methane-air as functions of flow and burner diameter. These data are replotted in Figure 13 to show the minimum flow and corresponding burner diameter for stable flames at reduced pressures. Here again the burner diameter and mass flow rates vary as 1/p.

At reduced pressures diffusion flames begin to approximate premixed flames in structure[2], owing to the increased diffusion rate coupled with the usual 1/p thickening of the reaction zone. This seems to occur at pressures below 60 mm Hg.

The effect of buoyancy of the burned gas was obviated in other experiments[10] where methane flowed downward from a sintered sphere to meet an upward flow of air. Although at the lower pressures, methane flame stability is very sensitive to blow-off, it is evident that diffusion flames can exist to pressures below 20 mm Hg under favorable conditions (Fig. 14).

H_2 flames have much smaller quenching distances than methane flames and reaction rates are greatly increased. Thus hydrogen-air diffusion flames may well exist to below 1 mm Hg. At such pressures the differences between premixed and diffusion flames become, however, somewhat academic.

2.5 Flames - General Summary

The relative rates of heat generation in a flame and heat loss to the surroundings has notable effects. As pressure is reduced, the reaction zone thickens so that the volumetric heat release rate is reduced, while heat loss to the surrounding remains high because the flame surface remains nearly constant, and in the case of heat loss to a tube or burner orifice the heat transfer area remains constant. The proportionally greater heat loss at lower pressures is seen to affect quenching diameter, and to affect the minimum flame or burner size required to prevent extinction.

These effects are accompanied by lowering of flame temperature with expected reduction in stability, propagation velocity, and general radiation levels. These are known to occur qualitatively, but for H_2-air flames

quantitative information on these effects is generally lacking. Thus at greatly reduced pressure there is some uncertainty as to whether a flame can exist that is so weak as to produce no discernible evidence of its existence other than local heating of the environment.

On the other hand this problem may be academic, as in practice, flames at their low pressure limit are tenuous and may be extinguished by a slight further reduction in pressure, a slight increase or decrease in fuel flow velocity, a slight increase in heat abstraction, or a low velocity transverse air current or gust. Some treatment of this latter is found in reference (17), a study of flame persistence vs altitude on diffusion flames over a pool of liquid hydrocarbon burning in air. The quiescent flame had an apparent extinction limit of 70,000 ft (30 mm Hg). At an altitude of 40,000 feet, a transverse air current of only a few feet per second would sweep away the flame. At lower altitudes, "flame holding" devices greatly increased the transverse air flow for extinction, but at increasing altitudes, their effectiveness decreased, and the flames were easily extinguished.

2.6 Hydrogen-Air Detonations

Hydrogen-air mixtures can support detonations if a detonation is established by sufficiently intense ignition. The chances, however, of a detonation developing from a deflagration depend entirely on geometry and pressure factors (See section 2.2(4), Transition from Explosion to Detonation), and is not expected in the system we are considering. For completeness, however, we indicate below the nature of information available on the H_2-air system.

The lean and rich limiting mixtures (at 1 atmosphere initial pressure) that will propagate a detonation are 18.3% H_2 and 59% H_2 in air. The detonation velocity varies from about 1500 m/s to about 2100 m/s near the lean and rich limits respectively[1, 5]. The pressure ratio across the detonation front is 16.25 (initial pressure, 1 atm)[18]. The final temperature of the reactants is 2840°K[1].

H_2-air detonations propagate through tubes less than 10 mm diameter[5]. The above velocities were measured in tubes 10-20 mm diameter. Increase of tube diameter broadens the detonation limits owing to reduced energy losses at the walls. For a 305 mm tube, for example, the lower and upper limits became 15% H_2 and 63.5% H_2[5].

Detonation limits measured in rough-walled pipe are wider than for smooth-walled pipe[5]. Numerical data on limits in rough-walled pipes are not given.

Data on detonation limits for sub-atmospheric pressure are limited. Some data of Gordon, Mooradian and Harper indicates the lower limit is constant at 15% H_2 down to about 0.7 atm, rises to about 16% H_2 at about 0.2 atm, and thereafter increases very rapidly with further reduction in pressure[19]. A definite low pressure limit for detonations was not established but the data suggests that one may exist between 0.1 and 0.2 atmospheres. The disparity between the 15% lower limit there reported and the 18.3% limit usually quoted is probably owed to the different experimental conditions.

2.7 Radiation in the H_2-Air System

The two prominent spectral features in the H_2-air reaction are the radiation bands in the ultraviolet due to the excited OH radical and the water vibration-rotation bands in the infrared. A weak continuum in the visible disappears as pressure is reduced, and is not important with regard to detection of H_2-air flames and explosions. In H_2-O_2 flames, the O_2 Schmann-Runge structure, and higher-order OH rotation-vibration bands in the IR are evident, but are of no significance in the H_2-air flame[20].

2.8 The Ultraviolet OH Bands

The OH radiation in the UV is a well-documented feature in H_2-O_2 and H_2-air flames[2, 20]. A complete description of the complex band structures of the H_2-O_2 flame is given by Dieke and Crosswhite[21]. For our purposes it is sufficient to note that the most intense radiation in H_2-O_2 and H_2-air is in the (0, 0) band (head at 3064 A) followed in intensity by the (1, 0) band at 2811 A, (2, 1) at 2875 A, and (3, 2) at 2945 A. These bands appear also in other flames of H- and O- containing reactants (H_2-N_2O), hydrocarbon-air, H_2H_4-NO, etc)[2, 20].

The OH radical exists in the reaction zone as a carrier in the chain branching reactions[1]

$$H + O_2 = OH + O$$

$$O + H_2 = OH + H,$$

and in the reaction products through the dissociation equilibrium

$$H_2O = 1/2\ H_2 + OH$$

In the H_2-air flames, the OH concentrations are approximately those expected at thermal equilibrium for stoichiometric and fuel-lean flames at the adiabatic reaction temperature. Kaskan[22, 23], in experiments with

H_2-O_2-N_2 premixed flames in which the flames could be cooled, reports however that for cooled flames, especially H_2 rich, where thermal OH concentration is extremely small, the measured OH concentration (by absorption) exceeded the calculated equilibrium concentration by factors of up to 5000.

OH radiation from the hydrogen-air reaction zone at atmospheric pressure is not greater than from the burnt gases following the reaction zone, suggesting that the radiation is mainly thermal in origin. In contrast, the hydrocarbon-air reaction shows OH radiation from the reaction zone that is greatly enhanced over that in the burnt gases, and greatly in excess of that from the H_2-air reaction zone[2, 20]. This is attributed to chemiluminescence in the hydrocarbon case[2, 20].

2.8.1 Relevance of Data to Detection of Flames and Explosions

In general the questions of concern to detection of hydrogen-air flames are:

Intensity of UV radiation as a function of flame size (dimension and H_2 consumption rate)
Effect of pressure on UV radiation
Effect of flame temperature on UV radiation
Rate of appearance of UV radiation after ignition

The H_2-O_2 reaction, with and without diluent gases (N_2, He, Ar, Ne), has been extensively studied as a reaction of fundamental importance, representing a "simple" chain branching system. In such studies, OH has frequently been measured in emission or in absorption, because of its accessibility as a spectral feature and because of the important role played by this radical in the reaction mechanism.

Information gained in such studies is indicated below, and later on mention will be made of what conclusions can or cannot be drawn from them with regard to our objective.

2.8.2 Detectability of OH

Schott and Kinsey measured OH concentration (absorption) in shock tube studies of the H_2-O_2 reaction induction time[25]. OH concentrations were measured of 10^{14} molecules/cc (equal to about 0.002% at 1 atmosphere or about 0.05% at 30 mm Hg). Further, the OH concentrations (ground state) reached peak values rapidly after shock wave ignition of a weak mixture. For example, after passage of a 1600°C shock through 2% O_2-4%H_2-94%Ar, an OH concentration of 10^{15} molecules/cc was

reached in 18 μs. These authors found an initial excess (compared to equilibrium) of OH and H concentrations similar to that reported by Bulewicz and Sugden for flame gases[26], which leads them to conclude that the reaction mechanism in detonations was the same as in flames, and characteristic of the branched-chain H_2-O_2 reaction in general, and not of a detonation only.

Kaskan[24] studied the probable excitation mechanisms for OH* in the H_2-O_2-N_2 system. In these studies also, absorption measurements detected OH ground state concentrations at as low as 10^{14} molecules/cc (0.005% at 1 atm). He also reports emission from the excited species OH* which he relates to the OH ground state concentration. According to this data, ground state concentrations as low as the 10^{14} to 10^{15} mol/cc range can give rise to measurable OH* emission in the (0, 0) band, for pressures between 0.15 and 1.0 atmospheres. Further, he reported that the intensity of the (0, 0) emission, per cm of optical path, was proportional to $(OH)^3$, and that the proportionality constant increased at reduced pressure (i.e. at a lower total pressure, a given OH gound state concentration yielded a more intense emission).

Three implications are of interest in Kaskan's data

1) Low concentrations of OH are detectable
2) Low pressure may enhance emission in the (0, 0) band
3) As flame temperature is reduced (by heat abstraction) below theoretical adiabatic for the mixture being reacted, OH concentration remains at levels substantially higher than equilibrium.

There is no need to review here the kinetics aspects of these papers.

2.8.3 Timeliness of Detecting OH

Norrish and Porter[27] studied the rate of change of OH concentration in H_2-O_2 explosions at low pressures, using their flash photolysis technique. Relative OH concentrations were measured by absorption. Typical results found were, that for $2H_2 + O_2$, and total pressures from 7.5 to 15 mm Hg before ignition, OH concentration was significant in less than 1ms, and peaked (prior to the onset of OH-consuming reactions) at under 2ms. The effect of O_2/H_2 ratio is covered, and although the persistence of OH varies, in all cases peak concentrations appeared in about 1ms. Their results are interpreted in terms of OH disappearance kinetics; this is not pertinent to the detection problem.

Minkoff, Everett, and Broida[28] observed OH in absorption at 3090A during the propagation of low-pressure explosions of 1.6H_2 + O_2 in a 2 cm x 30 cm combustion tube. They were concerned primarily with reactions in the burned gas, so that the development phase of the explosions was not well documented. They refer, however, to the OH intensity (in absorption) rising steeply for 1ms. Flame propagation over the 30 cm tube length took 0.7ms at an initial pressure of 15 cm Hg.

Reference is again made to Schott and Kinsey[25] who indicated a rapid rise in OH concentration (18μs) after initiation of the H_2-O_2 reaction behind a shock wave.

2.8.4 Effect of Pressure on Radiant Intensity

From the literature it is not clear in what manner, for a given size flame (i.e. H_2 consumption rate), the radiant intensity from the reaction should vary in an optically thin system such as a flame reaction zone. For the case of collision activation of the excited state, and where there is thermodynamic equilibrium between collision activation and the inverse collision deactivation, reduced pressure should deplete the excited population and emission should decrease. This is due to reduction in collision frequency with pressure which however does not reduce the time for radiative decay (lifetime OH* is about 10^{-6} sec)[2]. However the reaction zone in flames generally is not in thermodynamic equilibrium, and the extent of departure from equilibrium and its variation with pressure is not, in general, explicitly known[2, 20].

The data of Kaskan[23, 24], Sugden[26], and Gaydon and Wolfhard[2] on flames, and that of Schott and Kinsey[25], and Minkoff et al[28] on explosions do show that in the reaction zone, the H, O, and OH concentrations are in excess of equilibrium and that the degree of excess is highly dependent upon reaction conditions. However hydrogen flames seem to be much less subject to excess population than hydrocarbon flames. Thus it is not possible to be sure from existing literature what the effect of pressure would be.

One set of experimental results, thos of Kaskan previously mentioned, does suggest that emission intensity can be enhanced at reduced pressures as low as 0.15 atm.

2.8.5 Summary of Background Information on OH Emission

1. The OH radical appears in substantial concentration in the initial phases of the H_2-air reaction.

2. The reaction mechanism (and thus the role and appearance of OH) is the same for flames, high order deflagrations, and detonations.

3. The OH radiation in the UV is sufficiently intense to be of interest as a detectable property.

4. Concentrations of OH (ground state) as low as 10^{14} molecules/cc can be detected by absorption. This is equivalent to .002% at 1 atm, and .05% at 30 mm Hg. Concentrations of about 10^{15} molecules/cc result in detectable emission under normal conditions of flame temperature.

5. OH concentrations greater than equilibrium can occur in flames, thus analytical calculations of equilibrium concentrations would give an unreal (pessimistic) view of limits of UV detectability.

6. Data on radiant intensity of OH emission versus flame size, flow, pressure etc. for H_2-air flames is lacking.

7. Data on radiant intensity of OH emission versus time for H_2-air explosions is lacking.

8. The pressure dependence of radiant intensity of OH emission in the H_2-air system is uncertain for subatmospheric conditions.

2.9 The Infrared Water Bands

There is an extensive system of water bands extending from the near infrared into the microwave region. The emission bands centering at 1.4, 1.87, and 2.7 microns are of most interest for detection because of their relative intensity[20, 29, 30] and because at the hydrogen-air flame temperature, about 2300°K, this is also the region of maximum spectral intensity (Planck radiation law).

A large body of information exists on water band absorption[31] arising out of studies of the atmosphere, and some data on water vapor emissivities developed largely with regard to industrial heat transfer applications[32]. Application of these latter data, and more recent data on premixed hydrogen-oxygen flames[33, 34, 35], in relation to flame and explosion detection requires a knowledge of the temperature and concentration fields in and around the flame. Estimation of these for the hydrogen-air system can only be approximate, and is not accurate enough for the evaluation of radiant intensity at limiting conditions needed for assessing detection techniques.

The effect of reduced pressure on the emissivities of hydrocarbon-oxygen flames in the region of 4.2μ to 4.7μ, which includes a CO_2 band, has been measured[34] and shows a lowering of emissivity with pressure (1.00 at 760 mm, .8 at 203 mm, and .4 to .5 at 40.5 mm: path length 12.7 cm). This is consistent with the expected thermal nature of the water band emission, and although the spectral region 1.4 to 3 is not covered, a similar pressure dependence is to be expected.

With regard to explosions, no experimental data has been found relating the time rate of increase of IR emission in the early stages of the hydrogen-air reaction. Since, however, water is a major reaction product, it is reasonable to expect that emission should rise promptly.

From the available information it appears that IR emission has reasonable potential as a detectable property, and in fact commercial detection systems are based upon IR emission[9].

However, the seriousness of the pressure dependence of radiant intensity, and the quantitative relationship between emission and rate of rise of emission, and flame and explosion properties, need to be determined.

2.10 Ionization

The ionization level to be expected in H_2-air flames is too low or too variable to be attractive for detection. Our own previous measurements on ionization in the H_2-O_2 flame[36] and those of others[2] lead us to an estimated ionization level of about 10^6 ions/cc for the stoichiometric H_2-air flame. These values apply to flames from highly purified (electrolytic) hydrogen; these ionization levels are so low that in practical cases the ionization is dominated by impurities such as trace quantities, parts per million, of hydrocarbon or inorganic salts. Therefore the ionization levels in H_2-air flames would vary according to the extent of fortuitous contamination, thereby introducing unreliability.

3. EXPERIMENTAL PROCEDURE AND INSTRUMENTATION

3.1 Glass Vessel

The initial experiments on hydrogen-air diffusion flames were made in a pyrex glass vessel, Figure 15, having several ports of various sizes to which burners, electrodes, detectors, and exhaust lines were connected.

The pressure in the vessel was controlled by adjusting the exhaust valve to achieve an exhaust rate which would produce the desired pressure for a given flow of gases (H_2 and Air) introduced into the vessel.

The amount of air introduced into the chamber through the opening below the burner was maintained at a level large enough to react all the hydrogen. This was achieved by reducing the air to an amount where the radiant intensity was slightly reduced for a fixed hydrogen flow rate*, and then increasing the air flow rate to twice this value. By using this excess amount of air and considering the flow pattern in the vertical system, complete combustion was assumed to have been achieved.

The gases were ignited at low pressures, 20-30 mm Hg, by high voltage electrodes, which produced an arc discharge at the mouth of the burner.

The chamber pressure and photomultiplier current were recorded simultaneously on an X-Y recorder. The pressure transducer was of the strain gage variety giving continuous pressure readings. The photomultiplier current was measured as a voltage drop through the internal impedance of the X-Y recorder.

After ignition, the radiation versus pressure recording was made by gradually increasing the pressure to one atmosphere and then decreasing the pressure until the flame blew off at approximately 15 mm Hg.

This pressure cycle was accomplished over a period of approximately 15 minutes for large flow rates (560 cc/min and greater) and up to 25 minutes for smaller flow rates. These low rates of pressure change were necessary to maintain a stable fuel flow condition, owing to the relatively large fuel line capacity. A rapid increase in chamber pressure would compress the gas in the fuel line and decrease the flow; an increase in flow rate would occur for rapid decrease in chamber pressure.

The radiation measurements were made in the ultraviolet region using an RCA Type 1P28 photomultiplier and a Corning Type 7-54 filter. This photomultiplier filter combination covered the spectral region from 2200 to 4000A with a maximum, and approximately flat, sensitivity between 2600 and 3600A, which includes the major OH emission bands.

The diffusion flame burners used in the flame experiments were simple cylinders made from standard stainless steel tubings. A burner was of two part construction; the body of the burner consisted of two concentric

---

* This reduction in light intensity occurred at air/hydrogen ratio of about 3.5, as compared to the 2.5 air/hydrogen ratio for stoichiometry.

cylinders, (5/8" O. D. and 3/8" O. D.), the burner cylinder extending well beyond the outer and terminating as a flare; the burner tips were tubing sections 1/8", 3/8", 3/4" O. D. flared at one end and machined flat at the other. The burner tips were connected to the body of the burner with a full-flared union. The burner was introduced into the chamber through a rubber stopper and always positioned with the mouth of the burner opposite the center of the detector(s).

A series of measurements was made to determine the effect of heat abstraction from a flame to the burner (flame holder) on radiation. This was accomplished by monitoring the temperature of the burner tip with a thermocouple. The thermocouple e. m. f. and the photomultiplier current were recorded simultaneously on the X-Y recorder. The experiments for these measurements were run only at one atmosphere pressure.

3. 2 Metal Chamber

A large metal chamber was designed and constructed specifically for these studies, Fig. 16. This chamber allowed flexibility in operating conditions and was used for additional hydrogen-air flame studies and an extensive series of experiments on hydrogen-air explosions.

3. 2. 1 Flames

Additional UV radiation versus pressure measurements (see Fig. 17) were made on hydrogen-air diffusion flames using a procedure and instrumentation identical to that used for the glass vessel except for the distance from the flame to the photomultiplier. These measurements were made to check the measurements made in the smaller glass vessel where the distance was relatively small and the field of view possibly restricted for low pressure flames. These limitations can produce errors due to the inverse square-law for radiation and the increase in the size of the flame at low pressure (discussed in section 4. 1).

The radiation versus pressure measurements were extended in the metal chamber to include the 2. 7μ water band in the infrared, using a Mullard Type 61SV Pbs cell and a band-pass filter made from two NOTS filters (471 and 726) having sharp cut-offs at a half width of 2. 2 to 2. 75μ.

The radiation at the IR detector was chopped at 900 cps and the resulting output was condenser-coupled to a peak-to-peak voltmeter. This system was calibrated with a black-body.

In order to extend the flame radiation measurements to very small flow rates two special burner tips were fabricated, one of glass and one

of stainless steel, both having bore diameters of 1 mm. The burners were made of different materials to provide information about the effect of burner material on radiant intensity caused by heat abstraction from the flame.

Finally, a series of ultraviolet and infrared spectra were taken of the hydrogen-air diffusion flame using a Perkin-Elmer 12-C monochromator.

These spectra were taken for a fixed fuel flow rate on a 1.75 cm burner at several ambient pressures, 30, 60, 100, 300, 760 mm Hg) to get qualitative information about the band structure and its distribution with pressure. The transmission path length from flame to monochromator was 150 cm for both the IR and UV spectra, and a calculation of the atmospheric absorption over this path showed no absorption in the UV and a maximum of 5% absorption in the IR.

3.2.2 Explosions

The metal chamber was instrumented as follows (see also Fig. 18) for measurements of radiation and pressure versus time for hydrogen-air explosions:

(a) A pair of aneroid pressure gages for measuring the initial charging pressures, to an accuracy of 1 mm Hg at all pressures.

(b) Two piezo-crystal transducers, one located 30 cm from the ignition source and the other 150 cm. The upper frequency response of the crystal transducers is about 150,000 cps and the static decay time is about 4 sec. The output of the crystals were displayed on two channels of a four channel oscilloscope, calibrated to permit pressure levels to be read from the film record.

(c) The ultraviolet detector was the same as that used for the flame measurements and was mounted 150 cm from the ignition source. The output of the photomultiplier was displayed on one channel of the four-beam oscilloscope, and calibrated for irradiance to be read as a displacement on the film record.

(d) The infrared detector, filter, and chopper were the same as that used for the flame measurements, and was mounted 38 cm from the ignition source. The radiation was again a chopped input to the detector and this was displayed on one channel of the four-beam oscilloscope, the peak to peak magnitude of which was calibrated for irradiance at the detector.

(e) The recording system was a 35 mm drum camera (see Fig. 19 for typical records) focussed on the oscilloscope. One millisecond timing marks were recorded on all information channels and the total film strip records were 50 cm long, or approximately 250 millisecond recording time.

(f) The ignition system consisted of a high voltage power supply, an electrolytic capacitor, and a surface gap spark plug located at the center of one metal "cross", Figure 18. The ignition energy was four joules for all explosion experiments.

The explosion experiments were conducted at a wide range of mixture ratios and for three initial pressures; 100, 300 and 760 mm Hg. The desired combustible gas mixture was attained by first evacuating the chamber and charging the vessel to the desired ratio by partial pressure values measured on the aneroid pressure gages*. The aneroid pressure gages also provided a quantitative determination of complete combustion by accurate measurement of pre-ignition and post-ignition pressures.

Several ionization measurements were made on hydrogen-air explosions using a probe configuration consisting of a thin metal rod (wire) for the positive electrode located at the geometric center of a half cylinder which was the negative electrode. The ionization current was measured as a voltage drop at the input to the oscilloscope and recorded on one of the channels formerly used for pressure measurements.

4. EXPERIMENTAL RESULTS - FLAMES

4.1 Pressure Dependence of Ultraviolet (OH) Radiation

Two sets of similar data are presented in Figs. 20 and 21. The data in Fig. 20 were obtained in the small glass vessel, and the data in Fig. 21 obtained at a later date in the large metal vessel when it had been assembled.

The conditions for the two sets of measurements were identical except for the distance from burner to detector which was 15 cm for the glass system and 150 cm for the metal system. This distance is measured from the center of the burner to the entrance aperture at the photomultiplier.

---

* The filling procedure used was shown to produce a homogeneous mixture by comparing film-strip records of these explosion runs with those where the vessel was charged by flowing properly metered streams of H_2 and air simultaneously until the desired pressure was reached.

In Figs. 20 and 21 the values for radiant intensity at one atmosphere are the same within the experimental error for both systems while the values at 60 mm Hg are greater for the glass vessel measurements by approximately 30%. A possible explanation for this difference is based on an error introduced at low pressures in the glass vessel where the distance from burner (flame) to detector is small compared to the diameter of the flame. At one atmosphere the diameter of the flame is approximately the diameter of the burner (1.75 cm) while at 60 mm Hg the flame is about 9 cm diameter. Although the average separation remains constant, the inverse square law dependence of the radiation on distance produces an error when the increase in flame diameter is large compared to the distance between burner (flame) and detector. In view of this possible source of error the data taken from the measurements made in the large metal chamber are considered more accurate. The data in Fig. 21 indicates a OH radiant intensity at 60 mm Hg four times as great as at one atmosphere.

The increase in OH emission with decreasing pressure is probably due to an increasing departure from thermodynamic equilibrium at lower pressures (to 60 mm Hg) since a pure collision activation process would produce a negative effect at lower pressures. Below 60 mm Hg a sharp decrease in OH emission is apparent and is probably due to the cooling of the flame by heat loss to the surroundings as in this range the flame was becoming unstable and approaching extinction. The decrease in temperature with pressure below 60 mm Hg can be seen in Fig. 24 where the infrared radiation, a purely thermal effect, is falling markedly with pressure. No attempt has been made in this report to describe analytically the mechanism responsible for the increase in OH radiation with decreasing pressures as this would require in itself an extended study. However, for the purpose of this investigation, the worst condition (i.e. least radiation for a given flow rate) occurs at one atmosphere. Further measurements on flames in the ultraviolet were therefore conducted at one atmosphere, since even below 60 mm Hg, at near extinguishment, the radiation level is still greater than the radiation at one atmosphere.

4.2 Ultraviolet Radiation versus Flow Rate

Figs. 22 and 23 show that radiant intensity is a simple function of flow rate for a given burner over the laminar flow conditions at one atmosphere.

However, the value of the radiant intensity cannot be extrapolated for burner size or material, because total flame temperature varies with heat loss to the burner, which depends upon size (surface to volume effect) and burner material (thermal conductivity and heat capacity). In Fig. 22, the radiation measurements for flow rates above 1800 cc/min are not

markedly different for burner size at a given flow rate whereas there is an increasing difference for lower flow rates between the small burner (. 165 cm) and the larger burner (1. 75 and 2. 21 cm).

A probable reason for this is a decrease in flame temperature due to an appreciable percentage heat loss to the large stainless steel burner for low flow rates. This argument is again applicable to Fig. 23 where the radiation magnitude differs for burner material, the heat loss to the stainless steel burner being greater than the heat loss to the glass burner. In Fig. 23 the radiant intensity current measurements made for the lowest flow rate which could maintain a flame on the 1 mm glass and stainless steel burners were on the order of the dark current of the photomultiplier detector, requiring the radiant intensity values in Fig. 23 to be determined as difference values. The dark current value was subtracted from the dark current plus current produced by the incident power to obtain the value of the radiant intensity. The magnitude of the dark current introduces an important value for expressing the limit of detection in terms of an equivalent radiant intensity. In Fig. 23 the broken line labeled "Radiant Intensity Equivalent to Dark Current" at 30 cm represents that value of radiant intensity from a source 30 cm from the detector which would produce a current from the photomultiplier equal to the dark current.

To calculate a radiant intensity value for a flame equivalent to this dark current of a photomultiplier the following equation can be used:

$$J_{DC} = \frac{P_{DC} R^2}{A}$$

where: J_{DC} = radiant intensity equivalent to dark current of photomultiplier in μwatt/ster.

P_{DC} = incident power equivalent to dark current of the detector in μwatts; usually given with the photomultiplier tube specifications.

R = distance from detector to flame in cm

A = area of photomultiplier emissive surface exposed in cm^2.

This simple relationship is to be applied over the spectral bandwidth of interest and must be modified if any optics are introduced between detector and radiation source.

The object is, of course, to design a system with the lowest practicable "Radiant Intensity Equivalent to Dark Current". From the equation it is evident that a photomultiplier tube with low dark current and large emissive area, placed near possible flame sources, would have the lowest J_{DC}.

4.3 Pressure Dependence of Infrared (H_2O) Radiation

The emission of radiation energy in the infrared is mainly a thermal process and therefore related directly to the temperature and concentration of water vapor product of the hydrogen-air diffusion flame. The measurements for infrared radiation versus pressure were made on diffusion flames in the large vessel at a distance of 150 cm. The curves in Fig. 24 show some scatter over the measurements. They are attributed to flow rate fluctuations and absorption variations of the water band radiation along the transmission path.

The radiant intensity remains approximately the same for ambient pressure between 760 mm Hg and 100 mm Hg and decreases to 50% of this value at 19 mm Hg, below which a sharp decrease in radiant intensity occurs as the flame approaches extinction at 13-14 mm Hg.

4.4 Infrared Radiation versus Flow Rate

The radiant intensity value at one atmosphere in Fig. 24 and the radiant intensity versus flow rate curve in Fig. 25 show that radiant intensity is approximately a linear function of flow rate. The radiant intensity values of Fig. 25 were taken at one atmosphere and the values for radiant intensity for lower pressures can be estimated from the pressure dependence relationship established in data of Fig. 24.

In comparing the radiant intensity values for the 1 mm glass and metal burner at the same flow rate, the radiant intensity is higher for the glass burner due to lower heat abstraction.

The high noise level of the IR detector did not permit accurate measurements to be made below radiant intensity levels of 4×10^{-3} watt/ster.

The same method of evaluating the noise level of a detector can be applied here as in section 4.2. Whereas dark current was determining factor for photomultiplier, noise level is the factor for the PbS photo conductive cell.

Therefore, the radiant intensity value for a flame equivalent to the noise level of the photo conductive detector can be found from the following expression:

$$J_n = \frac{P_n R^2}{A}$$

where: P_n = noise equivalent power NEP in watts; usually given with cell specifications

R = distance from detector to flame in cm

A = area of detector area exposed in cm^2

At this point it should be made quite clear that this noise level for the detector used in these experiments is not representative of the state of the art. In fact, the detector system was of very simple design and had a noise level equivalent to power (NEP) of 10^{-7} watts. This high value of NEP was not limiting for the measurements made in these experiments, and is a reasonable value for a practical system if simplicity of design is the important criterion.

NEP's of 10^{-12} watts and lower have been achieved through the use of chopper lock-in amplifier combinations, narrow band pass filters, cryogenic techniques, and other methods involving relatively complex equipment.

4.5 Effect of Heat Abstraction on Radiant Intensity

Heat abstraction affects radiant intensity indirectly by lowering the temperature of the flame. In order to evaluate this effect, radiation versus temperature measurements were made on a 1.75 cm burner where the regenerative heating cycle was as follows:

The burner was at room temperature when ignited, therefore the greatest temperature gradient across the flame to the burner and along the burner existed and also the highest rate of heat abstraction.

Fig. 26 shows that the value of radiant intensity is lowest for the lowest burner temperature, that is, for the highest state of heat abstraction and thus lowest flame temperature.

As the burner temperature increases, heat abstraction rate decreases, flame temperature rises, and radiant intensity increases.

This cycle continues until an equilibrium point is reached at a burner temperature of about 450°F, where the heat gained by the burner is balanced by regeneration to the flame and heat loss from the burner-flame system to the environment.

These effects of heat abstraction from the flame upon radiant intensity were determined coincidentally with other experiments. There was no opportunity to study this factor as a separate subject. It is pointed out however, that heat abstraction may affect limiting cases of detection in real compartments, but this effect will be extremely environment sensitive and should be studied under a set of conditions relating to design practice. The seriousness of heat abstraction may be mitigated by the high non-equilibrium radiation reported for cooled H_2-air flames by Kaskan (See Section 2 and references 22 and 23).

5. EXPERIMENTAL RESULTS - EXPLOSIONS

The explosion data presented in Fig. 27 through 35 were reduced from film records (see Fig. 19) of twenty experimental runs made in the steel vacuum chamber for three initial pressures and several mixture ratios. These initial pressures and mixture ratios do not cover the entire reported ignitable range for hydrogen and air but are considered representative for the scope of this evaluation. In particular, mixture ratios outside the limits reported here did not ignite reliably in our system.

The data of Fig. 27 through 35 are real values of time vs. IR irradiance, UV irradiance, and chamber pressure for the experimental chamber and the source position. These curves can be applied to other systems if corrected as explained in section 5. 1, 5. 2 and 5. 3.

Probably the most important "value" to be assessed from the data in this report is a number we shall call "lead time". This time is determined from the data as the time from detection to the time when an assigned pressure has been reached. The assigned pressure is dependent on a suppressant system, a personnel ejection system or other corrective actions which may be used. For a sample analysis of "lead time" the experimental chamber was chosen as the compartment, the IR detection time at irradiance value 60μwatt/cm^2, the UV detection time at irradiance value .03μwatt/cm^2, and the assigned pressure increase as 5 psi.

The "lead times" determined from Fig. 27 through 35 are presented in Tables V and VI, pp. 50 and 51,

The values chosen to determine lead time in Tables V and VI are purely arbitrary and chosen only as an illustration of applicability of these data.

5.1 Pressure Measurements

The curves in Fig. 27, 28, and 29 show the total pressure in the vessel vs time from ignition. These pressures represent total vessel pressure since the pressure measurements taken at two points in the vessel were identical except for an out of phase oscillation which corresponded exactly to the acoustical resonance of the vessel. In all cases the pressure increases could be plotted as smooth curves as shown and no sharp rises indicative of shock waves were present.

It is important to realize that these pressure vs time curves are unique to the size and geometry of the vessel used, and ignition point chosen. The worst case (i.e. greatest $\frac{dp}{dt}$) exists for a very small spherical vessel ignited at the center (non-detonating mixtures); the lowest $\frac{dp}{dt}$ is for cylinder where length/diameter is very large and ignited at one end (non-detonating condition). It is emphasized that such generalization can only be made for the early stages of combustion, that is, while the flame front is freely expanding. This is, of course, the stage of a developing explosion at which any corrective action must be taken to be effective. The remarks that follow must not be applied to the later stages of a confined combustion when pressure piling may develop as a function of compartment geometry and when pressure rises may very much exceed the values shown, for example, in Fig. 27.

Ideally, pressure measurements should be made on a scaled vessel whose geometry is the same as the compartment being considered. Where this is not practicable, "worst case" values should be used. However, the geometry of the vessel and the ignition point chosen in these experiments approximate a worst case design, and a linear extrapolation for size is all that is required for estimating pressure rise times for other vessels (compartments).

This extrapolation can be made as follows: Take the greatest distance from ignition source to wall of the experimental vessel, 5 feet for a standard reference. Then, assuming a compartment approximating a cube x feet on a side with ignition at the center, the pressure rise time for a pressure P can be found from the curves in Figs. 27, 28 and 29 as

$$t_x(P) = t_E(P)\,\frac{x/2}{5}$$

$t_x(P)$ = time to reach pressure P in compartment in milliseconds

$t_E(P)$ = time to reach pressure P in experimental vessel in milliseconds taken from curves in Fig. 27, 28 and 29

x = length of side of cube approximating compartment in ft

The pressure measurements can be related directly to the volume of combustible gases consumed during the earlier period of the process. That is; in a closed vessel, the percent pressure rise is directly proportional to the percent of gases by volume of combustible mixture consumed[1].

This relationship is useful in estimating the position of the reaction zone from the curves in Figs. 27, 28 and 29.

For example:

From Fig. 29, assume a mixture of 28.5% H_2 in air at an initial pressure of 760 mm Hg. The peak pressure achieved after complete reaction, assuming no cooling, is approximately 8 times the initial pressure for this mixture ratio, or 120 psia.

Therefore, from Fig. 29 curve No. 3, at 15 milliseconds from ignition the pressure in the chamber has measured 11 psi which corresponds to 10.5% of the combustible gases having been consumed. The volume of the experimental chamber is 6.25 ft^3 and 10.5% of this volume is .65 ft^3 or the volume of a sphere having a diameter of 1.1 ft. The reaction zone has reached a point only .55 ft from the ignition point.

The peak pressure achieved for closed vessel reaction for the other initial pressure and mixture ratios can be readily calculated from the specific heats of the product gases and the heat of combustion of the fuel oxygen reacted*.

5.2 Ultraviolet Measurements

The units of the ultraviolet measurements are irradiances rather than radiance, see Figs. 30, 31 and 32. This value is chosen rather than the radiant intensity because the reaction zone geometry and position are not defined except during the first few tenths of a millisecond after ignition. The irradiance is that value of radiant flux in μwatt-cm^{-2} within the bandwidth 2200-4000A incident at the detector surface, 150 cm from the ignition source and normal to it.

During the early stages of a deflagration which is propagating spherically from an ignition point remote from the detector surface, the irradiance at the detector will depend inversely upon the square of its

---

* Combustion wave theory is finely developed and presented by Lewis and von Elbe in reference (1).

distance from the ignition, and directly upon the instantaneous mass burning rate. The mass burning rate is directly proportional to the third power of time. In the UV no correction need be made for transmission losses.

Propagation from an ignition at a wall or bulkhead would be initially hemispherical. The same inverse square relation for distance and direct cube relation for time would apply to irradiance at the detector; for a given time from ignition the magnitude of irradiance for the hemispherical case would be one-half that for the spherical, because of the reduction in mass burning rate.

These relationships enable extrapolation to any size compartment of the irradiance data in Figs. 30, 31 and 32. The inverse square correction for distance must be made, and our reported irradiance values divided by 2. This factor of 1/2 represents the "worst case" assumption that our measured values are for spherical deflagrations, but that the postulated deflagration will be hemispherical.

5.3 Infrared Measurements

The infrared measurements are defined in the same way as the ultraviolet measurements, the major difference being the distance from detector to ignition source which is 38 cm for the infrared detector and 150 cm for the UV detector.

The correction for irradiance by the inverse square law is applicable for the IR, but, where transmission path lengths are great, corrections for atmospheric absorption must also be made. Those curves shown as broken lines in Figs. 34 and 35 contain a large uncertainty as to their shape. The reason for this uncertainty is the chopping rate of the energy at 900 cycles per second, or a peak to peak time interval of .55 milliseconds. For events that take place in less than 5 milliseconds quantitative measurements are not possible. However, the magnitudes of the radiation determined by the broken curves are significant since they are minimum values, that is, higher time resolution (chopping rate) could only show values of irradiance which are higher at a given time.

The chopping rate of 900 cps was chosen because it is the optimum value for a PbS cell having a time constant of 75 μs, and a higher chopping rate would have decreased sensitivity.

5.4 Discrimination of Explosions from Flames

The magnitude of the radiant intensity is a function of the cube of time, after the reaction has established itself over a spherical surface area

approximating statistically a perfect reaction zone. During the first few milliseconds after ignition the radiant intensity does not increase with time indicating that reaction zone is very small and a spherically propagating reaction zone is not established until after an induction period.

During the induction period, i.e., the time from ignition to the point where the radiant intensity increases as a cube of time, the radiant intensity is increasing as a power K of time where K varies from 0 to 3.

The signal voltage from a detector due to radiant energy can be expressed as a function of time which is empirically derived from the data.

$$V(J) = F(t^K)$$

Where K = 0, as for a steady state flame,

$$V(J) = \text{Constant}$$

and $\frac{dV(J)}{dt} = 0$

and where $K \neq 0$, as for a spherically propagating explosion

$$\left|\frac{dV(J)}{dt}\right| > 0$$

Therefore, a detector having a linear output, and differentiating output, could discriminate fires from explosions. This analysis is not rigorous because it is apparent that a flickering flame could produce the same effect as an explosion, but the suggestion is presented as an example of a possible technique.

The above relationship holds for the UV as well as the IR, the UV being possibly more flexible for this application because of the rapid direct coupled response of a photomultiplier compared to the slower intermittent (chopped) response of photoconductive cells.

6. SPECTRAL DISTRIBUTION OF H_2-AIR FLAMES

Two sets of spectra were taken in the ultraviolet spectral region. Figs. 36 through 40, were taken with the monochromator recorder gain fixed to record the peak value of the (0, 0) OH band which has a maximum intensity at 3090A. The spectra were taken at various pressures from 1 atmosphere to 30 mm Hg; the magnitude of the (0, 0) OH radiation exhibited the same pressure dependence as the earlier measurements made with the filter and

photomultiplier. Figs. 41 through 45 are a set of spectra taken with an expanded scale to permit a qualitative evaluation of the contributions made at shorter wavelengths. By dividing the spectrum up into three regions in Fig. 41, the contribution of each band can be evaluated.

Spectral Band	% of Total Energy
2200-4000A	100%
2600-3200A	65%
2600-2900A	11%

These bands were chosen for the following reasons;

(1) 2200-4000A - this is the band over which the absolute values of radiant intensity or irradiance were measured (see Figs. 21, 22, and 23), and chosen as the 100% value representing all the radiation from the OH bands.

(2) 2600-3200A - A detection system designed to sense radiation over the spectral band 2600-3200A, to utilize the 65% of the available energy could only be used under certain conditions. The compartment would have to be wholly closed and without illumination since the solar radiation between 3000-3200A is 35 μwatt-cm^{-2} and standard illuminating lamps radiate below 3200A. However, the compartment could be illuminated and have ports if the window materials and lamp envelopes were made from glass which absorbs radiation below 3200A.

(3) 2600-2900A - A detector filter blocking all radiation above 2900A would be solar-blind up to an altitude of 11 km since all radiation below 2900A is absorbed by the ozone and oxygen of the upper atmosphere. However, near sea level, the atmosphere transmits rather well at 2900A, and background radiation could come from sources in the lower atmosphere; such as aircraft, flares, rocket exhausts, etc. However, below 2900A only special window materials transmit, i.e. quartz, CaF_2, and other optical materials. Furthermore, most commercial glass including, for example, Pyrex brand glass do not transmit below 3000A, and standard glass envelopes of incondescent and fluorescent lamps do not transmit below 3000A. Therefore, compartments fitted with standard windows and illuminating sources would be free from background radiation for a system sensitive only to radiation below 2900A. This system appears the most promising if 11% of the OH radiation is sufficient.

The infrared water band emission spectra from the hydrogen-air flames (see Figs. 46, 47 and 48) show that there is little variation in qualitative structure with pressure and the total energy varies with pressure as shown previously in Fig. 24.

The arguments for the utilization of water band emission from hydrogen-air flames and explosions present severe contradictions. First, it must be assumed that water vapor is ubiquitous in the compartment as well as in the atmosphere. Then, consider a detector-filter combination that is sensitive only to wavelengths between 2.6 and 2.8 micron with sharp cutoffs on either side. This detector system would be free from solar background, since solar radiation is totally absorbed within this bandwidth. However, a humidity condition of 100% at a temperature of 107°F would absorb 80% of the radiation from a source over a path length of 10 feet. Alternately, and especially in cryogenic systems, condensation of water vapor on the detector is possible, rendering the detector impotent. A layer of water .05 cm thick absorbs 90% of incident radiation at 2.7μ.

7. IONIZATION MEASUREMENTS

In all tests made a certain degree of ionization was recorded. The magnitude of the ionization was highly erratic, while the time lapse from ignition to detection was repeatable for identical run conditions. The response from the ionization probe occurred a short time before the peak pressure was reached in the chamber.

This response indicates that the expected result was realized, that is, the ionization gauge responds to the reaction zone. The species that produce the ionization are unknown and probably incidental. It is highly unlikely that a pure H_2-air reaction could produce the ionization currents measured in these experiments. It is probable that the ionization was produced by hydrocarbons or salts present in the reaction zone. The most probable source of the ionization is salt species present in the air used or on the walls of the chamber, in fact, sodium was found present in the flame spectra, Figs. 36 through 45. The results of these experiments do show rather clearly that ionization cannot be precluded but is limited as a detection method. Pure H_2-air reactions do not produce a detectable amount of ionization within practical limits, but easily ionized species on the probe would enable detection of the reaction. The foregoing remarks apply to detectability per se by ionization measurements and do not include operational considerations such as timeliness of detection, number of detectors needed per compartment, etc.

8. DISCUSSION

8.1 General

A detailed discussion of the experimental data as such and comments concerning trends and extrapolation has been included in the presentation of Experimental Results, Sections 4, 5, 6, and 7, along with the data to which they apply. It is the purpose of this Section to consider the relevance of the

results to application, including mention of the main experimental results.

The adequacy of emission detection techniques will first be discussed purely from the standpoint of the radiation properties versus flame and explosion properties.

Considerations related to application will follow.

8.2 Detectability of Flames by Emitted Radiation

The radiation from hydrogen air flame products in the infrared and especially the ultraviolet has proved an extremely sensitive property for flame detection. It was initially expected that the flames occurring at high altitude (low pressure) would offer the most difficulty as the theoretical adiabatic flame temperatures decrease with pressure*, and any emission of thermal origin would thus also decrease with pressure. This was indeed true for the IR water band emission where the measured radiant intensity decreased significantly at pressures less than about 60 mm Hg (Section 4.3, Fig. 24). For this reason alone, the water band IR radiation is not considered a useful flame detection property.

In contrast, the OH radiation in the UV increased surprisingly as pressure decreased, so that the radiant intensity at 60 mm Hg was four times as great as from the same flame at 1 atmosphere (Section 4.1, Figs. 20 and 21); even at the point of extinction (about 13-20 mm Hg for the burners used) the radiant intensity was still greater than at one atmosphere.

One must also consider that owing to the stability characteristics of flames in general, the minimum flame that is self sustaining requires a higher mass flow as pressure is reduced (Sections 2.3(3) and 2.4).

In view of three factors:

1) Minimum flame size (fuel mass flow rate) increases with altitude.

---

* RMD calculated flame temperatures for stoichiometric H_2-air

Pressure mm Hg	1	5	30	100	300	760
Temperature ^{o}K	2072	2149	2230	2279	2316	2342

2) Radiant intensity in the UV is roughly linear with fuel mass flow rate

3) Radiant intensity in the UV, for any fuel rate, increases with altitude,

it is readily concluded that monitoring of UV emission is a reliable basis for flame detection, with the most stringent condition being at one atmosphere.

The one atmosphere condition was further examined by measuring the radiant intensity from small flames (Section 4. 2, Fig. 23), and it is seen that at H_2 consumption rates well below 1 standard cc/sec, the OH radiation from the flame was easily measured. It is of course a matter of engineering consideration as to how small a flame constitutes a hazard. From purely the point of heating the environmental structure, it may be illustrative that a 1 cc/sec (NTP) flame represents a thermal output of only 2. 5 calories/sec. In any case, it is difficult to visualize detecting promptly a flame of this size by pressure rise, flame product analysis, or by any other means except a most fortunately placed thermocouple.

It should also be recalled that the radiant intensity decreases as heat is abstracted from the flame by its environment (Section 4. 5). Here again, the magnitude of this effect is environment-dependent, and it is considered probable that if heat abstraction is great enough to render a flame undetectable by UV, the flame will be cooled to the point of extinguishment.

In this research, we have dealt with intrinsic limits rather than design limits; environment-dependent limiting factors as mentioned must be assessed for a specific design or if necessary evaluated experimentally with mock-up procedures.

As a final point, it is repeated that our experiments were intended to evaluate marginal conditions; clearly any flames larger than those herein considered would present no problems of detection.

8. 3 Detectability of Explosions (Deflagrations) by Emitted Radiation

It was explained in Section 2. 2(4) that this investigation was concerned with deflagrations and not detonations, which in any case would be preceded by a pericd of deflagration.

The point of concern was whether under all conditions of pressure and mixture ratio which could result in a dangerous pressure rise, the

existence of the explosion could be detected enough in advance of a dangerous pressure level to permit corrective action.

Our data is presented in terms of pressure and irradiance versus time from ignition. To these data can be applied any desired criteria of detectability threshhold, dangerous pressure level, and detection lead time that the designer wishes. An illustrated example is Table V.

The data (Figs. 27 through 35) show clearly that upon ignition, IR detection of the water emission and UV detection of the OH emission are prompt compared to the rate of pressure rise, and that detection of radiation is distinct from the initiating spark (see film records, Fig. 19).

For all initial pressures, the rate of pressure rise is greatest for near stoichiometric mixtures*. If a hazardous condition is defined as an absolute value of pressure rise, say 5 psi, then the time to achieve this pressure elevation becomes greater with decreasing initial pressure.

Consequently from the standpoint of timely detection, near-stoichiometric explosions at one atmosphere initial pressure, represent the greatest potential difficulty, as the detection lead time is least for this condition, about 10 milliseconds for a 5-foot propagation length (Table V). In this regard, attention is again called to the fact that the time to reach a given moderately large pressure depends directly upon the size of the vessel as well as its geometry (Section 5. 1). Approximate extrapolation from our data can be made (Section 5. 1) if there is no opportunity for modeling experiments to be performed on a specific compartment configuration.

Whether the measured or extrapolated detection lead times are adequate will depend upon the freedom of the designer to avoid small compartments, and upon the response characteristics of the corrective measures to be taken.

Detection lead times based upon UV and IR detection are equivalent except for very rich mixtures (70% H_2)** where the UV emission levels and rate of rise are depressed compared to the IR. The adaptability of UV techniques to detecting these latter explosions depends upon the sensitivity

---

* Slightly fuel-rich mixtures propagate as fast or faster than stoichiometric mixtures. This parallels the published burning velocity data, Fig. 1.

** In the apparatus used, 70% H_2 mixtures could not be ignited at 100 mm Hg. The 65% mixtures were detected at all pressures.

of the detector and the minimum level of irradiance that can be used as a criterion for detection. Considering detectability per se, IR detection would seem from the foregoing somewhat better than UV for explosions. However one must also consider the inherent susceptibility of IR to attenuation by atmospheric moisture, condensation, and thermal background (Section 6). Thus from the overall standpoint, the monitoring of UV radiation is judged more dependable and is to be recommended, especially since the UV emission is clearly superior for flame detection, leading to a single rather than dual system.

Limited explosion experiments at 30 mm Hg initial pressure resulted in a maximum pressure rise on the order of only 2 psia. Detection of both UV and IR emission was clear for all mixtures that ignited, 15% to 50% H_2. Ignition at 50% H_2 was marginal. Thus the monitoring of radiation is sensitive enough to detect explosions which are not dangerous.

8.4 Application Considerations for a Detection System

The size and weight of a detection system is dependent on the complexity of the compartment(s), the degree of sensitivity needed, and the shock mounting and shielding requirements.

In the instance where many compartments require detectors or where obstacles would restrict the view of a detector, several detectors would be used. Both the photomultiplier and photoconductive cell lend themselves well to a parallel arrangement of detection powered by a single power supply with the signal output from all detectors monitored by a central alarm actuator control. Therefore, a multiple detector system could consist of one power supply, a central alarm actuator, and the required number of detectors.

The photomultiplier detectors and power supply are, in general, larger than the photoconductive cell and associated power supply. However, where high sensitivity is required for the photoconductive cell, a chopper must be included with each cell and each chopper synchronized with every other chopper.

The choice between photomultiplier and photoconductive cell, based only on size and weight considerations, is dependent on the state of art and specific efforts in these fields could probably produce detectors of either type in a more compact form.

At this point, the question of photomultiplier versus photodetector can not be wholly answered. However, it can be generally stated that where

high sensitivity to a unique characteristic is required, photomultipliers are the better choice with little or no sacrifice in size or weight.

Probably the more important design criteria will be dependent on the aerospace environment where g-loading, vibration and irradiation are acute. Nose cone packages containing photomultiplier tubes and photoconductive cells have been launched successfully and have remained operable. However, it is not clearly known if a photomultiplier tube (for example) would be operable during launch or re-entry when stresses are maximum and if it would be free from spurious effects which might give rise to a false alarm.

To generalize about the stresses which a photomultiplier could withstand would be frivolous at this point and possibly misleading.

An intensive study supported by experiments is required to determine the feasibility of photomultiplier operation under the uncommon stresses of an aerospace environment.

Research and development of photomultipliers[38] and broad band filters[39] for application in the ultraviolet, especially in the regions which are unique for hydrogen fire (OH band) detection, has been intense in the last few years and remains so at the present time. The ASCOP photomultiplier[38] type 541F with Cs-Te on a LiF window has excellent solar blind properties with a spectral response from 1300 to 3000A and a sensitivity and dark current on the order of the RCA type 1P28 photomultiplier. A photomultiplier of this type (ASCOP 541F) shockmounted and possibly modified for maximum volume coverage, would be a sensitive detector unique to the characteristic of a hydrogen-air flame or explosion.

8.5 Limitations of Other Methods

At the beginning of this program it was postulated, in part based upon existing knowledge and in part intuitively, that emitted radiation from flames and explosions would be the best property for detection. The results of this program have answered many initial questions and have confirmed the value of radiation especially in the OH region. Other detectable flame properties are less useful for the detection and control of hazards as briefly stated below.

Ionization would need to be measured by a probe in contact with the flame zone, compared to the possibility of detecting radiation from a distance. Absorption methods might apply, still resulting in only a line of sight rather than a volume detector, and moreover requiring relatively bulky equipment. In the H_2-air system, ionization levels are low and variable.

Detecting temperature effects due to fires or explosions by thermocouples or resistance wires also would depend upon the detector being at or very near the flame zone. Furthermore, heating effects from very small flames might only slowly be detected owing to heat transfer and heat capacity considerations. In contrast, detection of small flames by radiation is prompt. The same considerations apply to the detection of thermal noise or temperature fluctuations in a flame.

Chemical or acoustic means of analyzing for combustion products are neither so sensitive, rapid, or insensitive to detector location as a radiation technique. This last, of course can be considered an optical method of product detection.

Absorption as well as emission techniques have been considered for detection. A disadvantage is that they are line of sight rather than volume detection methods. Additionally, apparatus is usually cumbersome calling for high resolution optics compared to emission detectors. Complexity would certainly apply to microwave absorption.

The disadvantages of monitoring pressure rise have already been mentioned as being altitude dependent in a vented compartment, insensitive to small fires, and offering little lead time in the case of explosions.

9. CONCLUSIONS

9.1 In general, the monitoring of emitted radiation from the hydrogen-air flame is the best basis for detecting fires and explosions under all operating conditions for reasons of sensitivity, detection from a distance within a solid angle of view, promptness of detection, and simplicity of equipment.

9.2 Monitoring the ultraviolet OH emission from hydrogen-air flames is intrinsically the best way to detect hydrogen-air fires. Very small flames on the order of 1 cc (NTP) H_2 consumption can be detected and for any constant H_2 consumption rate the radiant intensity increases as pressure decreases.

9.3 The H_2O band IR emission is not a suitable property for H_2-air flame detection, since the radiant intensity decreases with pressure below 60 mm Hg as the radiation is purely thermal, and flame temperature decreases with pressure.

9.4 In the case of explosions, the OH (UV) emission again is the best property for detection before vessel pressures rise to a dangerous level, over the complete range of mixture ratios tested and at all pressures where explosions may yield a dangerous pressure rise. Marginal cases exist for

mixtures near the rich limit (70% H_2) where OH concentrations are low and the radiation levels and rates of rise are unusually small.

9.5 Detection of explosions through the H_2O (IR) emission is in one sense easier than with the OH emission, insofar as the marginal rich mixture cases are not found. The susceptibility however of interference from background due to a warm environment and from atmospheric and condensate absorption render the IR approach less reliable overall than the UV.

9.6 A flame at one atmosphere pressure represents a more critical detection problem than at reduced pressures, owing to the pressure dependence of radiant intensity and minimum flame size.

9.7 An explosion at one atmosphere of a near-stoichiometric hydrogen-air mixture is the most critical detection problem because such an explosion yields the highest rate of absolute pressure rise, and thus the minimum lead time between radiation detection and some arbitrary absolute pressure rise. However, even in these cases, a conservative lead time of about 10 ms is available for a 5-foot explosion propagation path.

9.8 The time rate of pressure rise in a compartment due to exploding a given mixture at a given initial pressure varies with compartment geometry; for any given geometry, it is nearly inversely proportional to linear compartment dimension except during the final stages of propagation.

9.9 Heat abstraction from the reaction zone will decrease radiant intensity levels.

9.10 In any real situation, the limits of detectability of fires and explosions, and the detection lead time for explosions, depend upon environmental design factors such as (a) heat sink effects, (b) geometry, (c) and distance of detector from the flame or ignition, and upon detection system design factors such as (d) detector threshhold, (e) irradiance level criteria for detection, and (f) definition of hazardous conditions. The effect of many of these factors can be extrapolated from the data here reported.

9.11 Spectral distribution in the UV has shown small variations with pressure which however are not significant with regard to the detection problem.

9.12 Solar radiation in the UV becomes an increasing interference with altitude unless the compartment in question is closed or, if vented, light shielding of detectors is designed in.

10. RECOMMENDATIONS

10.1 Development and evaluation of an H_2-air fire and explosion detection system prototype based upon monitoring OH radiation in the ultraviolet should be undertaken.

10.2 An experimental study should be made of the geometry and size dependence of rate of pressure rise in explosions in relation to the flame velocity and position of the flame front.

10.3 A quantitative investigation of the effect of heat abstraction upon UV radiant intensity from hydrogen-air flames should be of value.

10.4 An evaluation should be made of the need for ruggedizing radiation detectors (eg. photomultipliers), extending their temperature range of operation, and otherwise fitting them for aerospace vehicular application.

10.5 Further research should be undertaken as needed to evaluate or develop suppression methods that are effective within the detection lead times herein reported.

10.6 In view of the marked effects of slight oxygen enrichment upon the hydrogen-air reaction, especially deflagrations and detonations (Section 2.2(3)), the data herein reported should be extended to cover the case of oxygen leaks along with hydrogen leaks.

10.7 Anticipating the eventual application of advanced propellant systems, such as those based upon fluorine compounds as oxidizers, an assessment of their hazards and detectability should be undertaken.

REFERENCES

1. Lewis, B., and von Elbe, G., "Combustion, Flames, and Explosions of Gases", Academic Press, 2nd ed., 1961.

2. Gaydon, A. G., and Wolfhard, H. G., "Flames, Their Structure, Radiation and Temperature", The Macmillan Co., 2nd ed., 1960.

3. Barnett, H. C., and Hibbard, R. R., (Ed.), "Basic Considerations in the Combustion of Hydrocarbon Fuels with Air", NACA Report 1300, 1959.

4. Van Dolah, R. W., et al., "Review of Fire and Explosion Hazards of Flight Vehicle Combustibles", ASD Technical Report 61-278, October 1961.

5. Zeldovich, Ia. B., and Kompaneets, A. S., "Theory of Detonation", Academic Press, 1960 (Original Russian edition, Moscow, 1955).

6. Seamans, T., Clark, A., and Tromans, R., "Research on Autoignition and Detonation", Final Report RMD 2005-F, 1960, Reaction Motors Division, TCC, Contract NOas 60-6047-c.

7. Lewis, B., and von Elbe, G., "Combustion, Flames, and Explosions of Gases", Academic Press, 1st ed., 1951.

8. Williams, F. A., "Progress in Spray-Combustion Analysis", Eighth Symposium (Int.) on Combustion, The Williams and Wilkins Co., 1962, p. 50.

9. Carlton, C., Gunket, W., and Yonill, C., "Study of Explosive and Fire Suppression of Aircraft Engine Sections", WADC Technical Report 57-300, April 1957, Contract AF 33(616)-3489.

10. Wolfhard, H. G., "Problems of Combustion under Altitude Conditions (From Fundamental Viewpoint)", Selected Combustion Problems - II (AGARD), Butterworths, London, 1956.

11. Wigg, L. D., "The Ignition of Flowing Gases", ibid.

12. Wolfhard, H. G., and Vanpee, M., "Ignition of Fuel-Air Mixtures by Hot Gases", Seventh Symposium on Combustion, Butterworths, London, 1959, p. 446.

REFERENCES (Cont.)

13. Coward, H. F., and Jones, G. W., "Limits of Flammability of Gases and Vapors", Bureau of Mines Bulletin 503, 1952.

14. Anagnostou, E., and Potter, A. E. Jr., "Quenching Diameters of Some Fast Flames at Low Pressures", Combustion and Flame 3, 453-7 (1959).

15. Friedman, R., et al., "A Program to Advance the Technology of Fire Extinguishment", Atlantic Research Corp. Report No. 62-5069-Q4, 15 July 1962, Contract AF 33(616)-8110.

16. Mullins, B. P., "Combustion in Vitiated Air", Selected Combustion Problems (AGARD), Butterworths, London, 1954.

17. Hirst, R., and Sutton, D., "Effect of Reduced Pressure and Airflow on Liquid Surface Diffusion Flames", Combustion and Flame, 5, 319-30 (1961).

18. Berets, D., Green, E., Kistiakowsky, G. B., "Gaseous Detonations I: Stationary Waves in Hydrogen Oxygen Mixtures & II: Initiation by Shock Waves". J. Am. Chem. Soc. 72, 1080, 1086 (1956).

19. Gordon, W. E., Mooradian, A. J., Harper, S. A., "Limit and Spin Effects in Hydrogen-Oxygen Detonations", Seventh Symposium on Combustion, Butterworths, London, 1959, p. 752.

20. Gaydon, A. G., "The Spectroscopy of Flames", Chapman & Hall, London, 1957.

21. Dieke, G. H., and Crosswhite, H. N., "The Ultraviolet Bands of OH", Johns Hopkins University Press, 1948.

22. Kaskan, W. E., "Hydroxyl Concentrations in Rich Hydrogen-Air Flames Held on Porous Burners", Combustion and Flame, 2, 229-43 (1958).

23. Kaskan, W. E., "The Concentrations of Hydroxyl and of Oxygen Atoms in Gases from Lean Hydrogen-Air Flames", ibid., pp. 286-304.

24. Kaskan, W. E., "Abnormal Excitation of OH in $H_2/N_2/O_2$ Flames", J. Chem. Phys. 31, 944-56 (1959).

REFERENCES (Cont.)

25. Schott, G. L., and Kinsey, J. L., "Kinetic Studies of Hydroxyl Radicals in Shock Waves. II. Induction Times in the Hydrogen-Oxygen Reaction", J. Chem. Phys. 29, 1177-82 (1958).

26. Bulewicz, E. M., and Sugden, T. M., "Recombination of Hydrogen Atoms and Hydroxyl Radicals in Hydrogen Flame Gases", Trans. Faraday Soc. 54, 1855-60 (1958).

27. Norrish, R. G. W., and Porter, G., "Spectroscopic Studies of the Hydrogen-Oxygen Explosion Initiated by Flash Photolysis of Nitrogen Dioxide", Proc. Roy. Soc., 210A, 439-460 (1952).

28. Minkoff, G. J., Everett, A. J., and Broida, H. P., "Ultraviolet Spectrophotometry of Low Pressure Explosions", Fifth Symposium on Combustion, Reinhold 1955, p. 779.

29. Penner, S. S., "Quantitative Molecular Spectroscopy and Gas Emissivities", Addison Wesley Publishing Co., 1959.

30. Ferriso, C. C., "High Temperature Infrared Emission and Absorption Studies", General Dynamics/Astronautics Report AE61-0910, AFCRL Contract AF 19(604)-5554, 14 Sept. 1961.

31. "Handbook of Geophysics" (Revised Edition), Macmillan, 1960.

32. McAdams, W. C., "Heat Transmission", 3rd ed., McGraw Hill, 1954.

33. Ryan, L. R., Penzias, G. J., and Tourin, R. H., "An Atlas of Infrared Spectra of Flames Pt. 1: Infrared Spectra of Hydrocarbon Flames in the 1-5μ Region", Warner & Swasey Company Report AFCRL-848, Contract AF 19(604)-6106, July 1961.

34. Perzias, G. J., et al., "An Atlas of Infrared Spectra of Flames, Part Two. Hydrocarbon-Oxygen Flames, 4-15μ; Ammonia-Oxygen, 1-15μ; Hydrazine-Oxygen, 1-5μ; and Flames Burning at Reduced Pressures". Warner & Swasey Company Report AFCRL-848 II, Contract AF 19(604)-6106, Oct. 1961.

35. Tourin, R. H., Babrov, H. J. Penzias, G. J., "Infrared Radiation of Flames". Warner & Swasey Company Report AFCRL-1071, Contract AF 19(604) 6106, Oct. 1961.

REFERENCES (Cont.)

36. Reaction Motors Report 204-Q7, AFOSR Contract AF 49(638)305, Nov. 1959.

37. Sugden, T. M., (oral information).

38. Causse, J. P. (ASCOP, Princeton, N. J.), Dunkelman, L. and Hennes, J. P. (NASA, Greenbelt, Md.), "Far Ultraviolet 'Solar Blind" Photomultipliers". Paper No. WC18, Opt. Soc. Amer. Los Angeles meeting, 18 Oct. 1961.

39. Childs, C. B., "Broad Band Ultraviolet Filters", J. Opt. Soc. Am. 51, 895-897, (1961).

TABLE I (Ref. 5)

Induction Distance For Detonation Versus Pressure

(Constant Tube Diameter)

Mixture	Induction distance, cm			
	30 mm Hg	100 mm Hg	200 mm Hg	300 mm Hg
$2H_2 + O_2$	--	--	78	52
$CH_4 + 2O_2$	--	134	78	51
$C_6H_{14} + 9.5O_2$	105	48	32	27

TABLE II (Ref. 5)

Induction Distance Versus Mixture Temperature

(Initial Pressure Constant)

$2H_2 + O_2$		$CH_4 + O_2$	
T^oC	cm	T^oC	cm
15	60	15	55
120-130	73	160-180	74
160-180	78	290-310	90
300-320	not in 1 meter	340-350	not in 1 meter

TABLE III (Ref. 5)

Induction Distance Versus Tube Diameter

For $CH_4 + 2O_2$ at 400 mm Hg and 15°C

Diameter, mm	13	32	38	48
Induction Distance, cm	112	117	150	220

TABLE IV

Comparison of Ignition Temperatures by Different Ignition Sources at 1 Atmosphere

Fuel	Hot Air Jet Ignition Temp. °C	Nichrome Wire (0.04 in) Ignition Temp. °C	Spontaneous Ignition Temp. °C
Methane	1180	1200	537
Ethane	920	980	472
Propane	980	1150	493
Ethylene	840	950	490
Acetylene	700	850	305
Hydrogen	670	750	572

TABLE V

Lead Time Values For UV Detection Of Explosions In Experimental Vessel (Fig. 18)

Initial Pressure	% H_2 in Air	Time to .03 μwatt/cm^2 Irradiance, ms	Time to 5 psi Pressure Increase, ms	UV-Pressure Lead Time, ms
100 mm Hg	15	35	>100	>65
	20	6.3	74	67.7
	28.5	2.5	37	34.5
	40	2.9	36	33.1
	50	7.4	43	35.6
	60	22	67	45
300 mm Hg	15	45	>100	>55
	20	6.2	37	30.8
	28.5	< 1	20	~19
	40	1	16	15
	50	3.1	20	16.9
	60	13.5	32	18.5
	70	(.03 μwatt/cm^2 not reached)	85	----
760 mm Hg	15	28	49	21
	20	5.4	25	19.6
	28.5	< 1	13	~ 12
	40	< 1	10.2	~ 9.2
	50	1.95	13	11.05
	60	11.2	21.5	10.3
	70	(.03 μwatt/cm^2 not reached)	58	----

TABLE VI

Lead Time Values For IR Detection of Explosions
In Experimental Vessel (Fig. 18)

Initial Pressure	% H_2 in Air	Time to 60 μwatt/cm^2 Irradiance ms	Time to 5 psi Pressure Increase ms	IR-Pressure Lead Time
100 mm Hg	15	15	>100	>85
	20	6.6	74	67.4
	28.5	4.7	37	32.3
	40	4.7	36	31.3
	50	5.4	43	37.6
	60	10.7	67	66.3
300 mm Hg	15	9.8	>100	>90.2
	20	3.3	37	33.7
	28.5	~1.1	20	~18.9
	40	~1.3	16	~14.7
	50	~1.7	20	~18.3
	60	4.9	32	27.1
	70	17.3	85	67.7
760 mm Hg	15	6.6	49	42.4
	20	1.8	25	23.2
	28.5	< 1	13	~12
	40	< 1	10.2	~9.2
	50	~1.1	13	~11.9
	60	1.9	21.5	19.6
	70	7.9	58	50.1

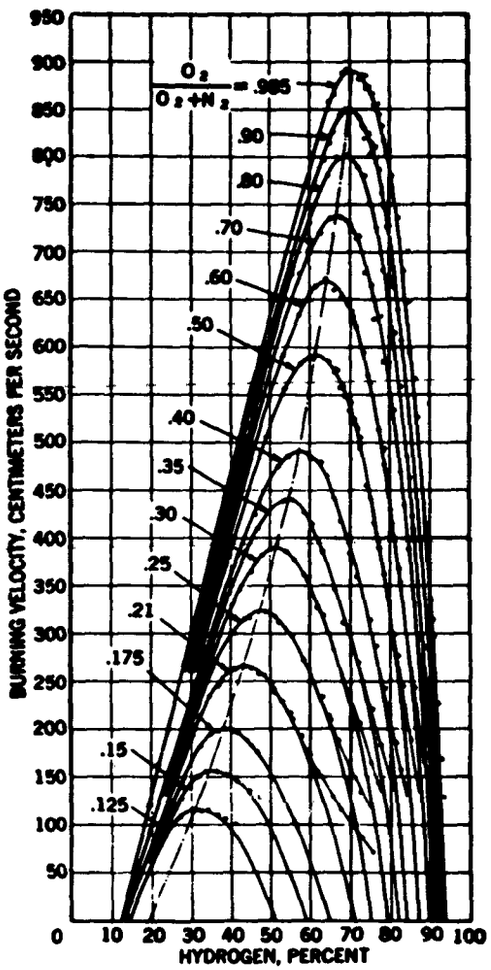

Fig. 1 Burning velocities of mixtures of hydrogen, oxygen, and nitrogen at room temperature and atmospheric pressure (Jahn)(1).

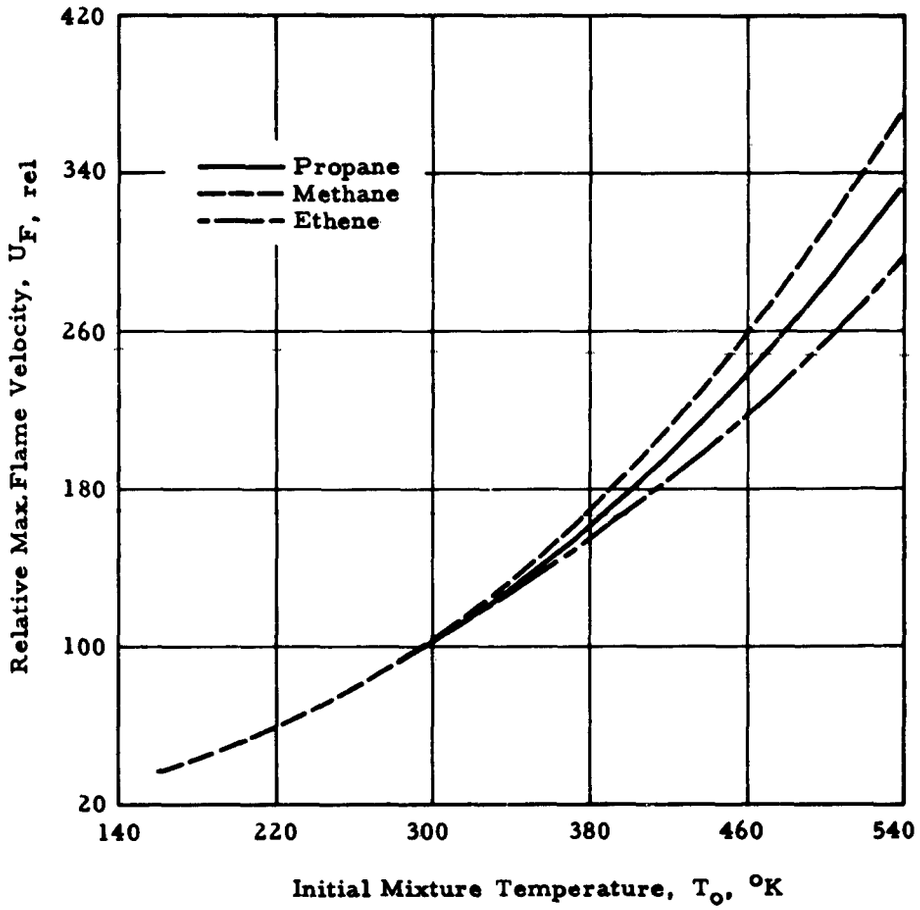

Fig. 2 Variation of relative maximum flame velocity with initial mixture temperature, referred to maximum flame velocity at 25°C[3].

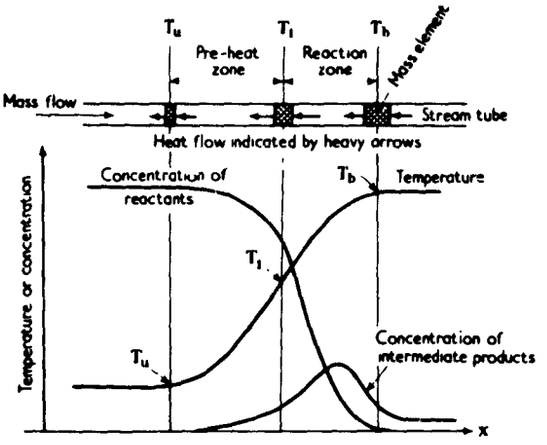

Fig. 3 Concentration and temperature profile of a plane (premixed) combustion wave(1).

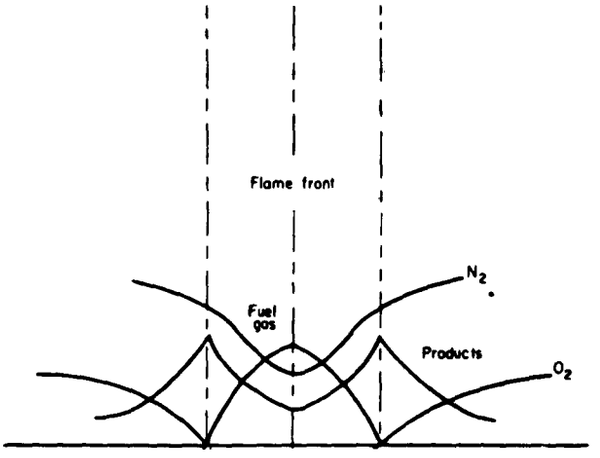

Fig. 4 Concentration profiles in a typical laminar diffusion flame(3).

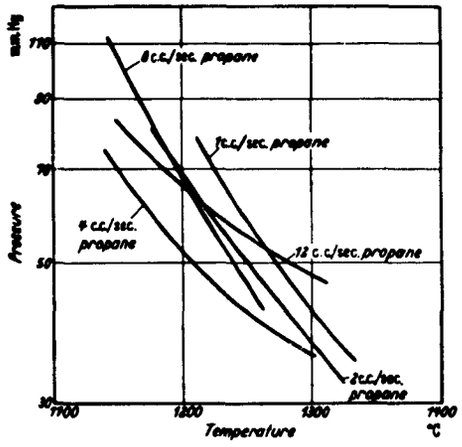

Fig. 5 Surface temperature of a Nichrome coil necessary to ignite stoichiometric propane-air in a 51-mm. diameter tube depending on pressure and mass flow of mixture(10).

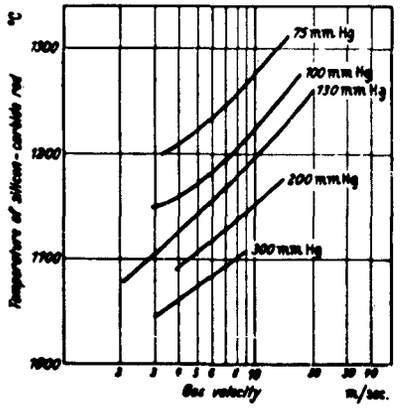

Fig. 6 Surface temperature of silicon carbide rod necessary to ignite stoichiometric propane-air mixtures depending on velocity of mixture for various pressures. Diameter of flow tube 51-mm.(10).

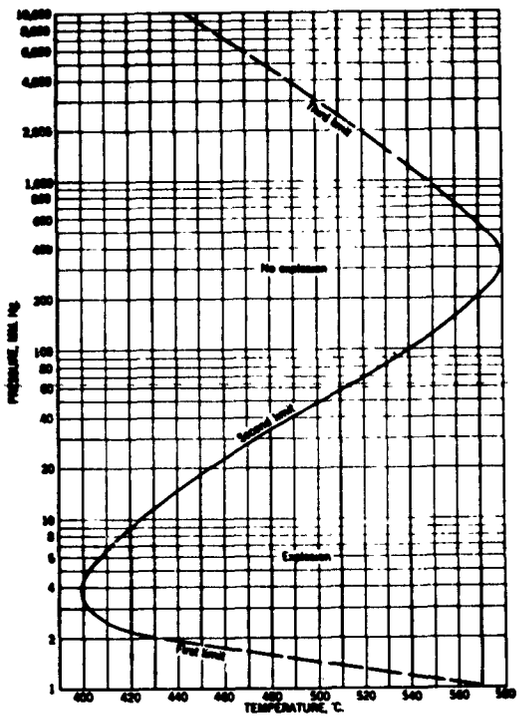

Fig. 7 Explosion limits of a stoichiometric hydrogen-oxygen mixture in a spherical KCl-coated vessel of 7.4 cm. diameter. First and third limits are partly extrapolated. First limit is subject to erratic changes(1).

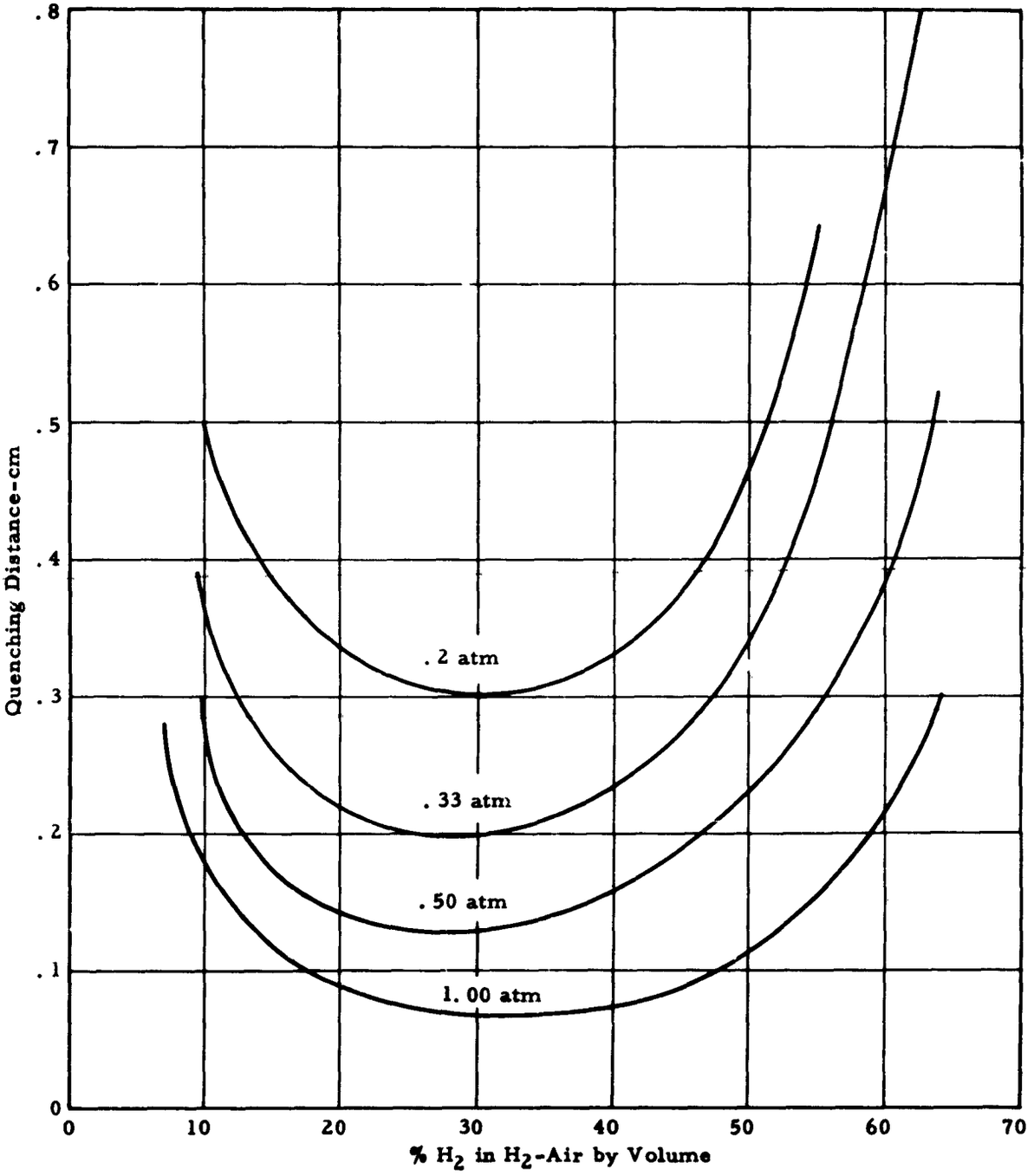

Fig. 8 Quenching distances for hydrogen-air mixtures at various pressures[7].

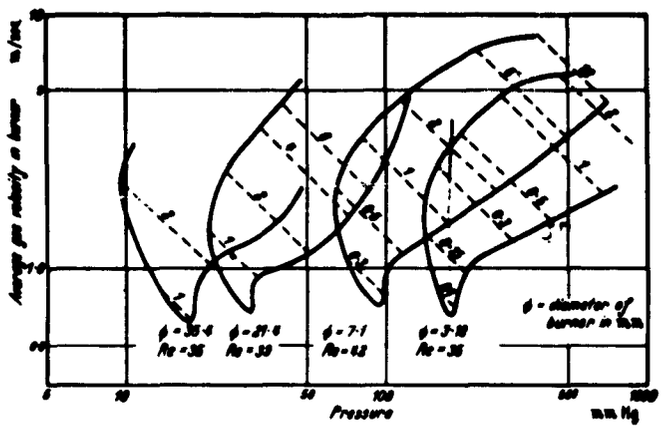

Fig. 9 Stability regions of stoichiometric acetylene-air flames on different size burners. The numbers inside the stability regions denote the mass flow of acetylene in c.c./sec. (N.T.P.). Reynolds number refers to the flow in the burner for the tip of the stability regions.(10)

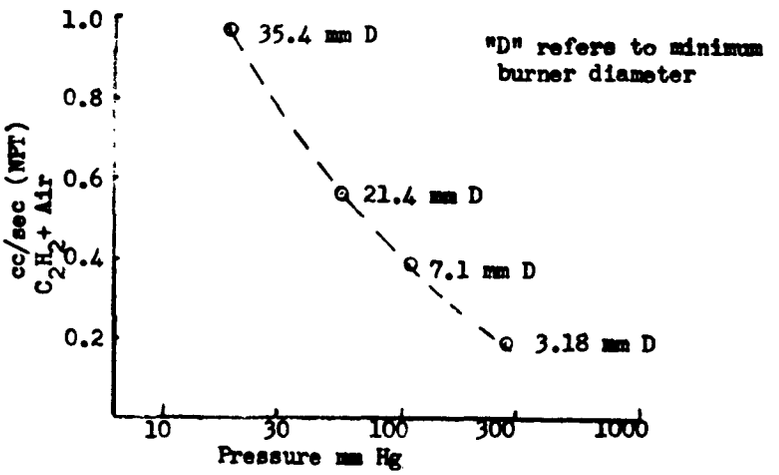

Fig. 10 Acetylene-air premixed flame: Minimum mass flow vs. pressure (from data of Fig. 9).

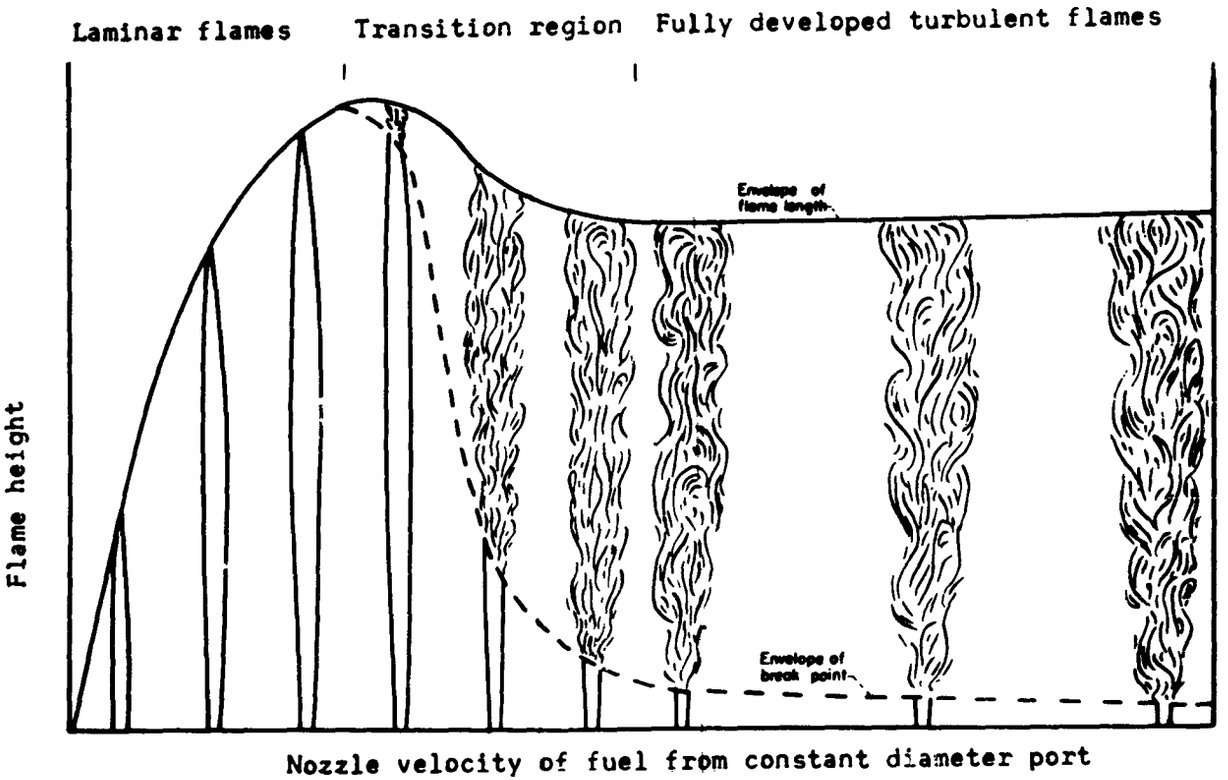

Fig. 11 Progressive change in flame shape for typical diffusion flame with increase in nozzle velocity of fuel issuing into air[3].

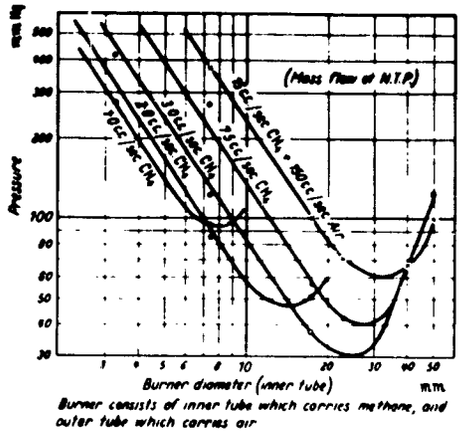

Fig. 12 Pressure at which a diffusion flame lifts off, depending on mass flow, which is always stoichiometric, and tube diameter.(10)

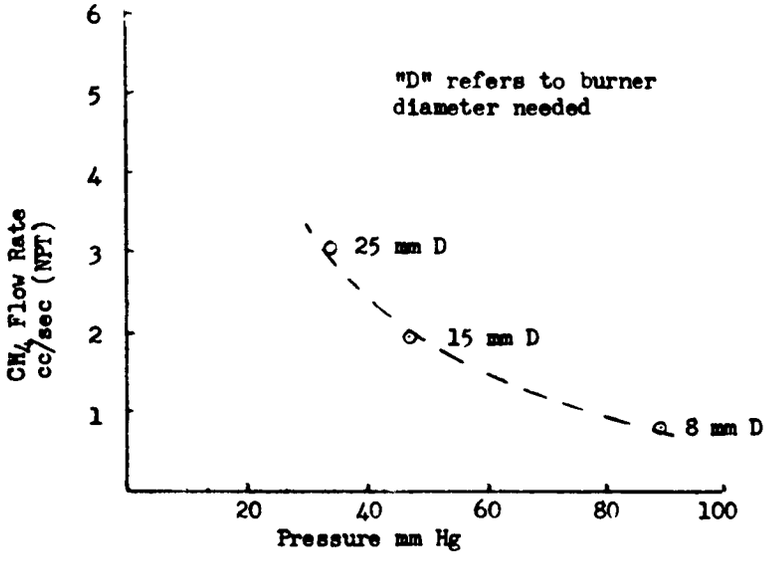

Fig. 13 Minimum fuel flow needed to maintain a flame vs. pressure for methane air diffusion flame (from data of Fig. 12).

A 20.8 cm. tube diameter
B 10.3 cm. tube diameter
C 5.3 cm. tube diameter

Diameter of sintered sphere 2.0 cm.

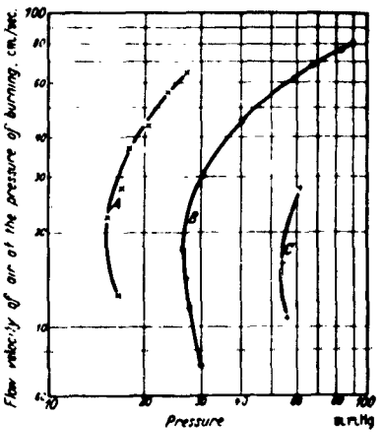

Fig. 14 Blow-off velocities of methane-air diffusion flames suspended on porous sintered spheres(10).

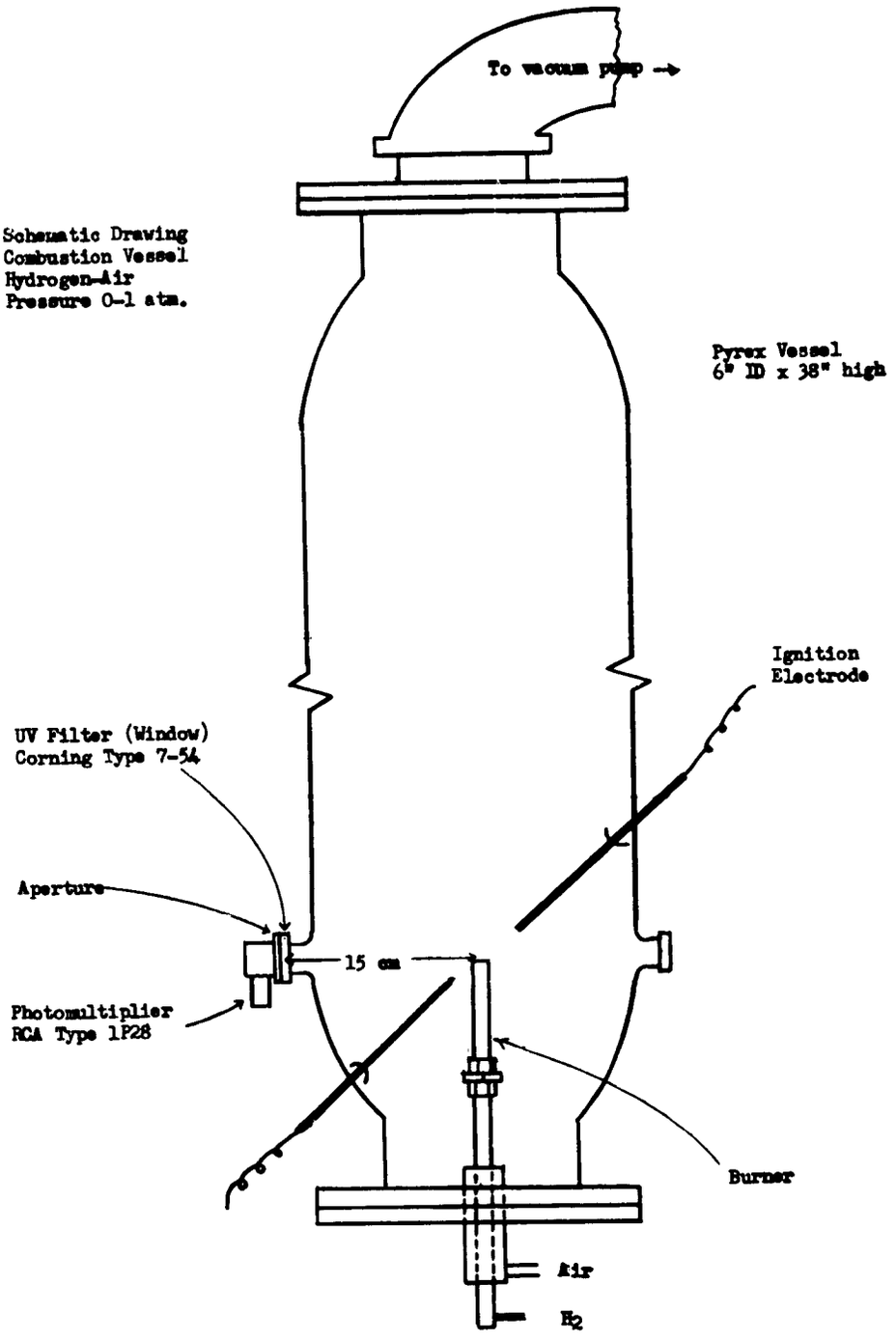

Fig. 15 Glass vacuum chamber used for hydrogen-air flames.

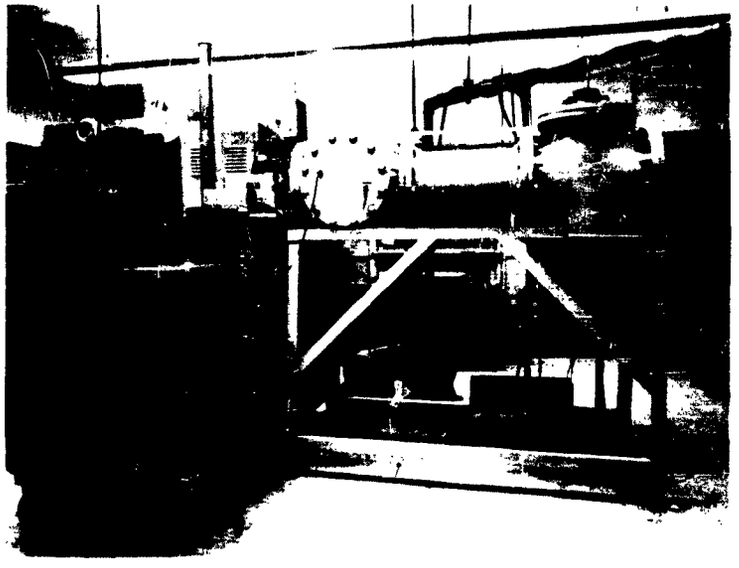

RMD No. 5508-1

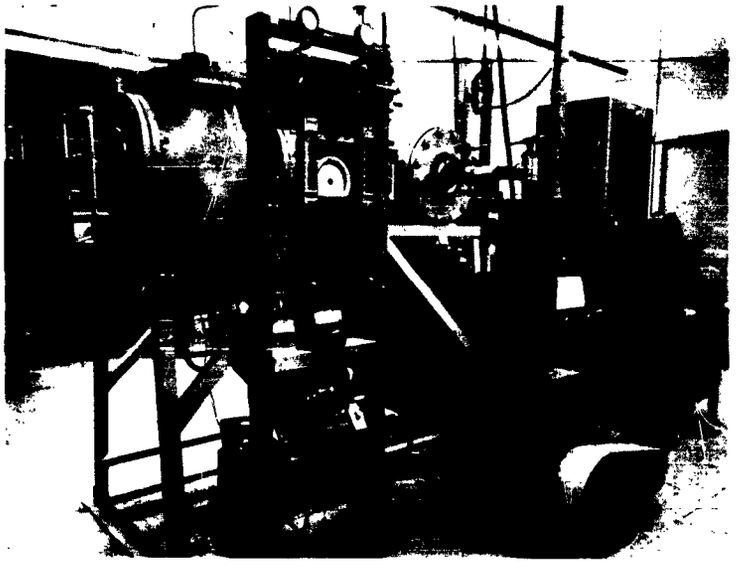

RMD No. 5508-3

Fig. 16 Steel vacuum chamber used for hydrogen-air flames and explosions.

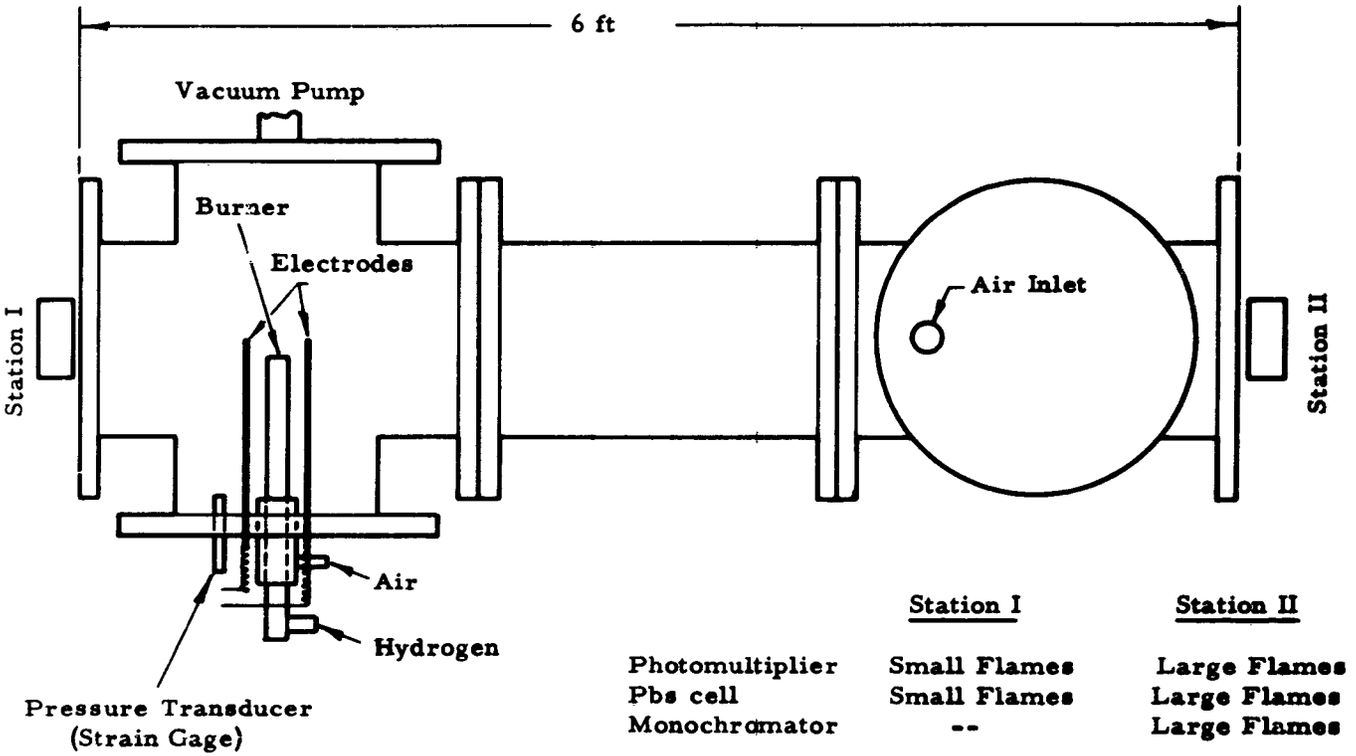

Fig. 17 Schematic-steel vacuum chamber set up for hydrogen-air flame experiments.

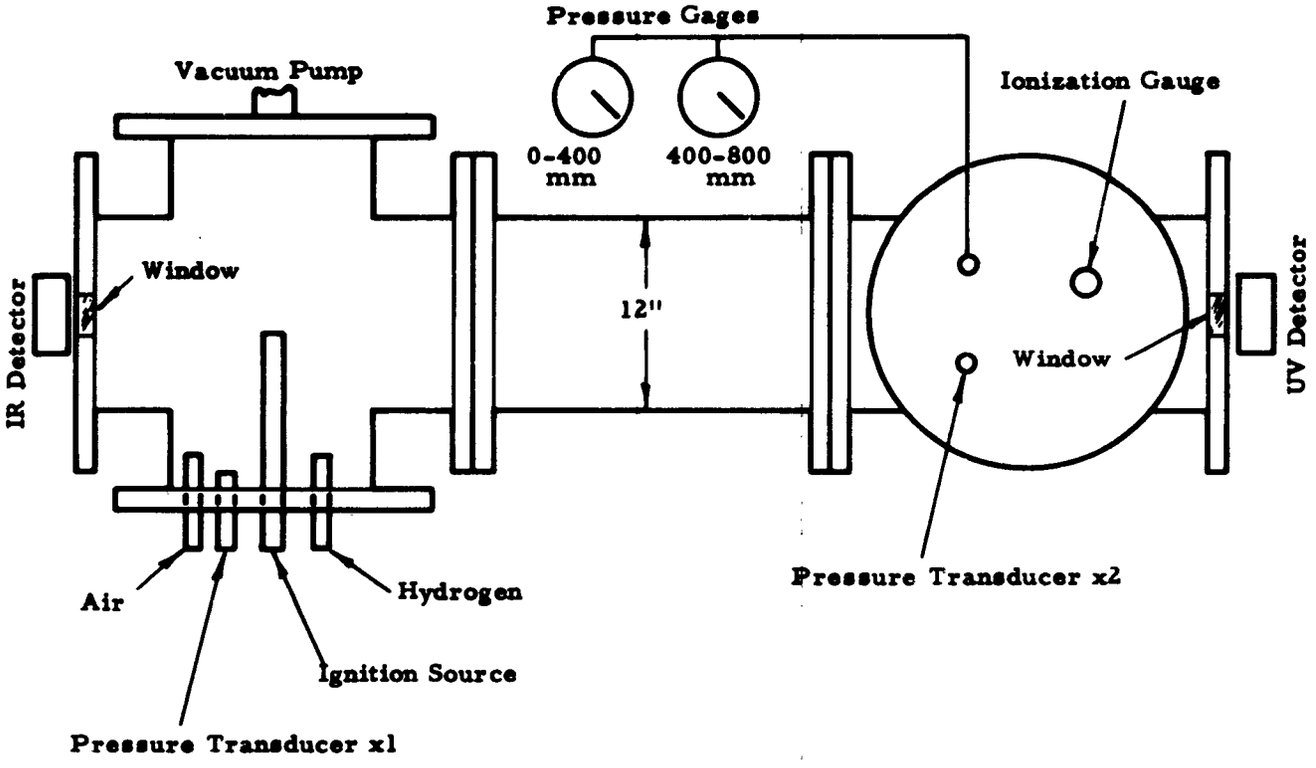

Fig. 18 Schematic-steel vacuum chamber set up for hydrogen-air explosion experiments.

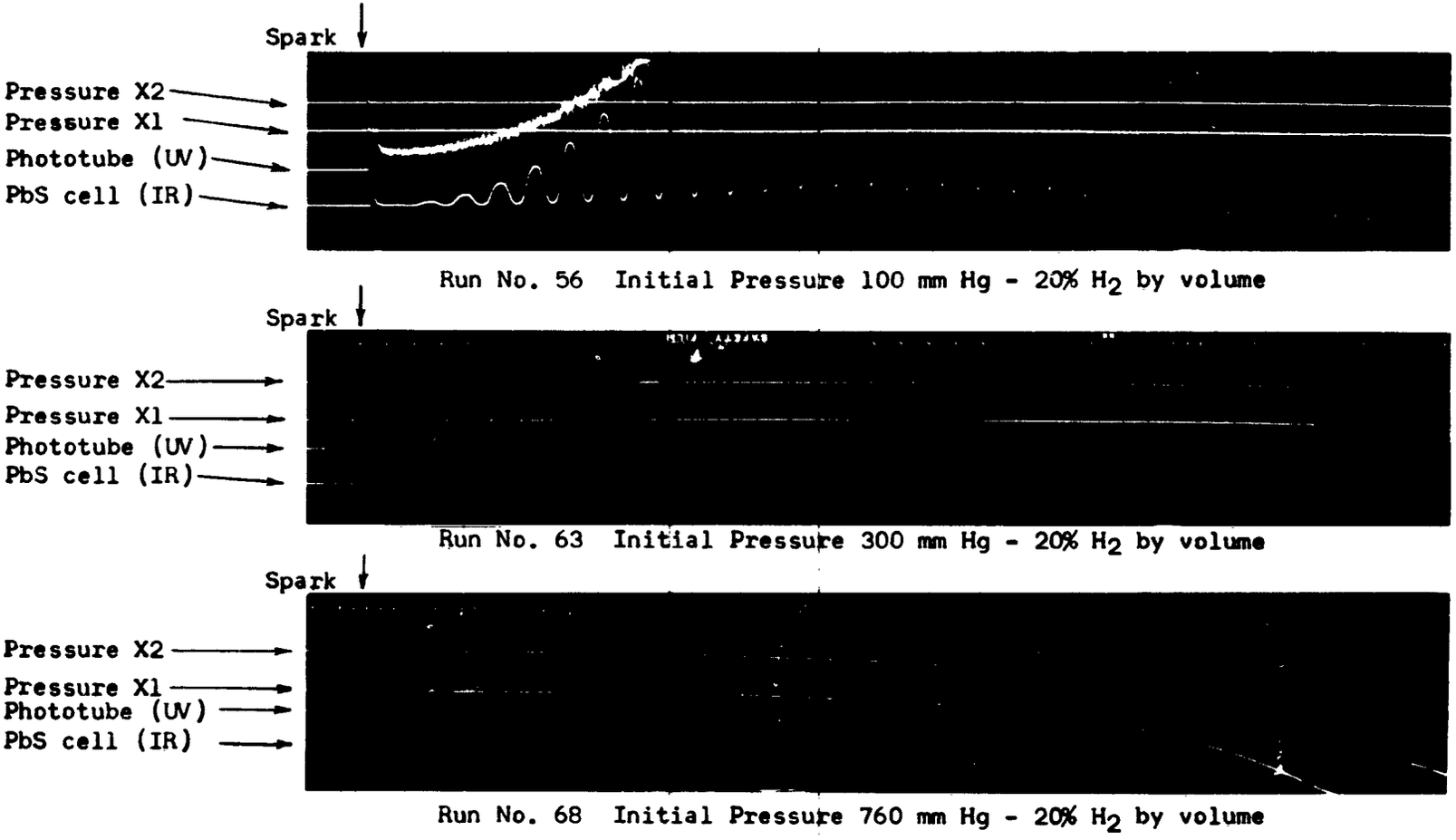

Calibrations identical for all runs

Fig. 19 Hydrogen-air explosions. Film strip records of pressure, UV radiation and IR radiation vs. time.

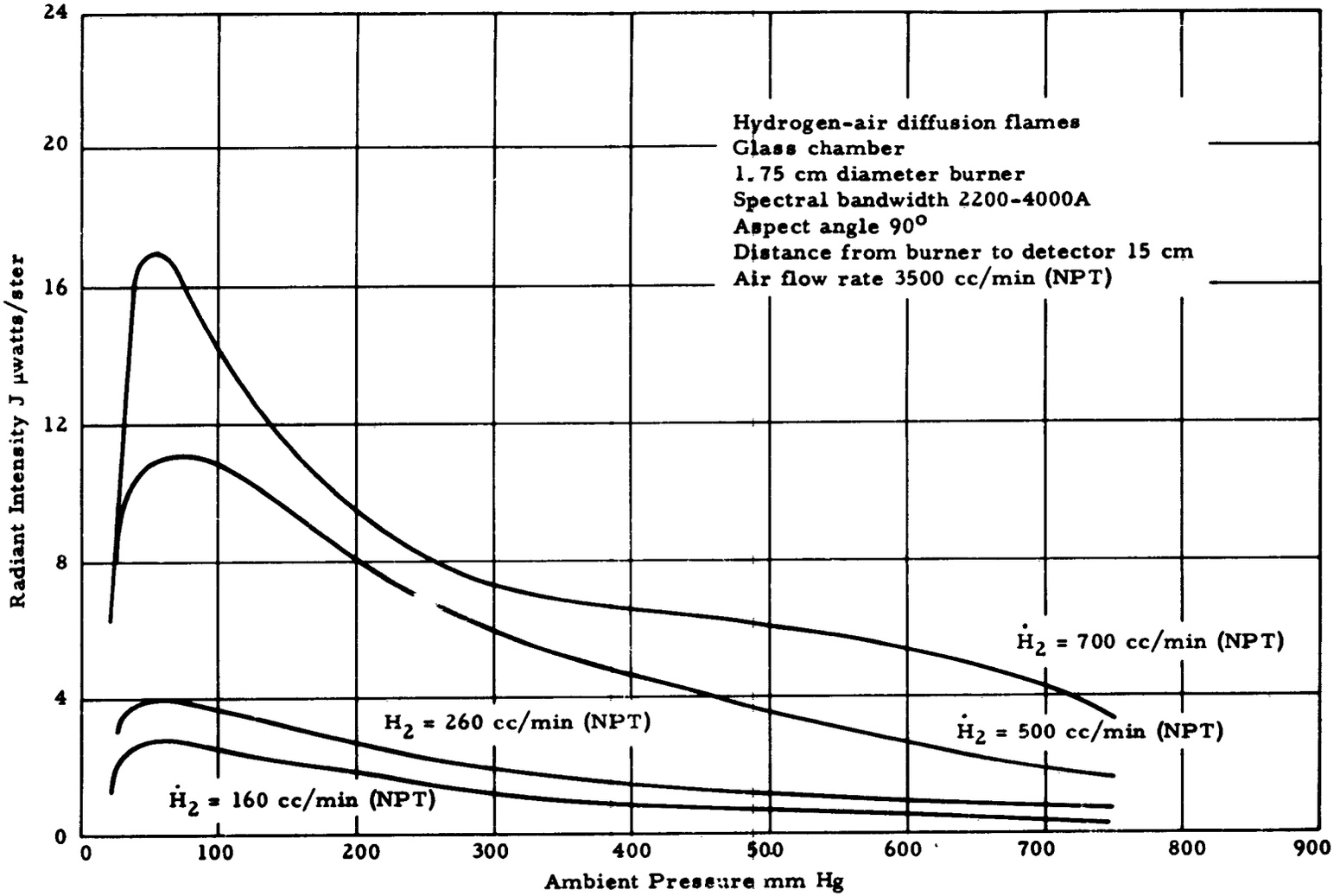

Fig. 20 Hydrogen-air diffusion flames: Radiant intensity (2200 - 4000A) vs ambient pressure - glass chamber.

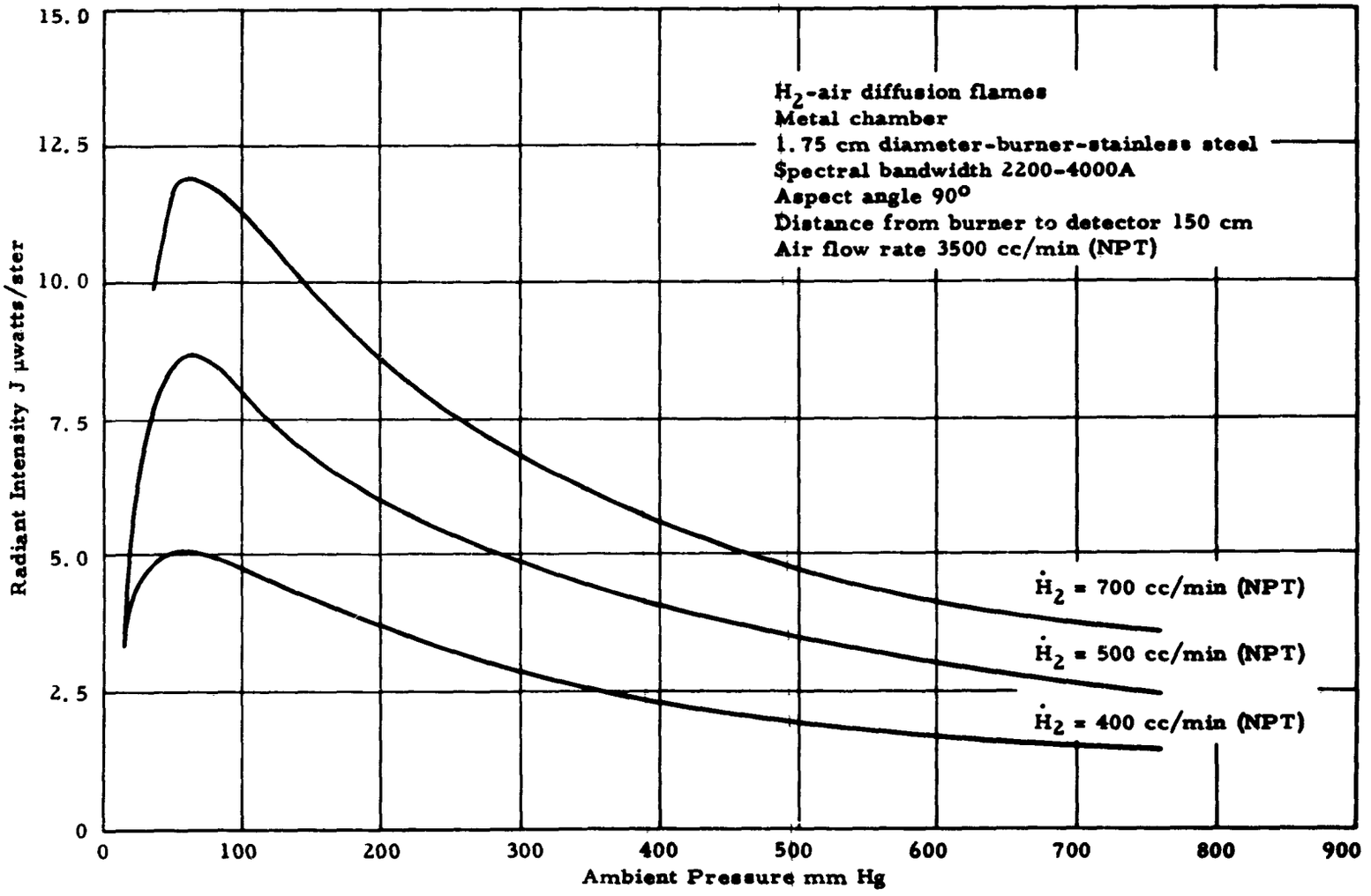

Fig. 21 Hydrogen-air diffusion flames: Radiant intensity (2200 - 4000A) vs ambient pressure - metal chamber.

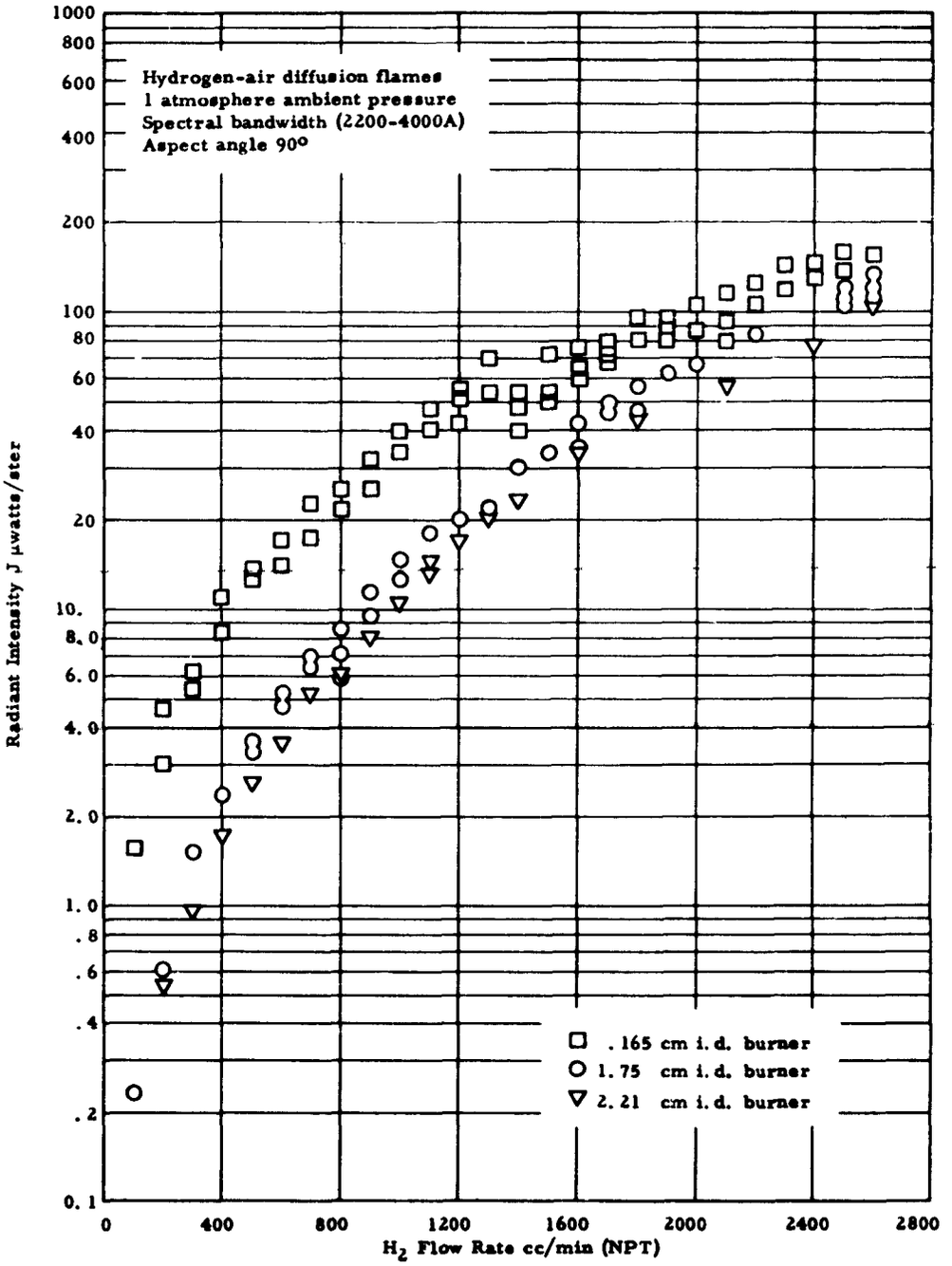

Fig. 22 Hydrogen-air diffusion flames: Radiant intensity (2200-4000A) vs H_2 flow rate at 1 atmosphere for various burner sizes.

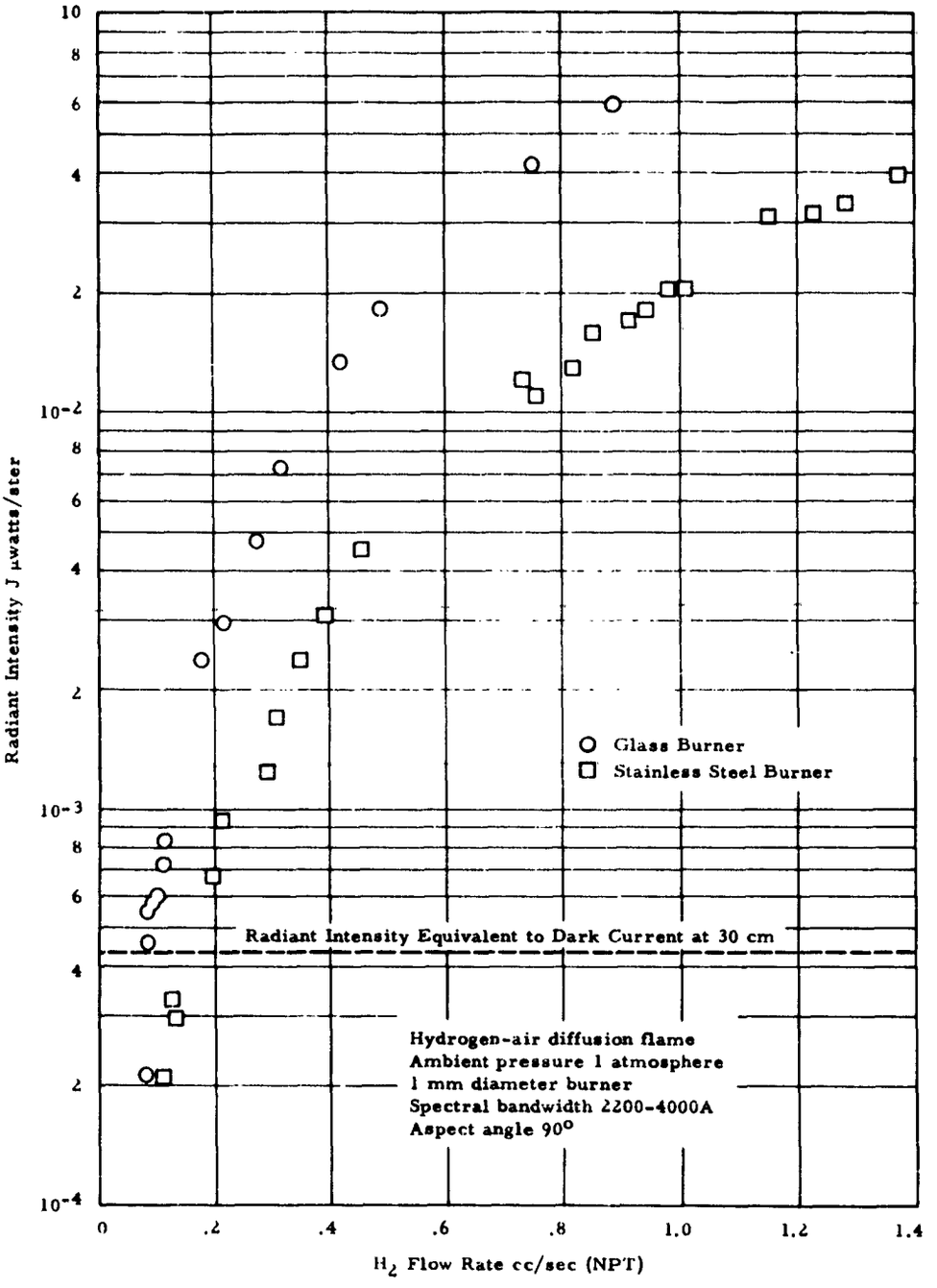

Fig. 23 Hydrogen-air diffusion flames: Radiant intensity (2200-4000A) vs H_2 flow rate-1 mm burner at 1 atmosphere.

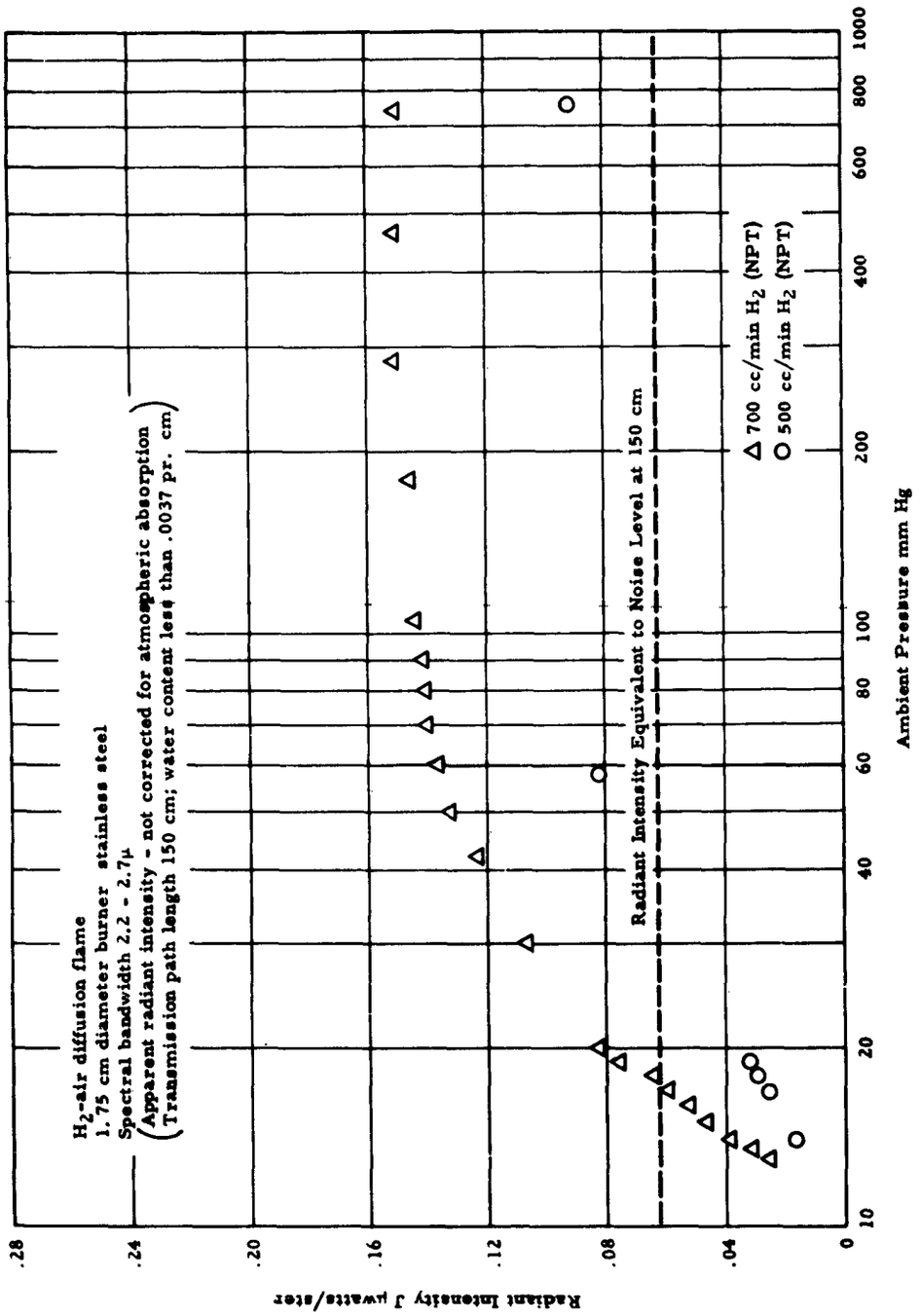

Fig. 24 Hydrogen-air diffusion flames: Radiant intensity (2.2 - 2.7μ) vs ambient pressure.

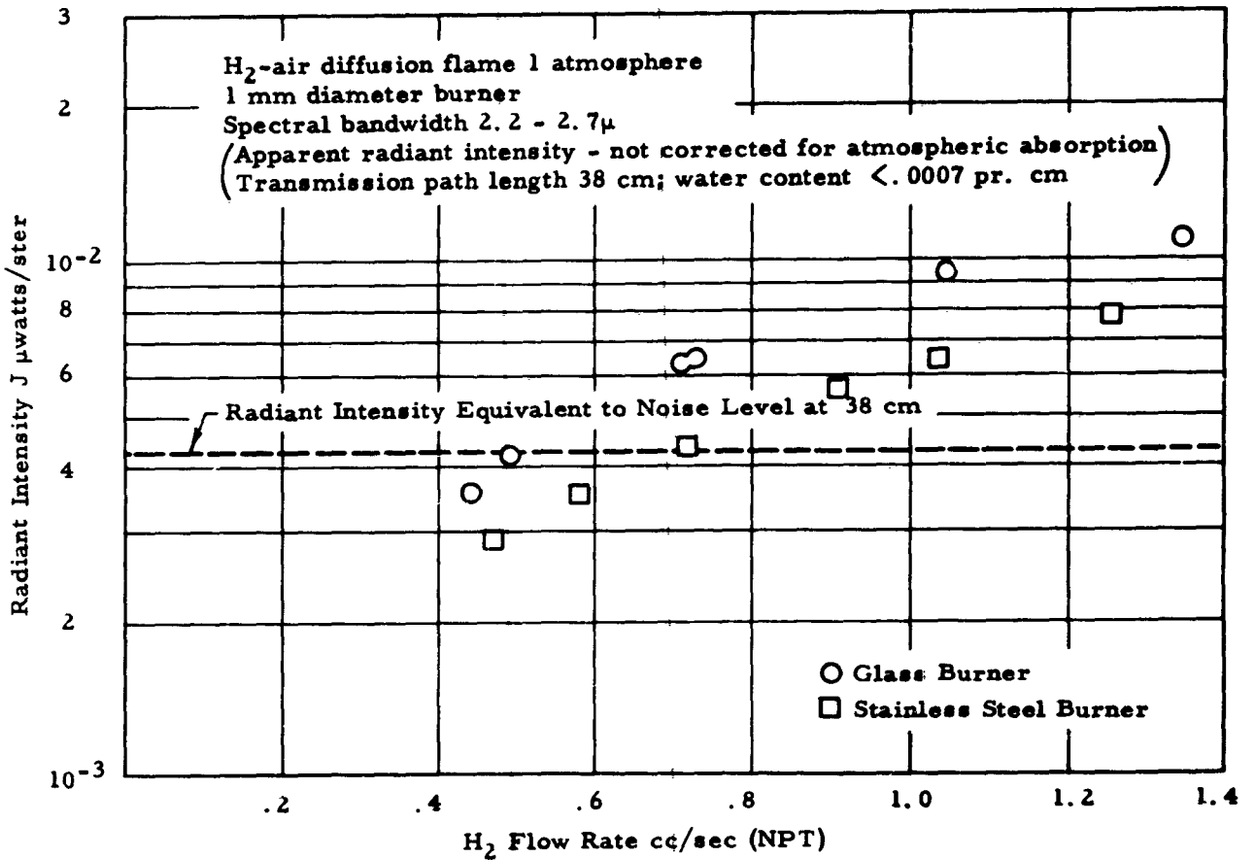

Fig. 25 Hydrogen-air diffusion flames: Radiant intensity (2.2 - 2.7μ) vs H_2 flow rate - 1 mm burner at 1 atmosphere.

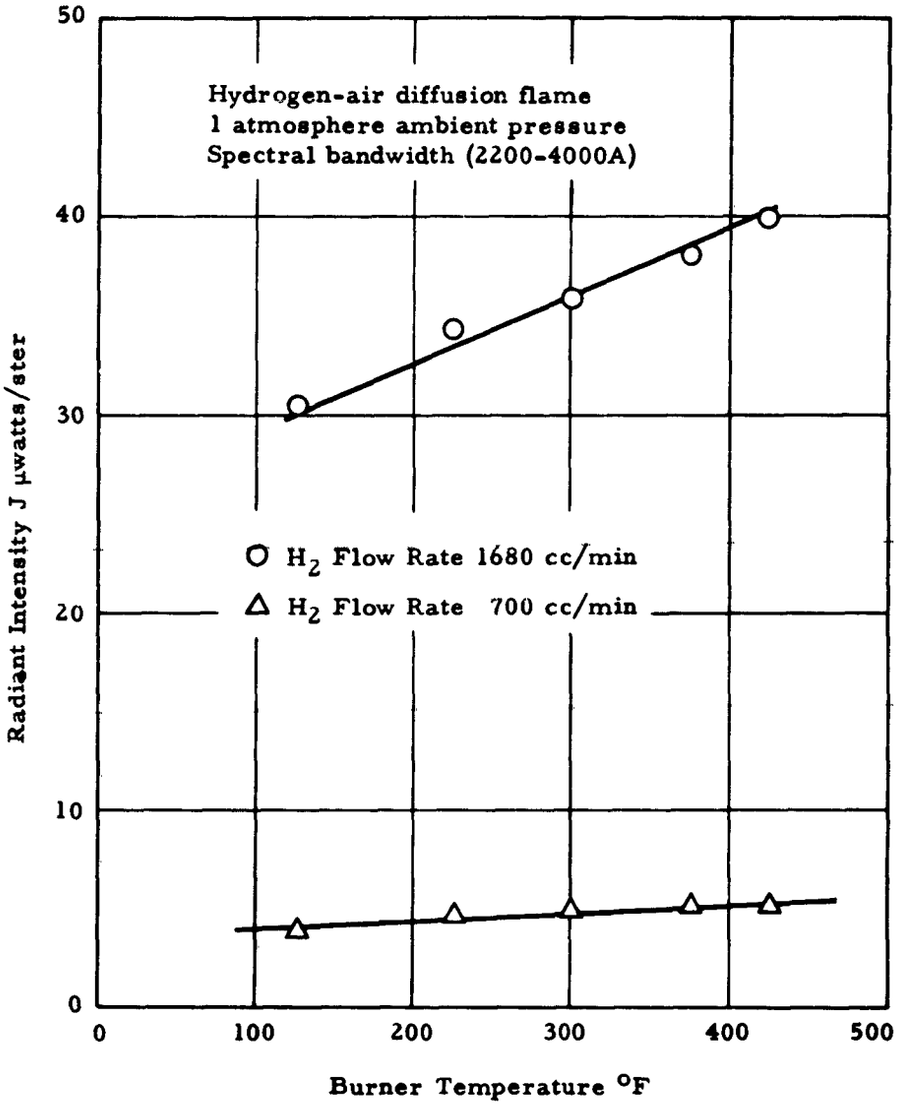

Fig. 26 Hydrogen-air diffusion flames: Radiant intensity (2200 - 4000A) vs burner temperature at 1 atmosphere.

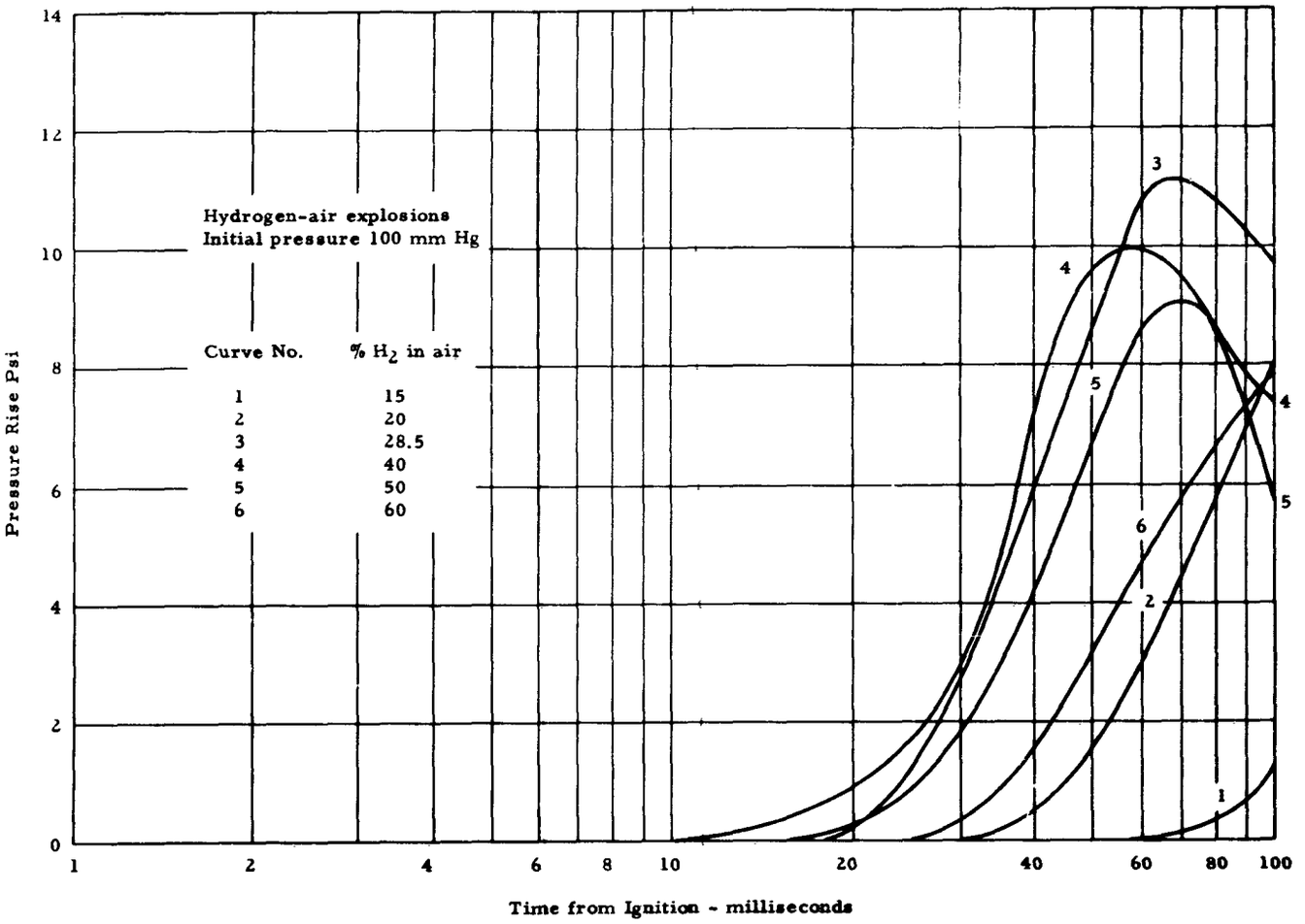

Fig. 27a Hydrogen-air explosions: Pressure vs time for initial pressure 100 mm Hg.

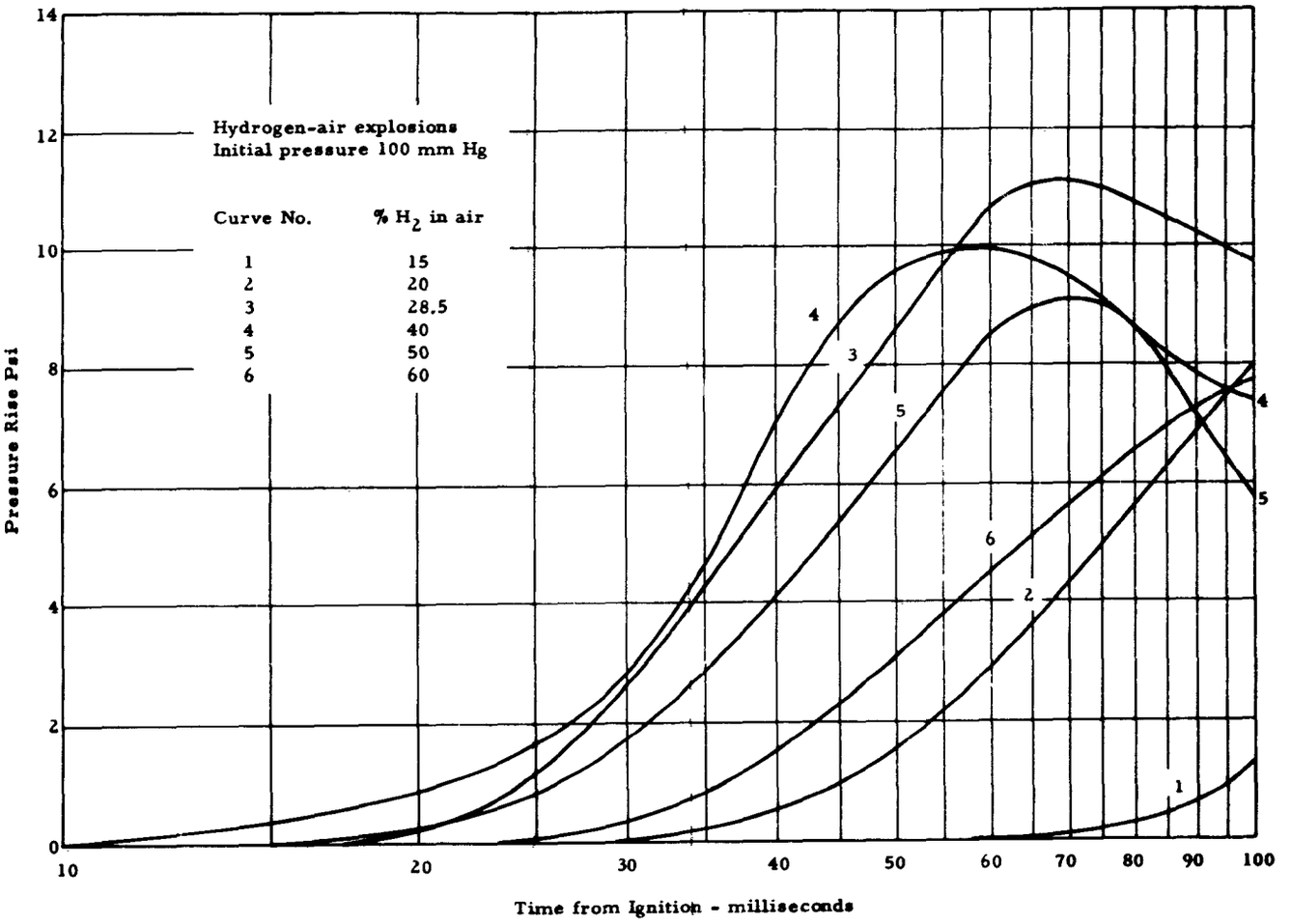

Fig. 27b Hydrogen-air explosions: Pressure vs time for initial pressure 100 mm Hg (replotted on expanded scale).

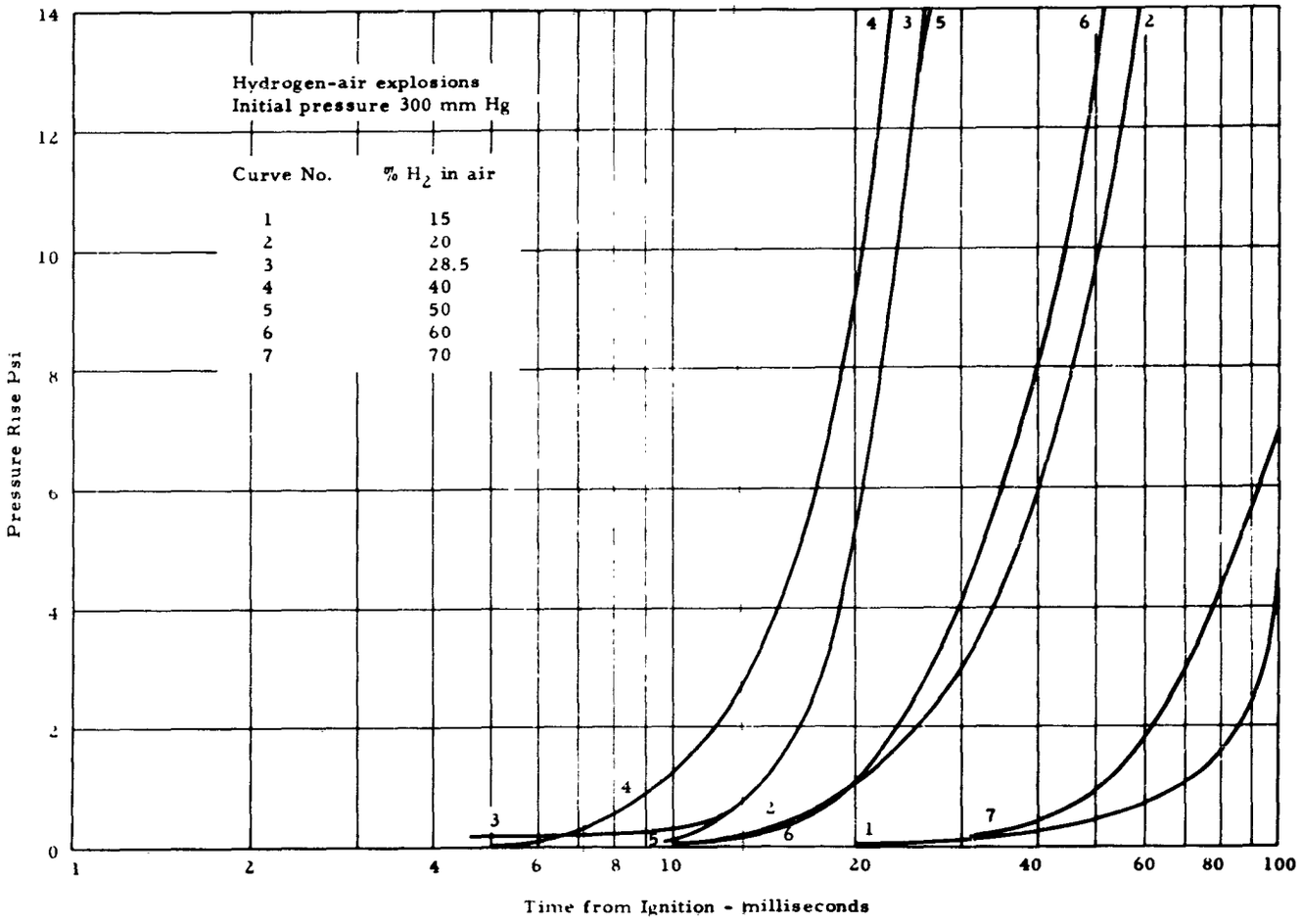

Fig. 28 Hydrogen-air explosions: Pressure vs time for initial pressure 300 mm Hg.

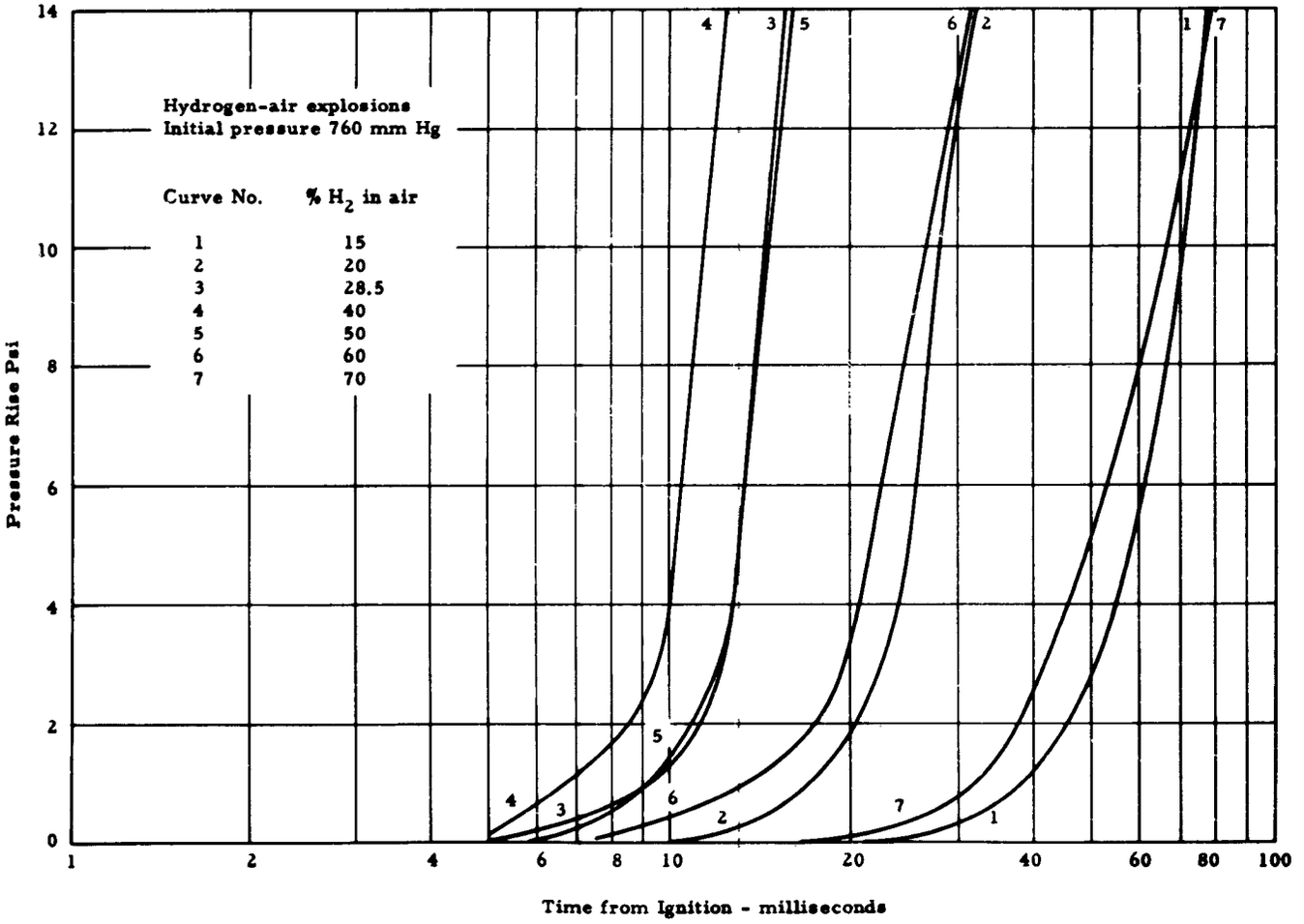

Fig. 29 Hydrogen-air explosions: Pressure vs time for initial pressure 760 mm Hg.

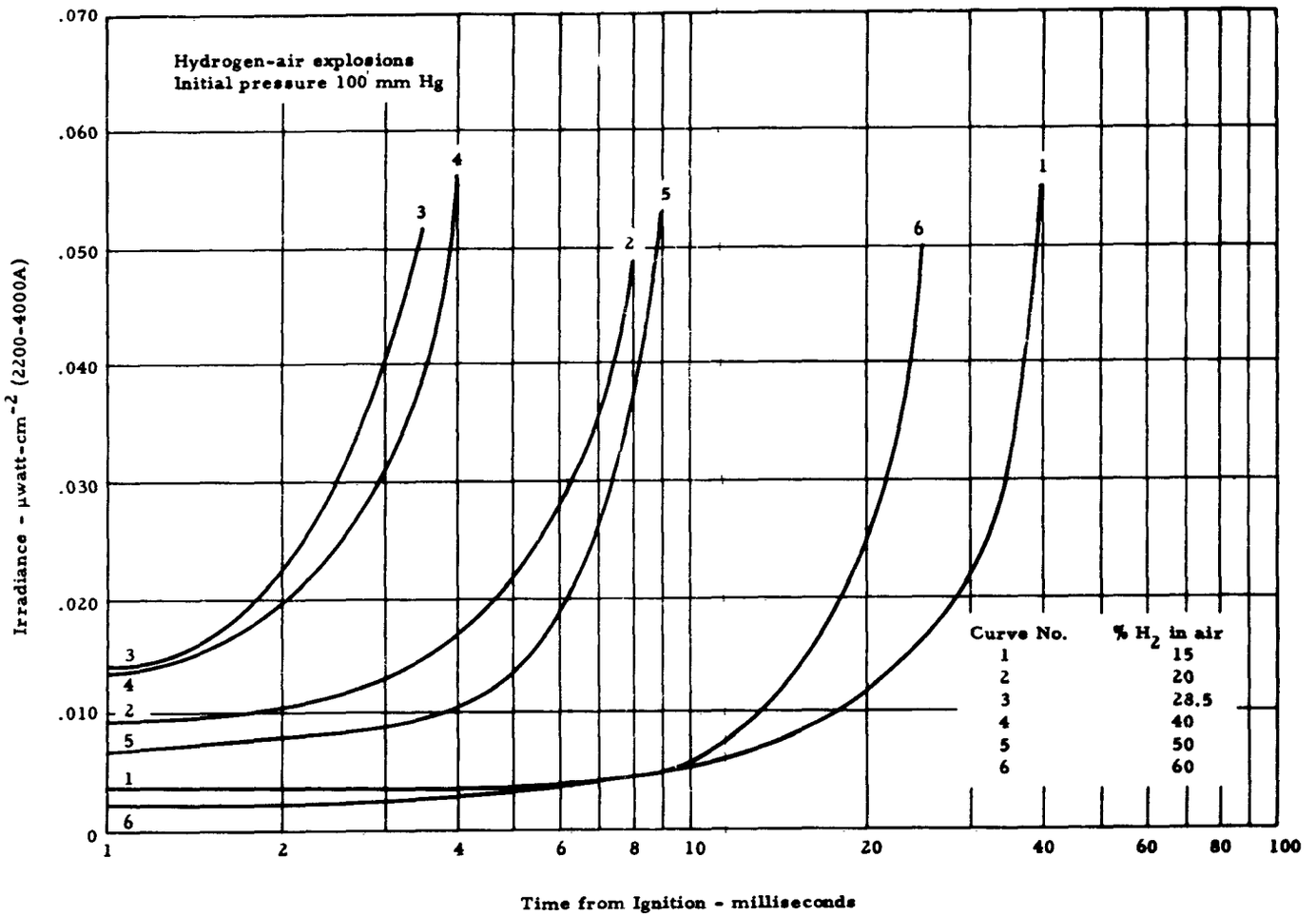

Fig. 30 Hydrogen-air explosions: UV radiation vs time for initial pressure 100 mm Hg.

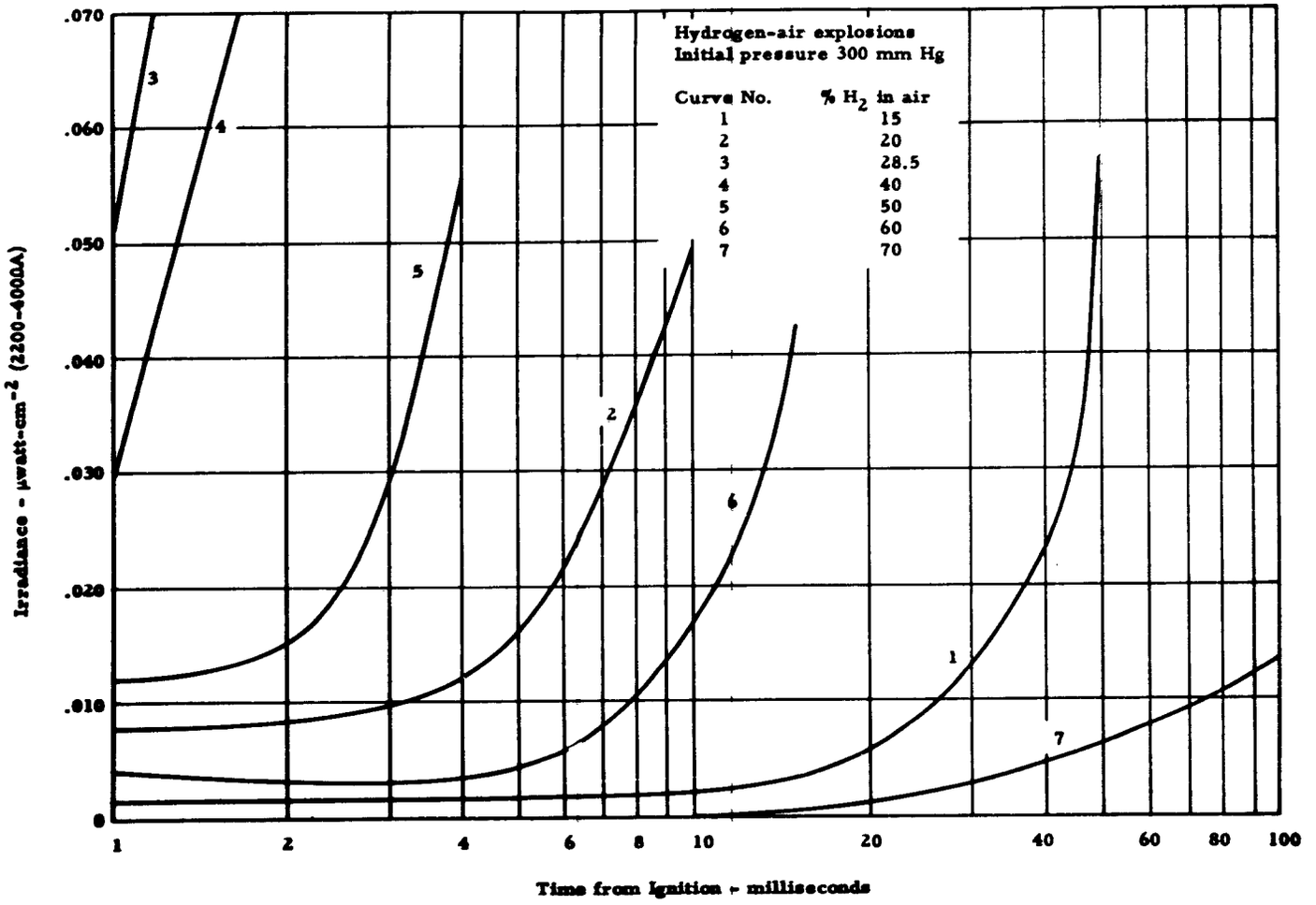

Fig. 31 Hydrogen-air explosions: UV radiation vs time for initial pressure 300 mm Hg.

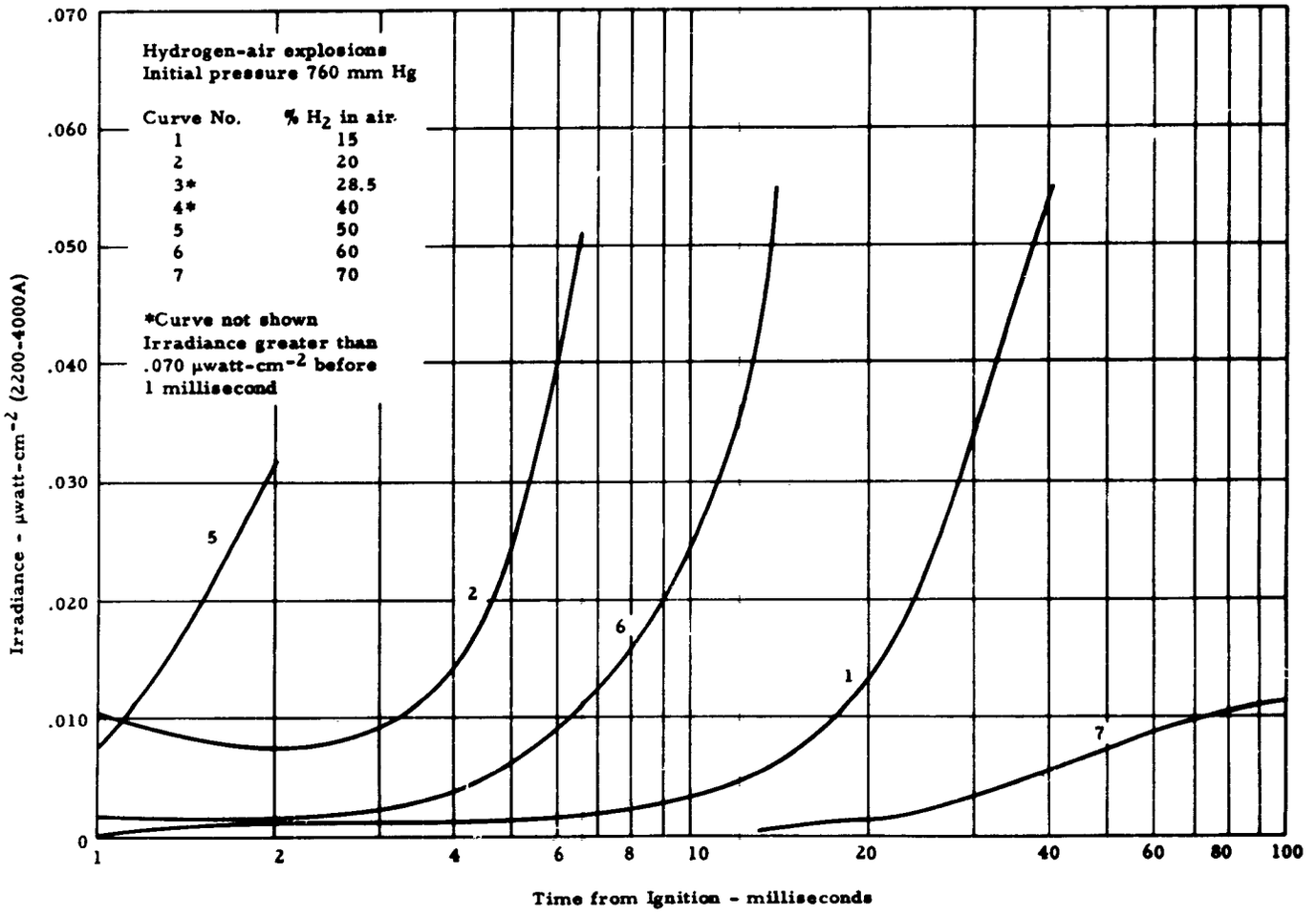

Fig. 32 Hydrogen-air explosions: UV radiation vs time for initial pressure 760 mm Hg.

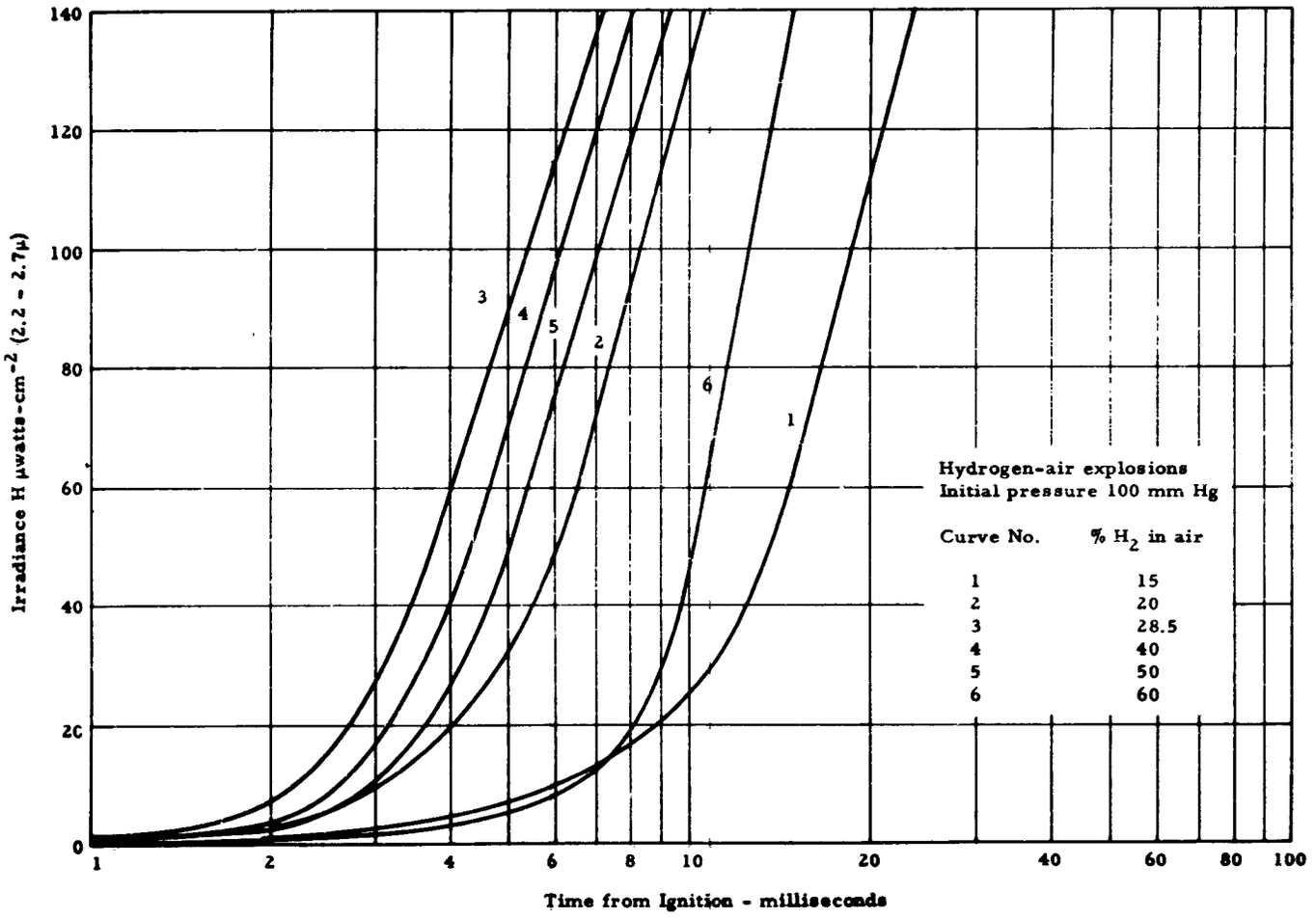

Fig. 33 Hydrogen-air explosions: IR radiation vs time for initial pressure 100 mm Hg.

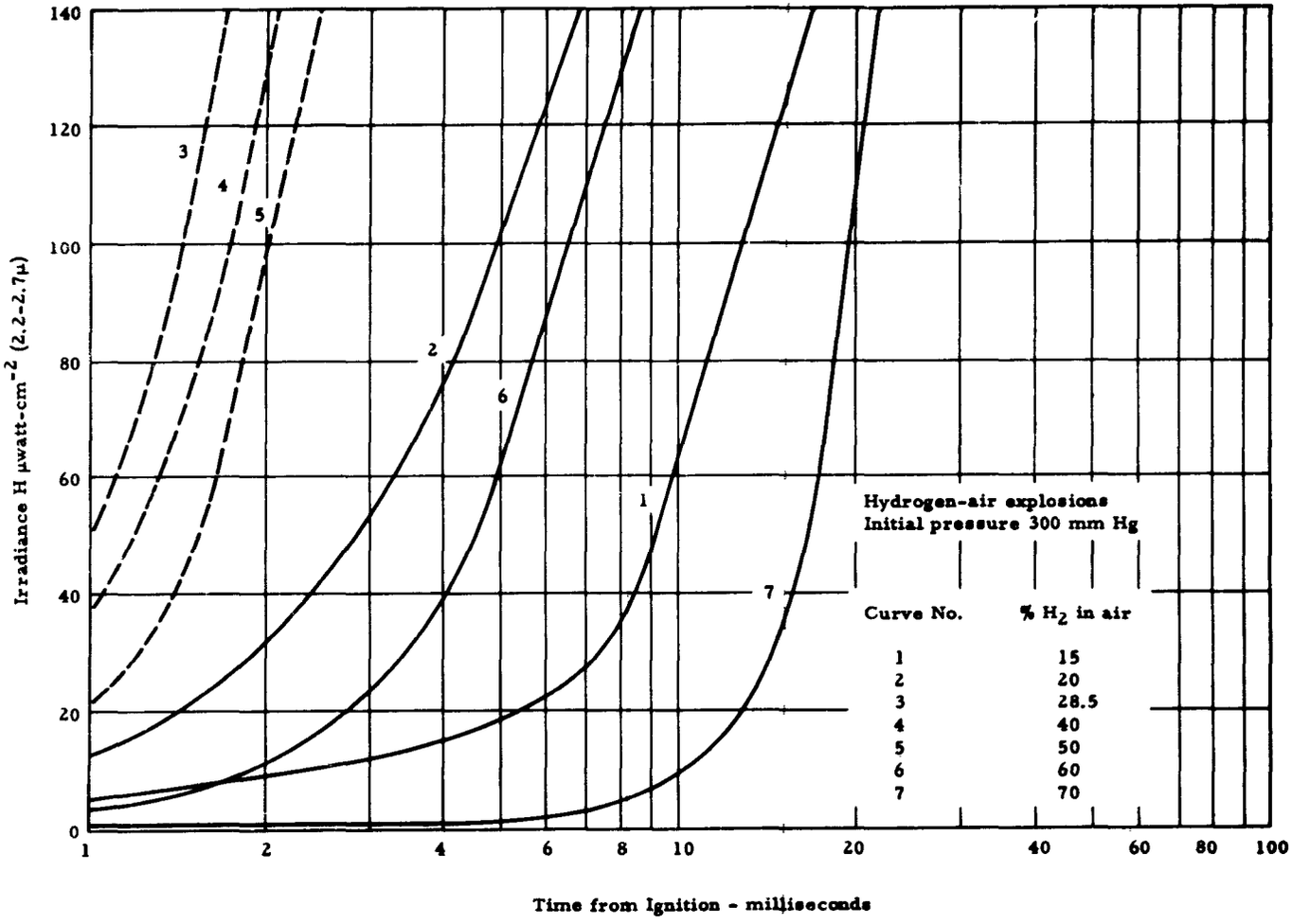

Fig. 34 Hydrogen-air explosions: IR radiation vs time for initial pressure 300 mm Hg.

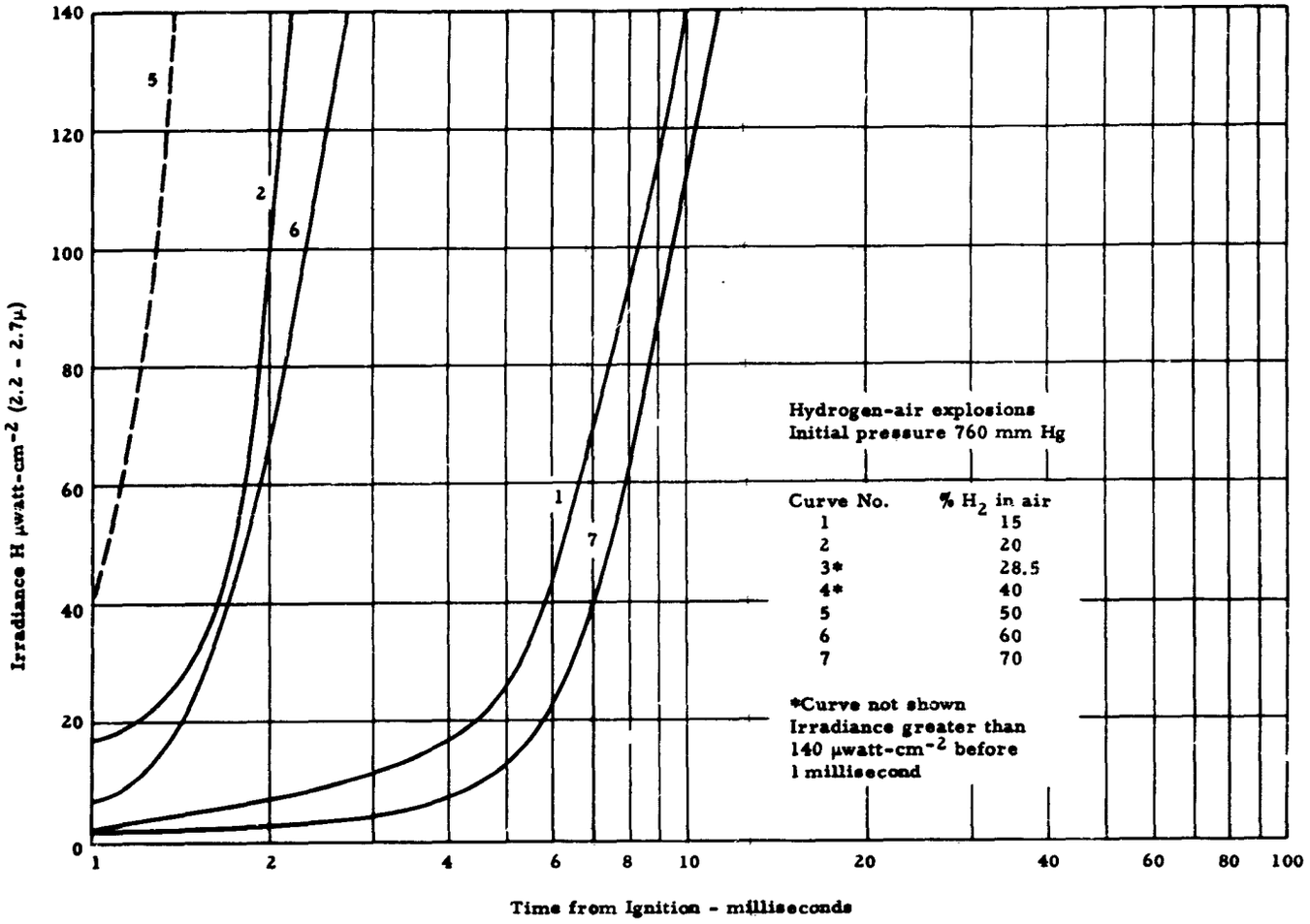

Fig. 35 Hydrogen-air explosions: IR radiation vs time for initial pressure 760 mm Hg.

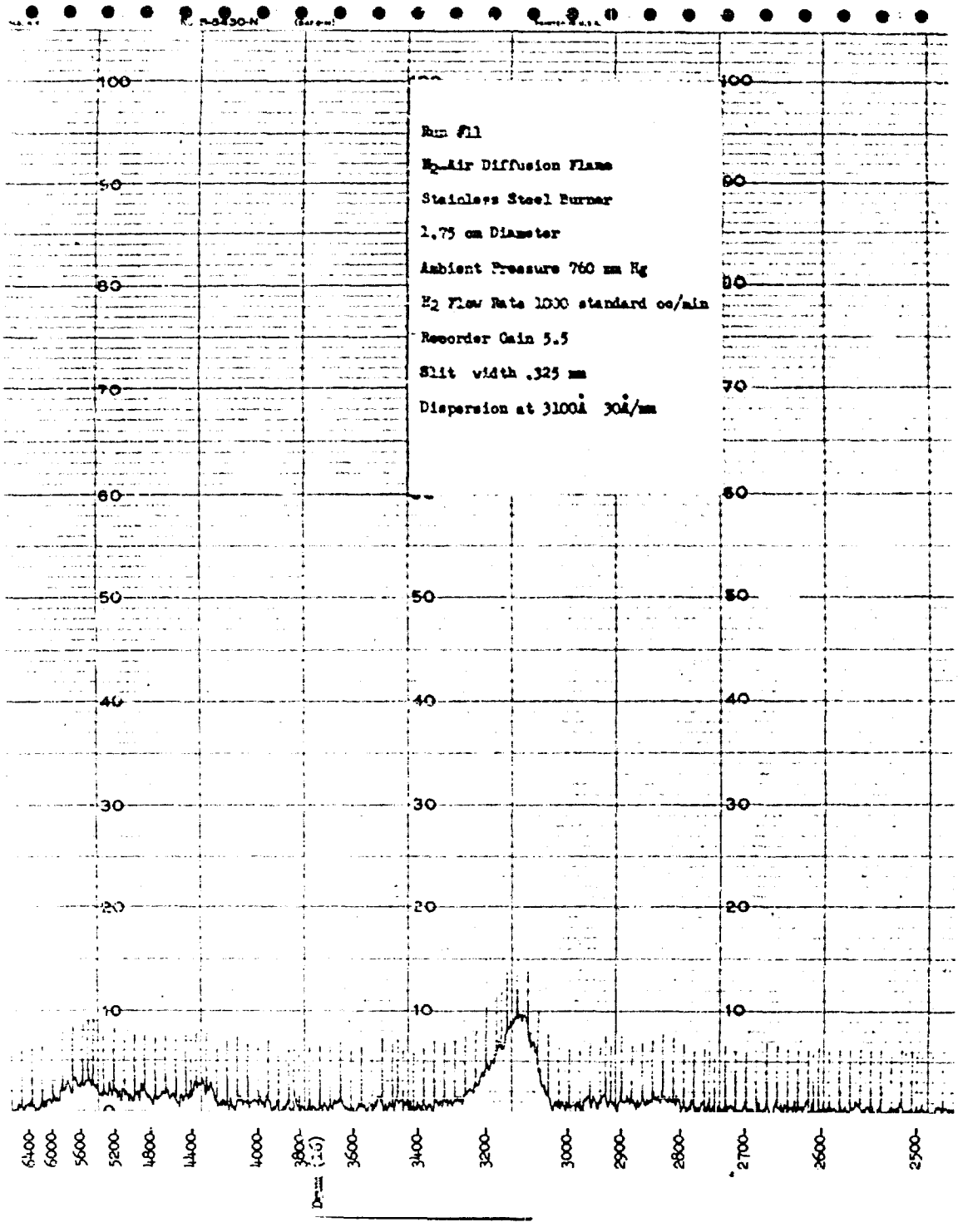

wavelength in angstroms

Fig. 36 UV-visible spectrum of hydrogen-air diffusion flame at 760 mm Hg. Recorder gain = 5.5.

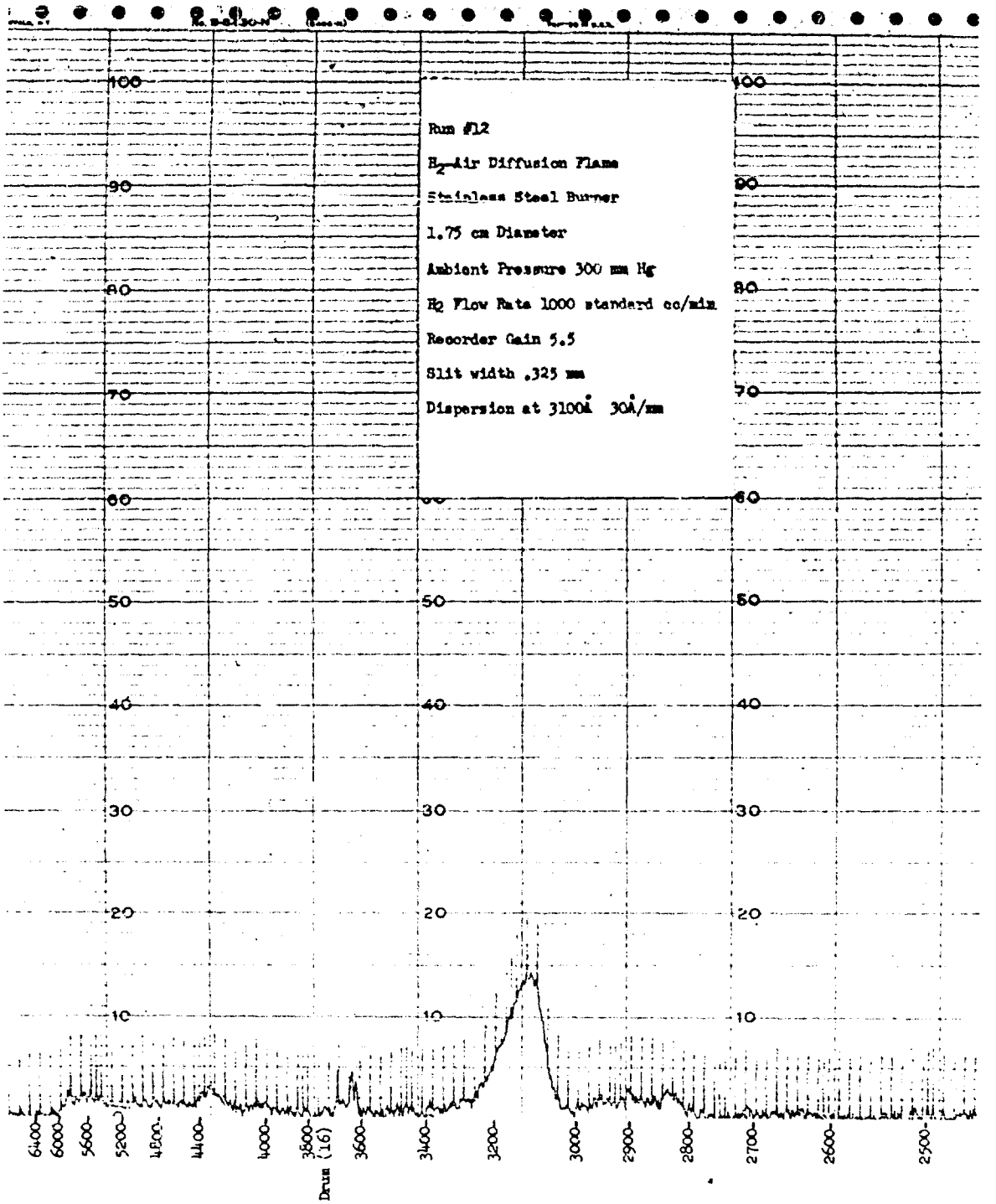

wavelength in angstroms

Fig. 37 UV-visible spectrum of hydrogen-air diffusion flame at 300 mm Hg. Recorder gain = 5.5.

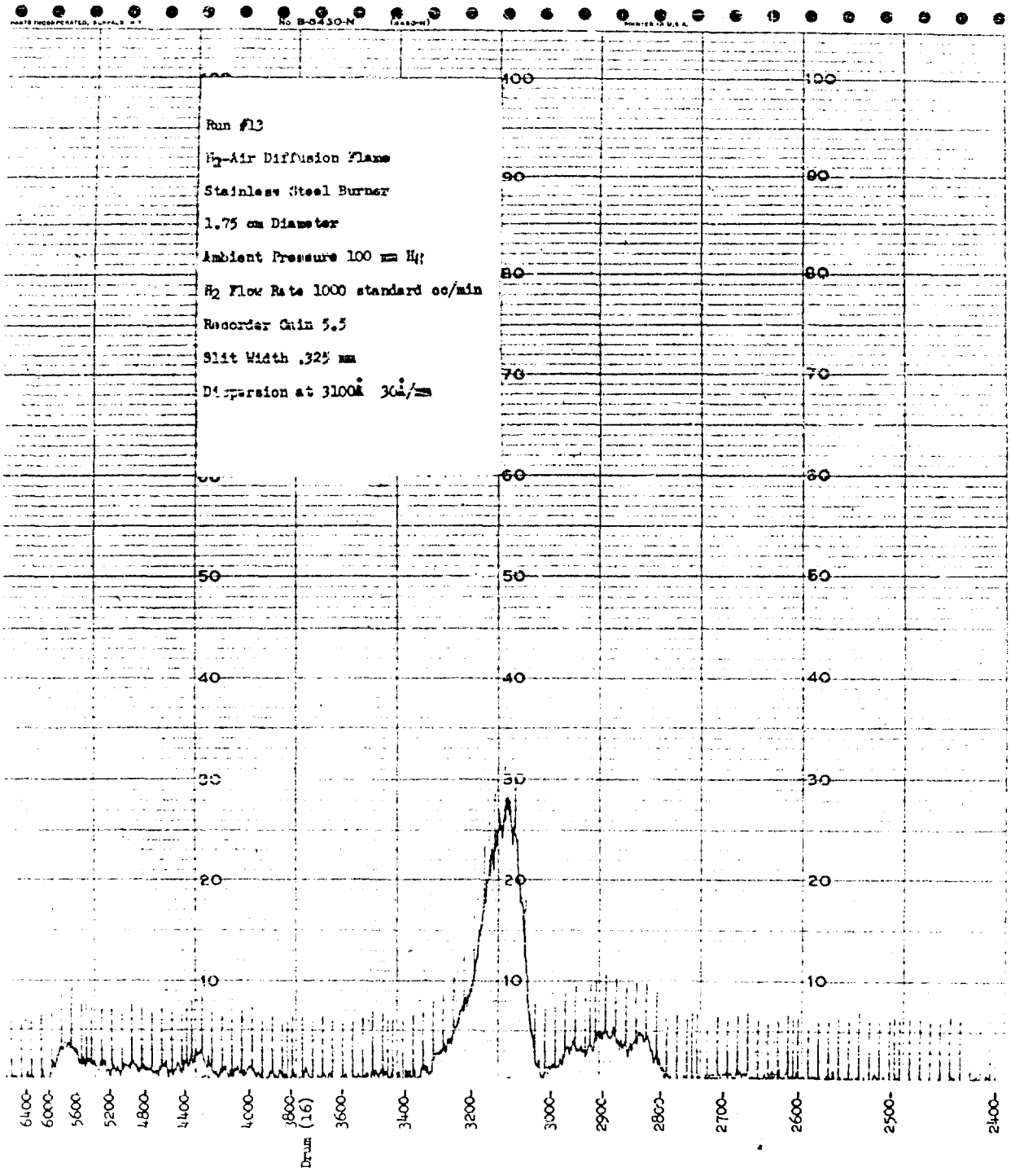

wavelength in angstroms

Fig. 38 UV-visible spectrum of hydrogen-air diffusion flame at 100 mm Hg. Recorder gain = 5.5.

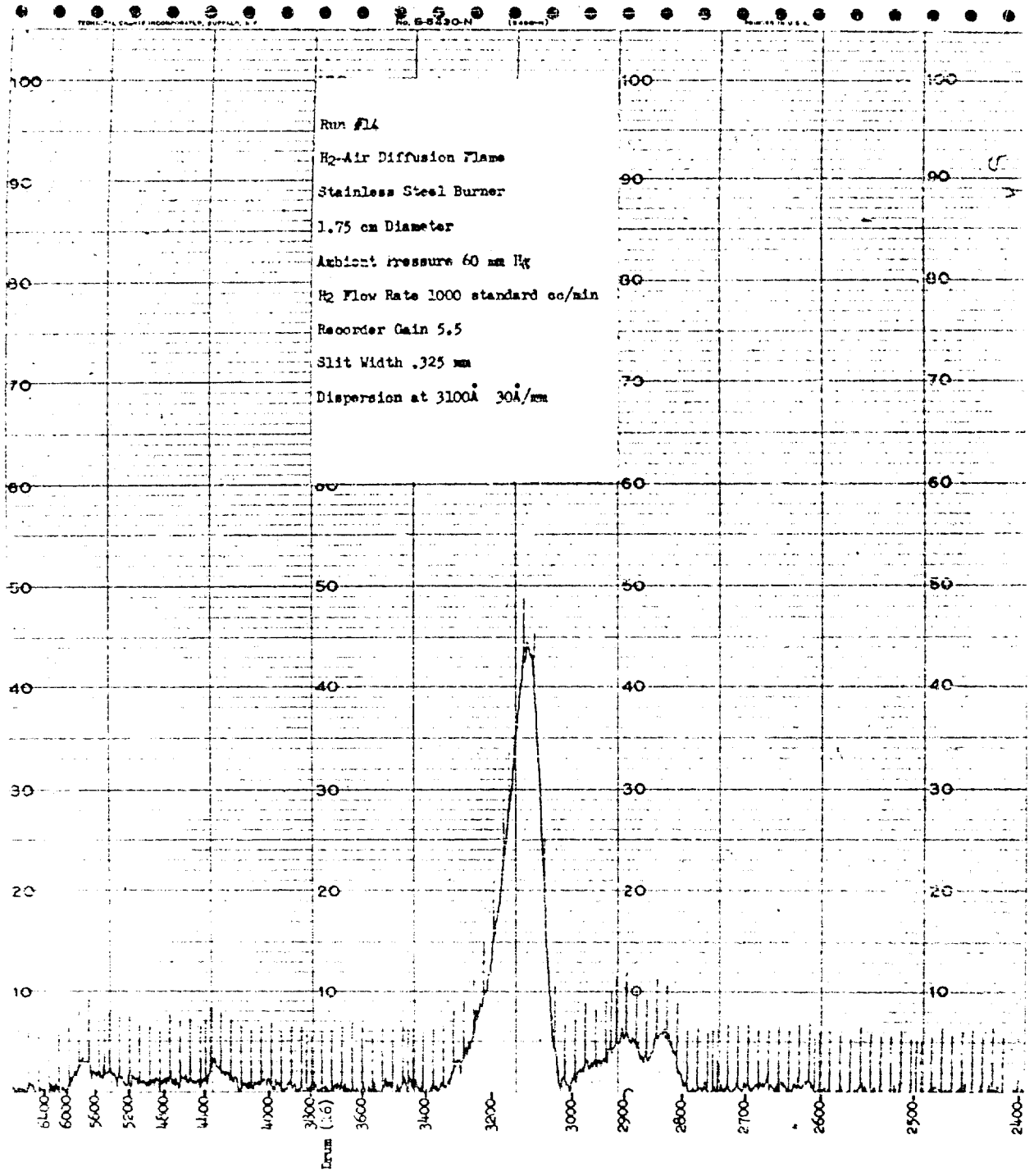

wavelength in angstroms

Fig. 39 UV-visible spectrum of hydrogen-air diffusion flame at 60 mm Hg. Recorder gain = 5.5.

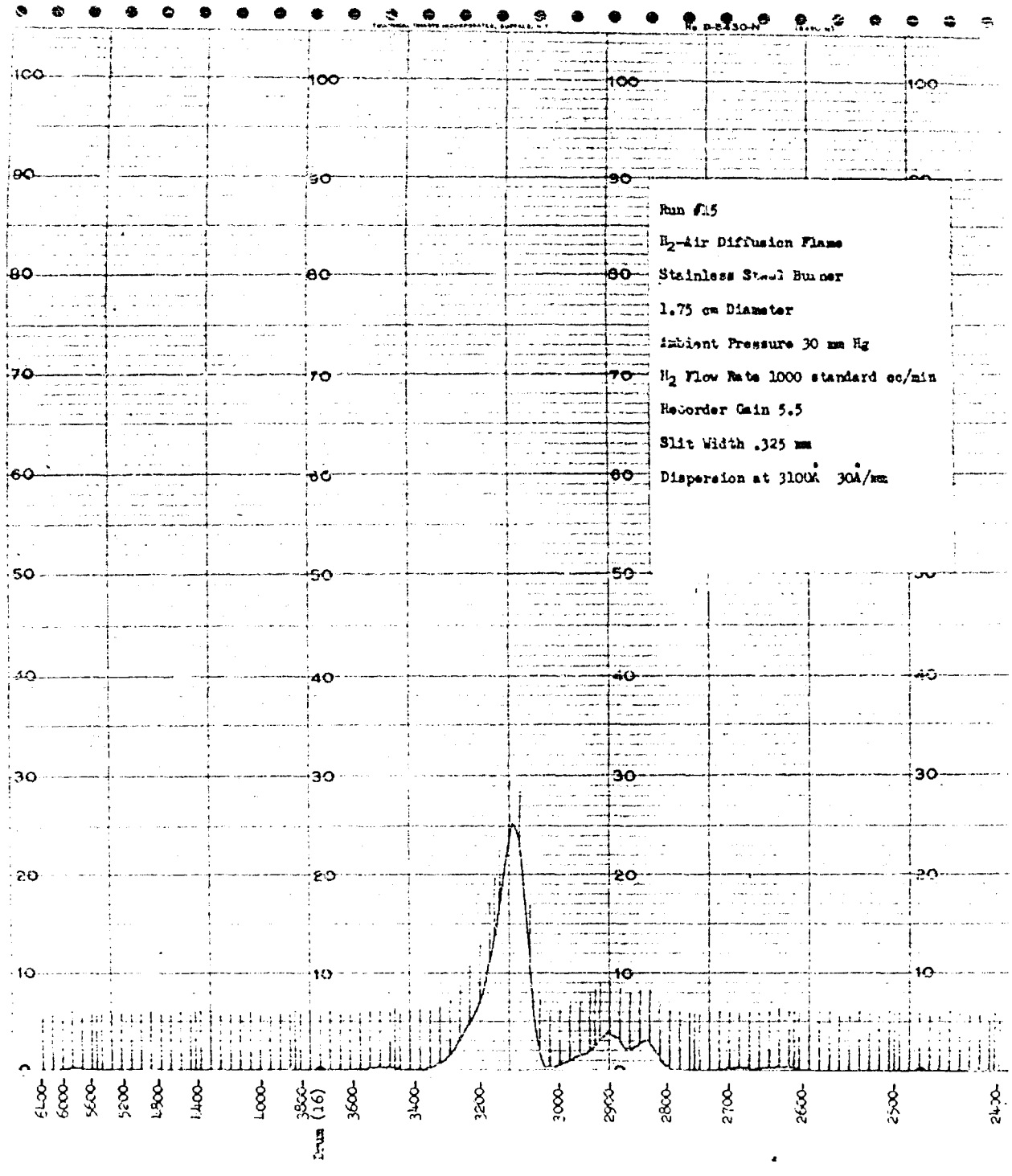

wavelength in angstroms

Fig. 40 UV-visible spectrum of hydrogen-air diffusion flame at 30 mm Hg. Recorder gain = 5.5.

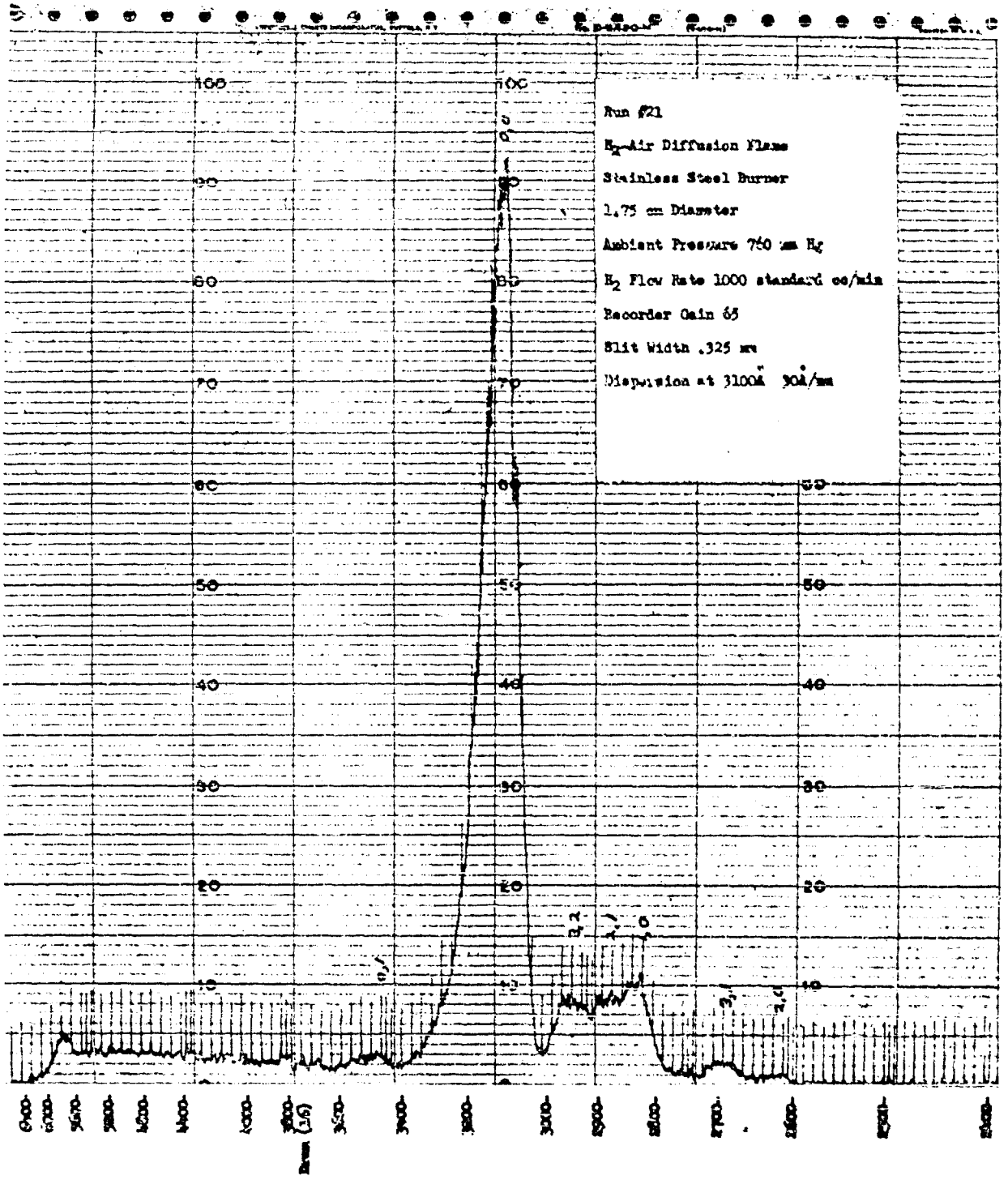

wavelength in angstroms

Fig. 41 UV-visible spectrum of hydrogen-air diffusion flame at 760 mm Hg. Recorder gain = 65.

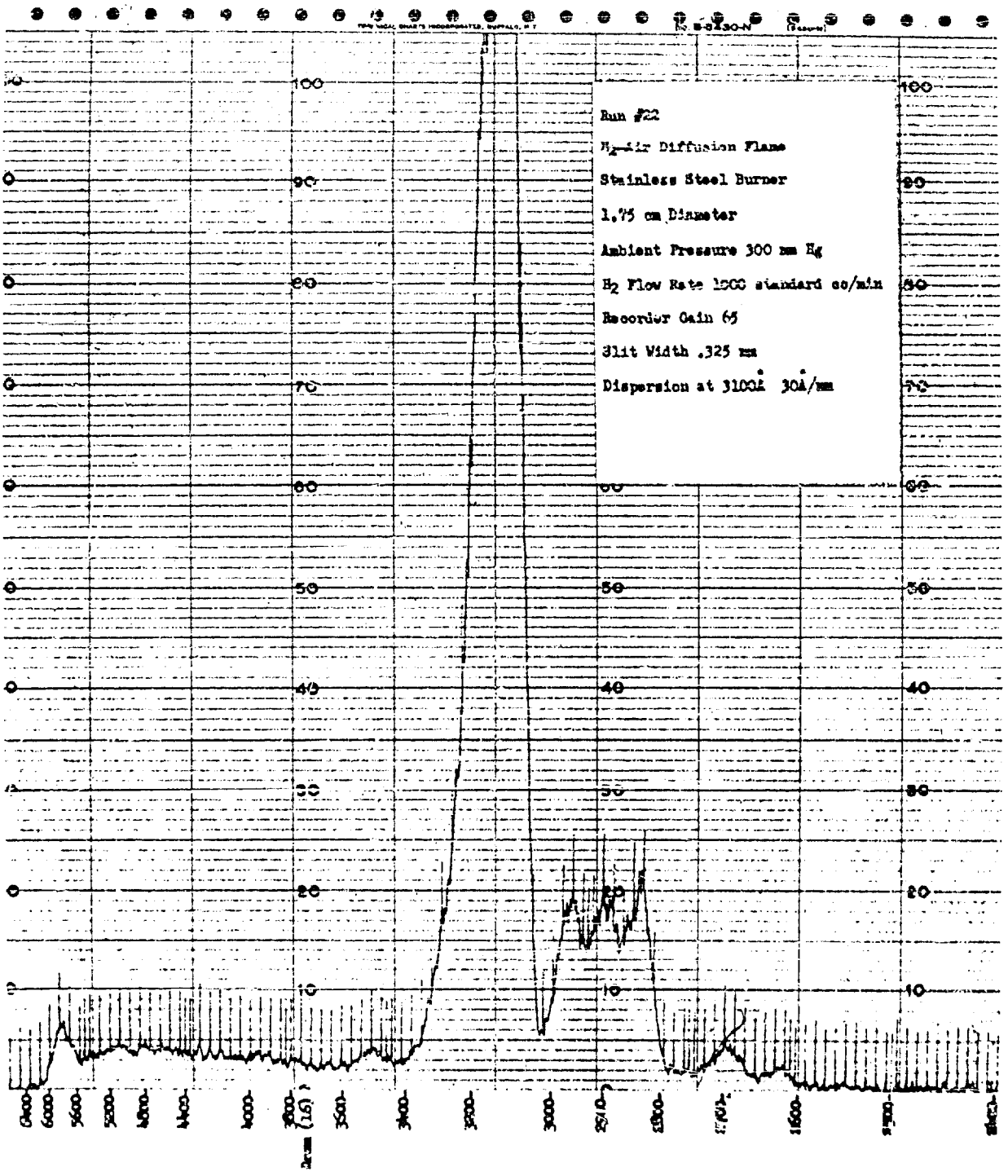

wavelength in angstroms

Fig. 42 UV-visible spectrum of hydrogen-air diffusion flame at 300 mm Hg. Recorder gain = 65.

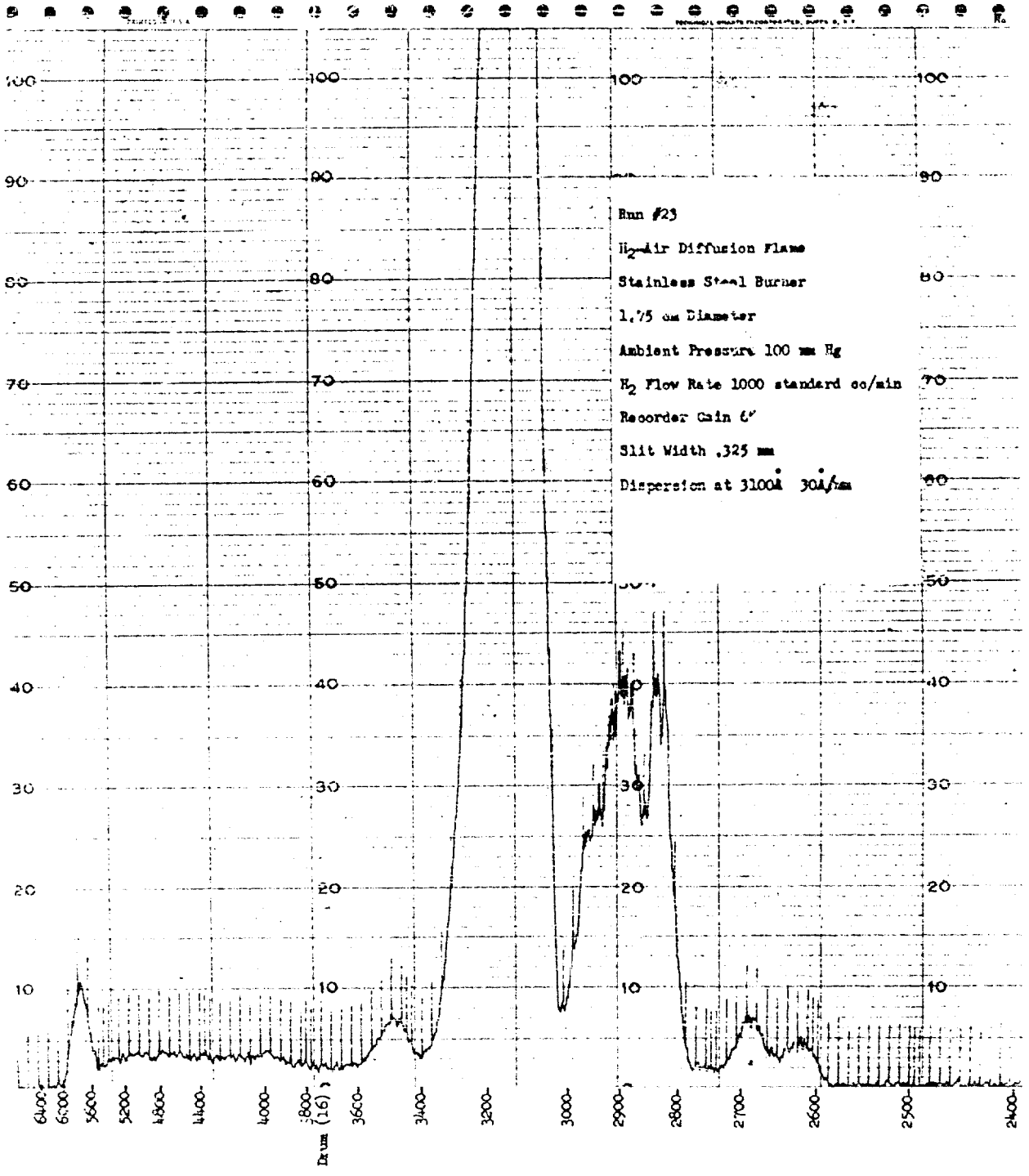

Fig. 43 UV-visible spectrum of hydrogen-air diffusion flame at 100 mm Hg. Recorder gain = 65.

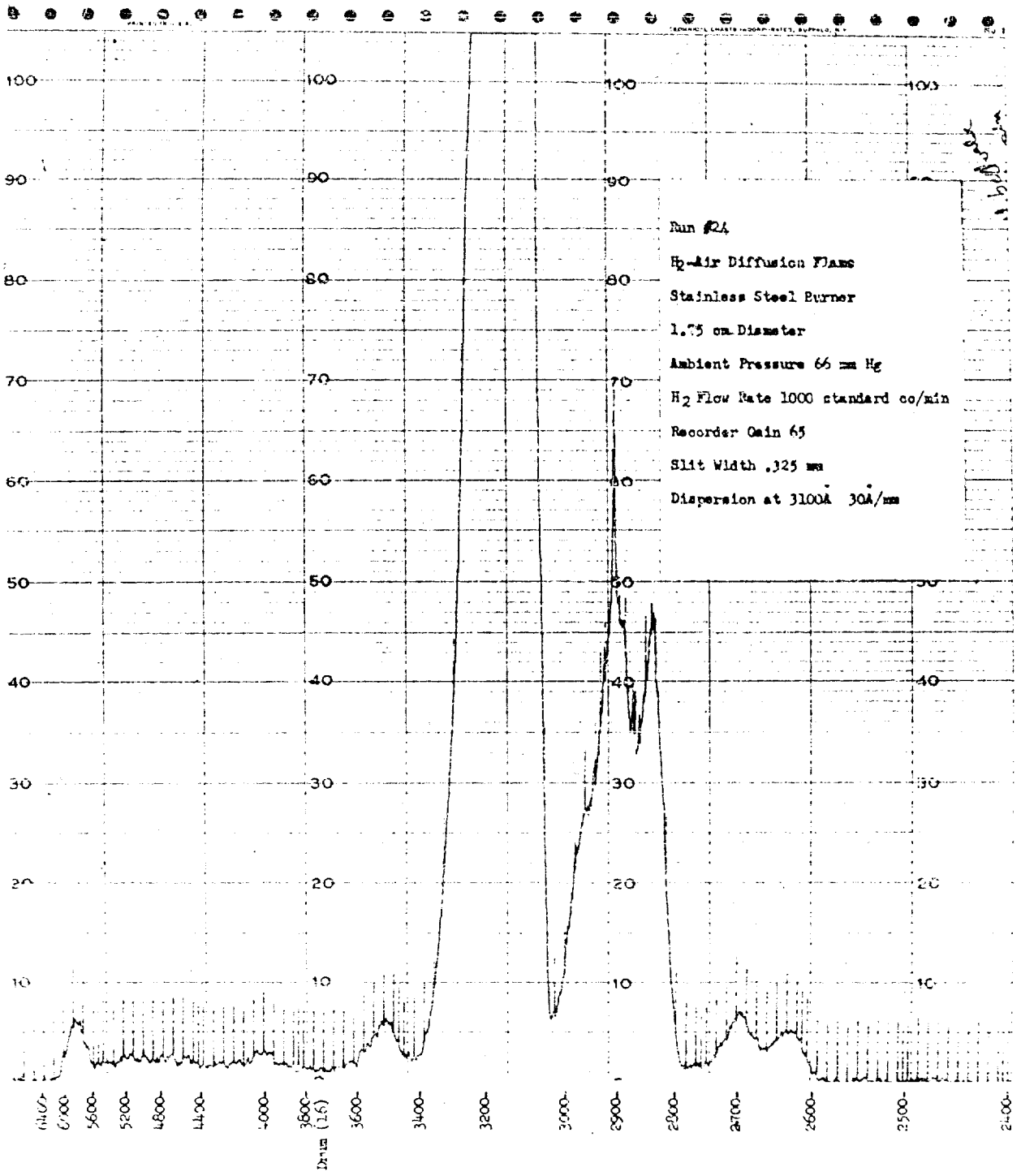

Fig. 44 UV-visible spectrum of hydrogen-air diffusion flame at 60 mm Hg. Recorder gain = 65.

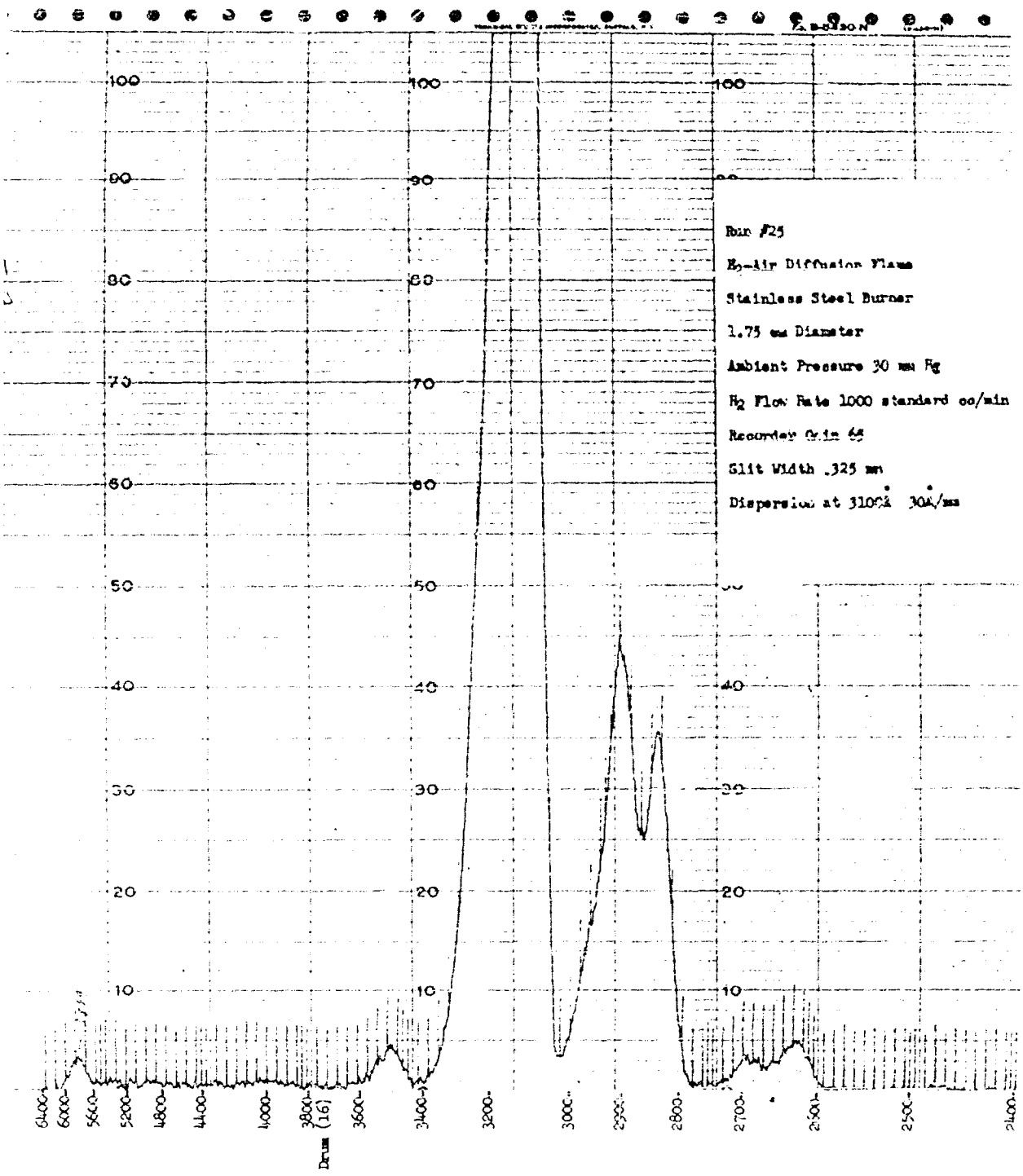

wavelength in angstroms

Fig. 45 UV-visible spectrum of hydrogen-air diffusion flame at 30 mm Hg. Recorder gain = 65.

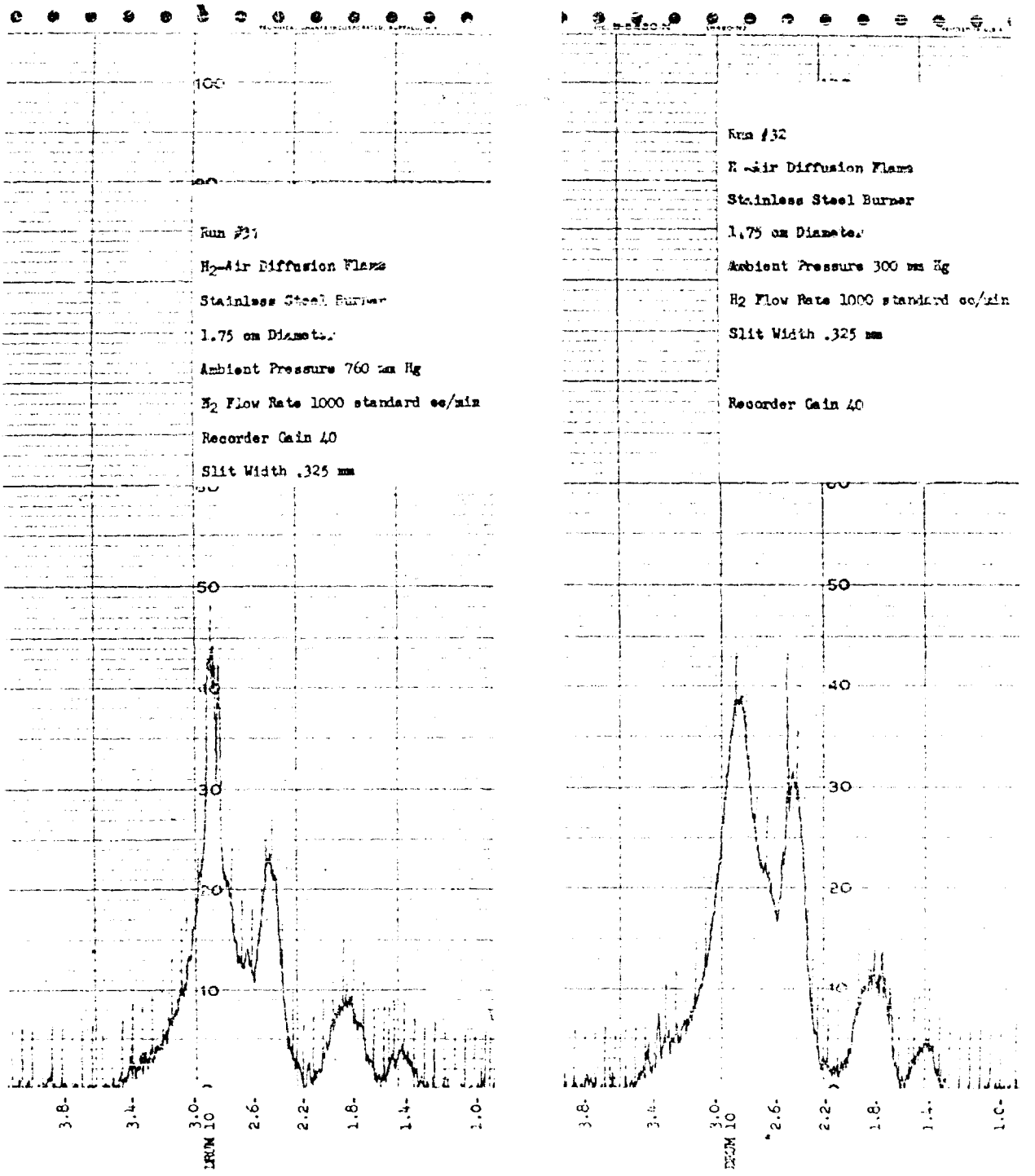

wavelength in microns

Fig. 45 Infrared spectra of hydrogen-air diffusion flame at 760 and 300 mm Hg.

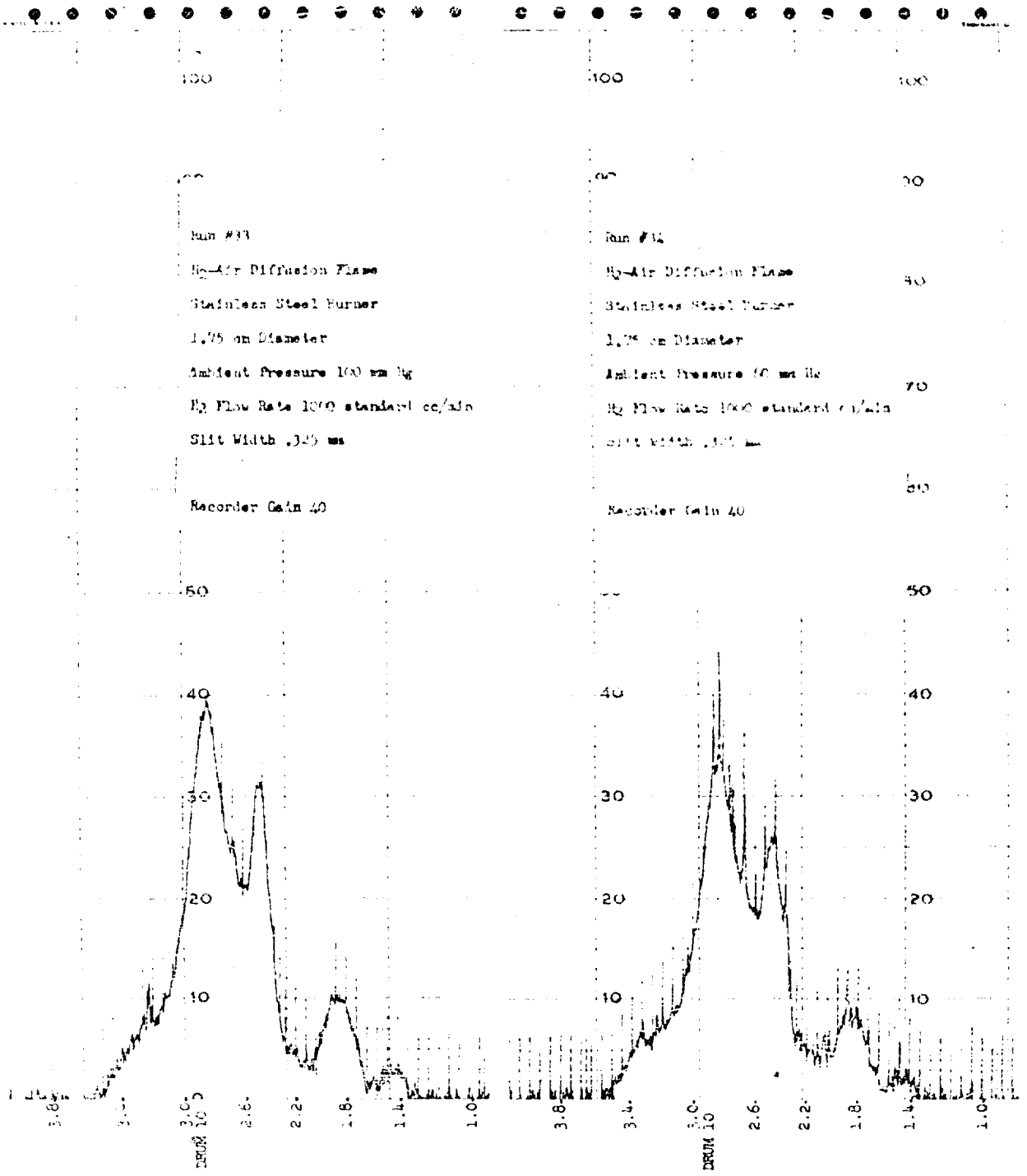

Fig. 47 Infrared spectra of hydrogen-air diffusion flame at 100 and 60 mm Hg.

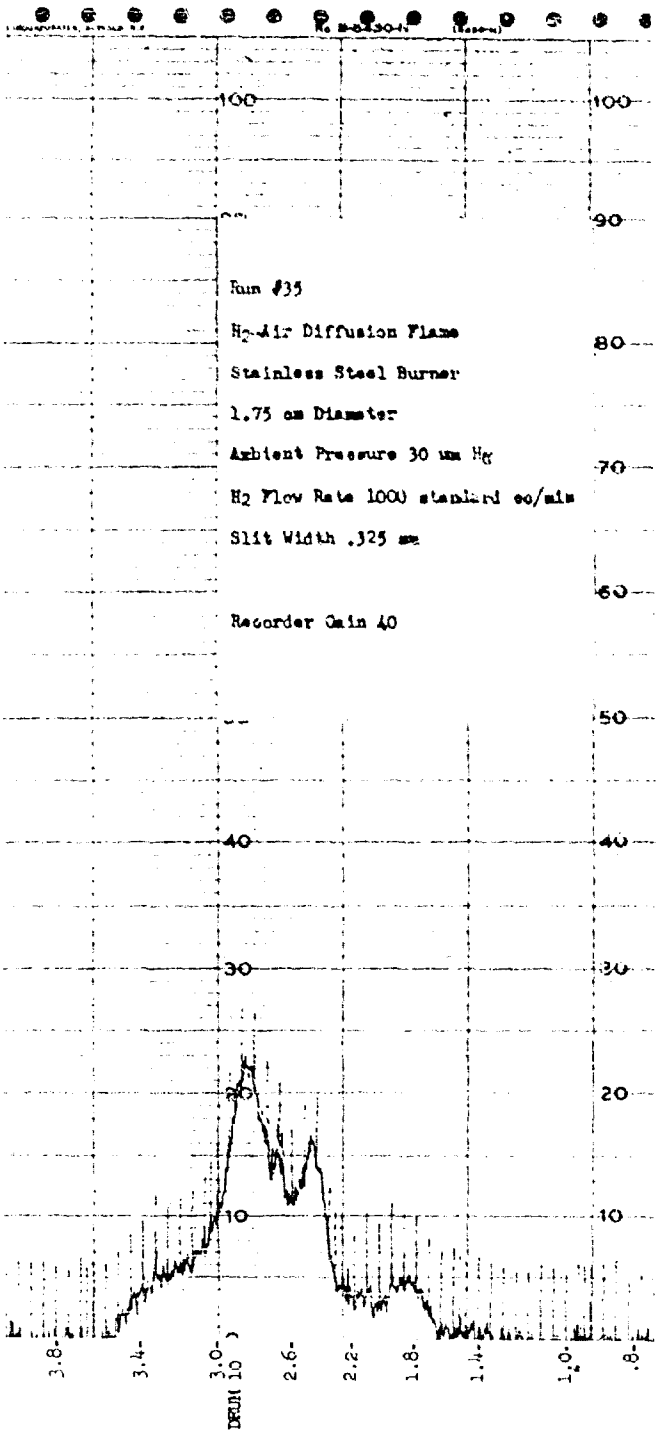

wavelength in microns

Fig. 48 Infrared spectrum of hydrogen-air diffusion flame at 30 mm Hg.

Aeronautical Systems Division, Directorate of Aeromechanics, Flight Accessories Lab, Wright-Patterson AFB, Ohio.
Rpt No. ASD-TDR-63-113. DETECTION OF HYDROGEN-AIR FIRES AND EXPLOSIONS IN AEROSPACE VEHICLES VIA OH BAND AND WATER BAND EMISSION. Final report, Apr 63, 96p., incl illus, tables and refs.

Unclassified Report.

To provide a basis for reliable hydrogen-air fire and explosion detection in aerospace vehicles, measurements of the absolute value of radiant intensity were made over the OH bands of the ultraviolet and the water bands in the infrared. A surprising

(over)

result was the increase in OH radiant intensity with decreasing pressure. Diffusion flame variables were hydrogen flow rate, port diameter, and pressure from 760 to less than 20 mm Hg. For explosions, mixture ratio as well as pressure were varied; the rate of increase of emission and pressure after ignition were measured to determine detection lead time. Results where possible are presented as fundamental quantities which can be applied with reasonable rigor to a variety of design situations. Detection based upon monitoring OH radiation is recommended over other properties such as IR radiation, ionization, temperature rise, or pressure rise. Application of the data to specific designs is discussed.

1. Fire Detection Hydrogen-Air
2. Aerospace Vehicles
3. Radiation, Infrared
4. Radiation, Ultraviolet

I. AFSC Project 6075 Task 607501
II. Contract AF 33 (657)-8969
III. Thiokol Chemical Corp., Reaction Motors Division, Denville, N. J.
IV. K. Hill B. Hornstein

V. Aval fr OTS
VI. In ASTIA collection

Aeronautical Systems Division, Directorate of Aeromechanics, Flight Accessories Lab, Wright-Patterson AFB, Ohio.
Rpt No. ASD-TDR-63-113. DETECTION OF HYDROGEN-AIR FIRES AND EXPLOSIONS IN AEROSPACE VEHICLES VIA OH BAND AND WATER BAND EMISSION. Final report, Apr 63, 96p., incl illus, tables and refs.

Unclassified Report.

To provide a basis for reliable hydrogen-air fire and explosion detection in aerospace vehicles, measurements of the absolute value of radiant intensity were made over the OH bands of the ultraviolet and the water bands in the infrared. A surprising

(over)

result was the increase in OH radiant intensity with decreasing pressure. Diffusion flame variables were hydrogen flow rate, port diameter, and pressure from 760 to less than 20 mm Hg. For explosions, mixture ratio as well as pressure were varied; the rate of increase of emission and pressure after ignition were measured to determine detection lead time, Results where possible are presented as fundamental quantities which can be applied with reasonable rigor to a variety of design situations. Detection based upon monitoring OH radiation is recommended over other properties such as IR radiation, ionization, temperature rise, or pressure rise. Application of the data to specific designs is discussed.

1. Fire Detection Hydrogen-Air
2. Aerospace Vehicles
3. Radiation, Infrared
4. Radiation, Ultraviolet

I. AFSC Project 6075 Task 607501
II. Contract AF 33 (657)-8969
III. Thiokol Chemical Corp., Reaction Motors Division, Denville, N. J.
IV. K. Hill B. Hornstein

V. Aval fr OTS
VI. In ASTIA collection